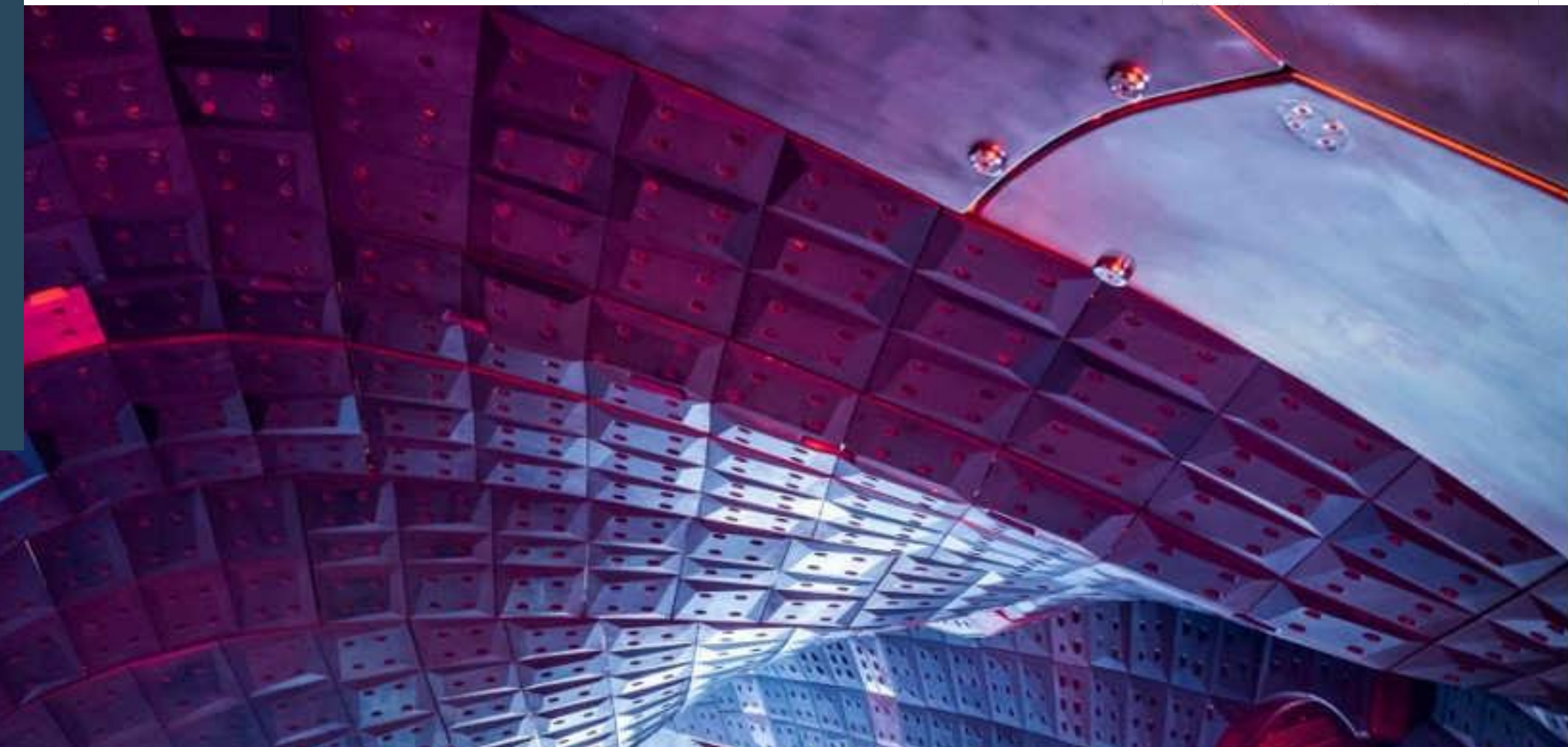




## Exploring sawtooth-like crashes triggered by current drive in Wendelstein 7-X.



EUROfusion

**Ksenia Aleynikova<sup>1</sup>, Rohan Ramasamy<sup>2</sup>, Nikita Nikulsin<sup>1</sup>, Joachim Geiger<sup>1</sup>,  
Alessandro Zocco<sup>1</sup>, Florian Hindenlang<sup>3</sup>, Matthias Hoelzl<sup>3</sup> and JOREK team**

Acknowledgements: Carolin Nührenberg, Erika Strumberger and Qingquan Yu

<sup>1</sup> Max-Planck-Institut für Plasmaphysik, EURATOM Association, Greifswald, Germany

<sup>2</sup> Proxima Fusion GmbH, Flößergasse 2, Boltzmannstraße 2, 81369 Munich, Germany

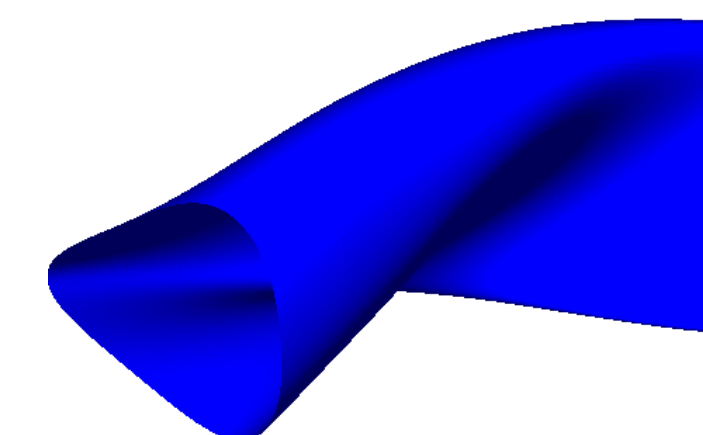
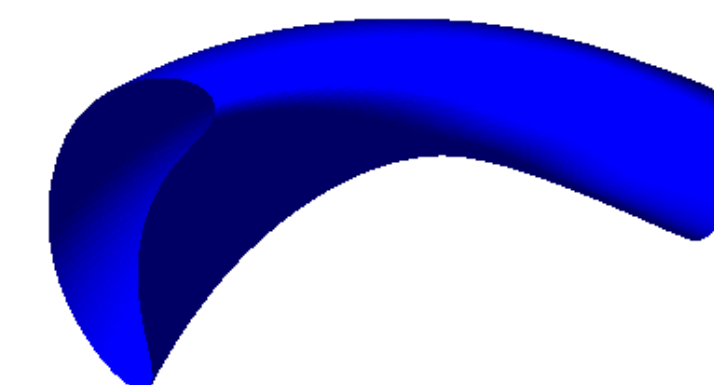
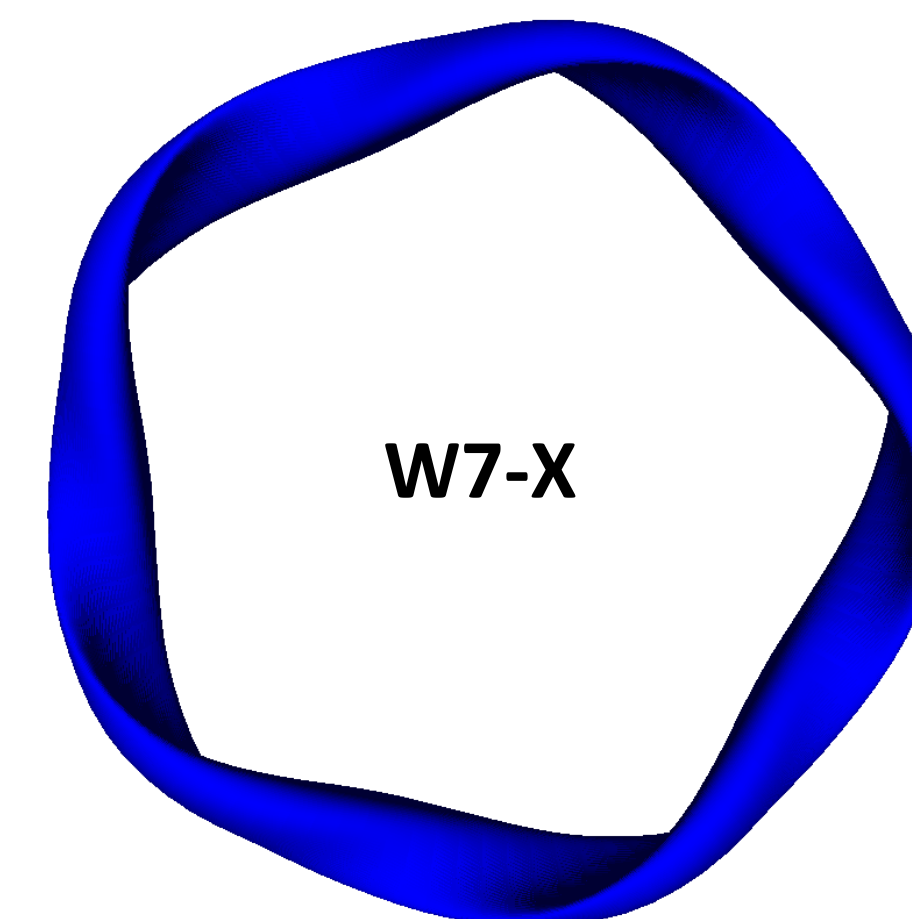
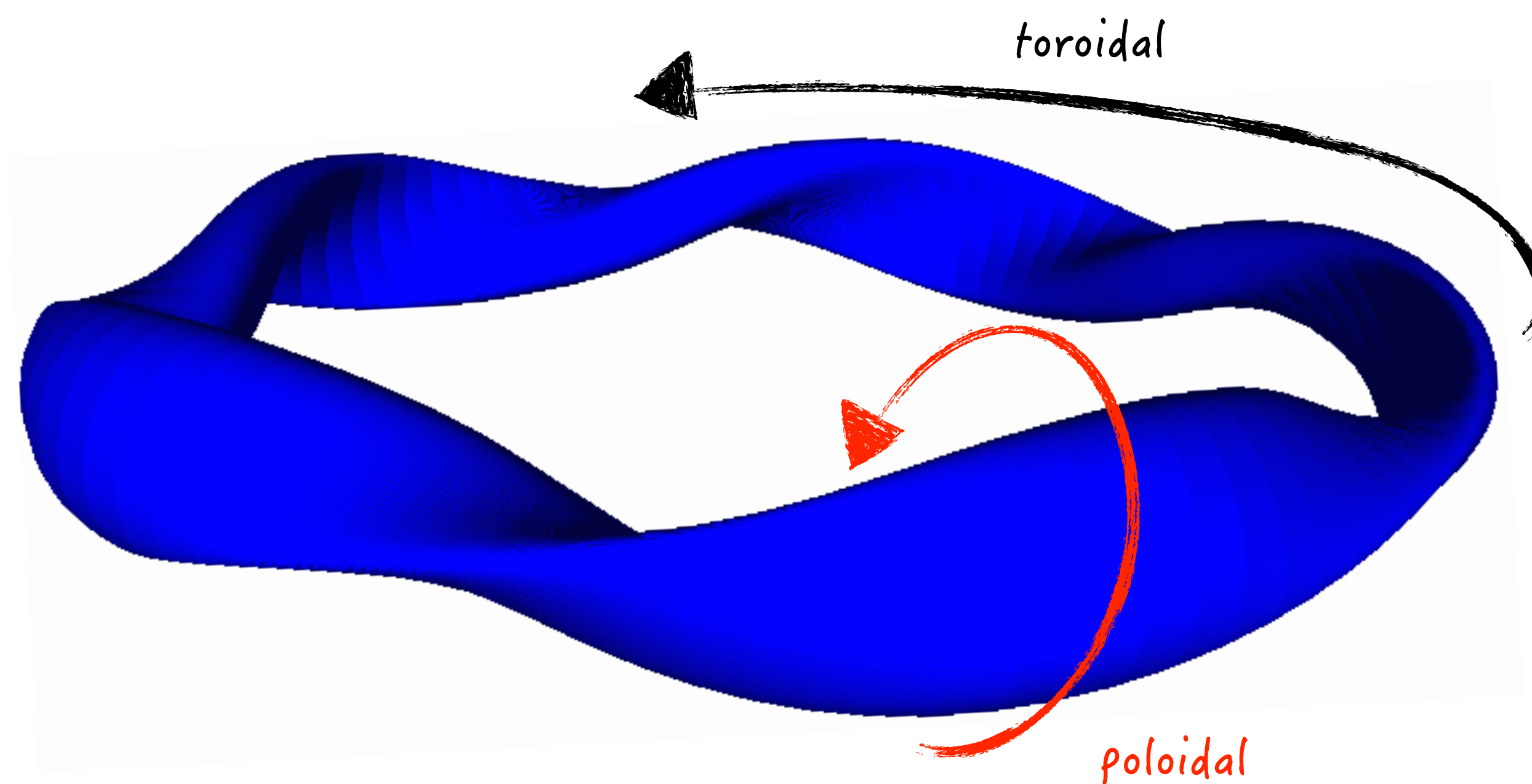
<sup>3</sup> Max-Planck Institut für Plasmaphysik, Boltzmannstraße 2, 85748 Garching, Germany



This work has been carried out within the framework of the EUROfusion Consortium, funded by the European Union via the Euratom Research and Training Programme (Grant Agreement No 101052200 — EUROfusion). Views and opinions expressed are however those of the author(s) only and do not necessarily reflect those of the European Union or the European Commission. Neither the European Union nor the European Commission can be held responsible for them.

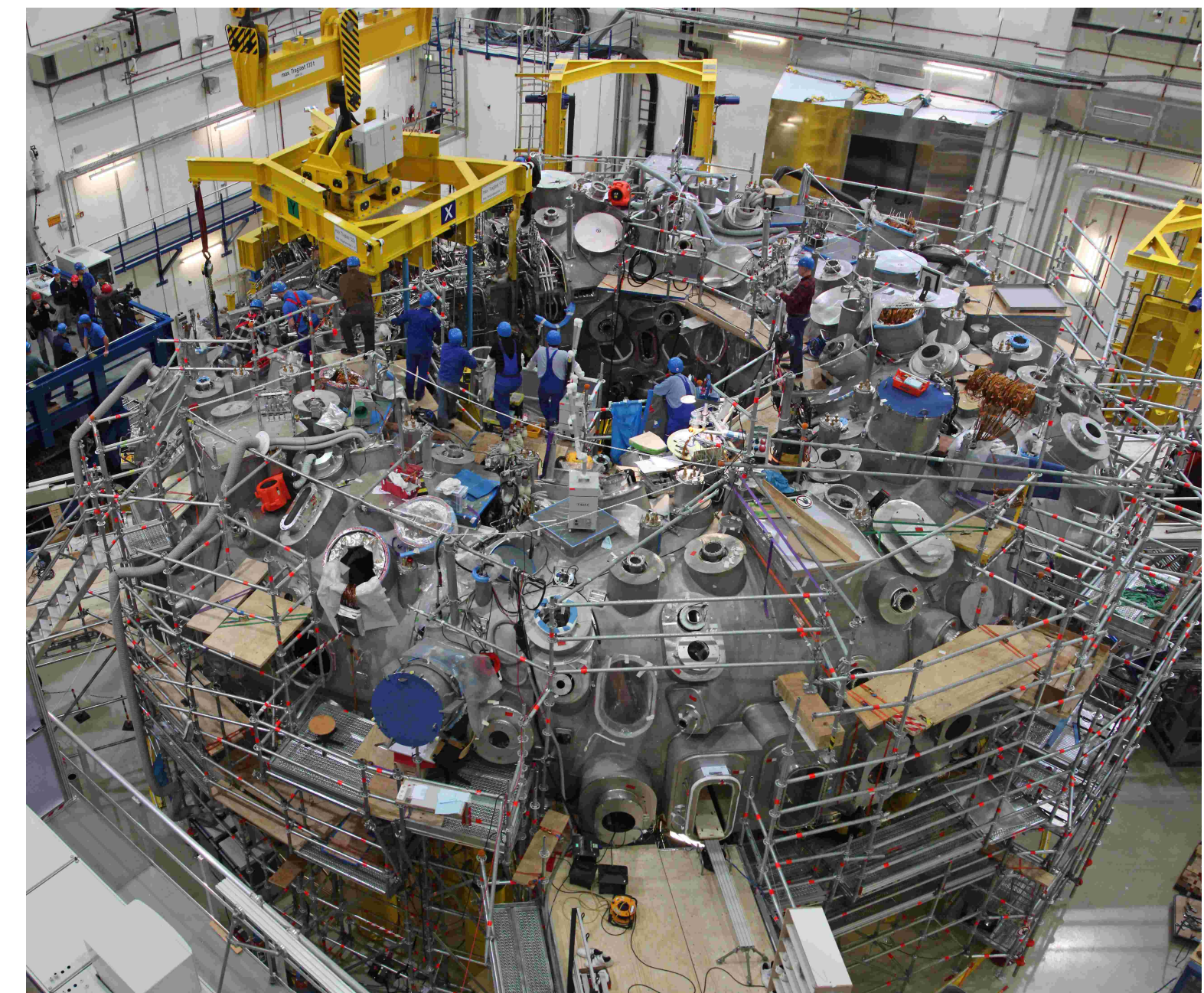
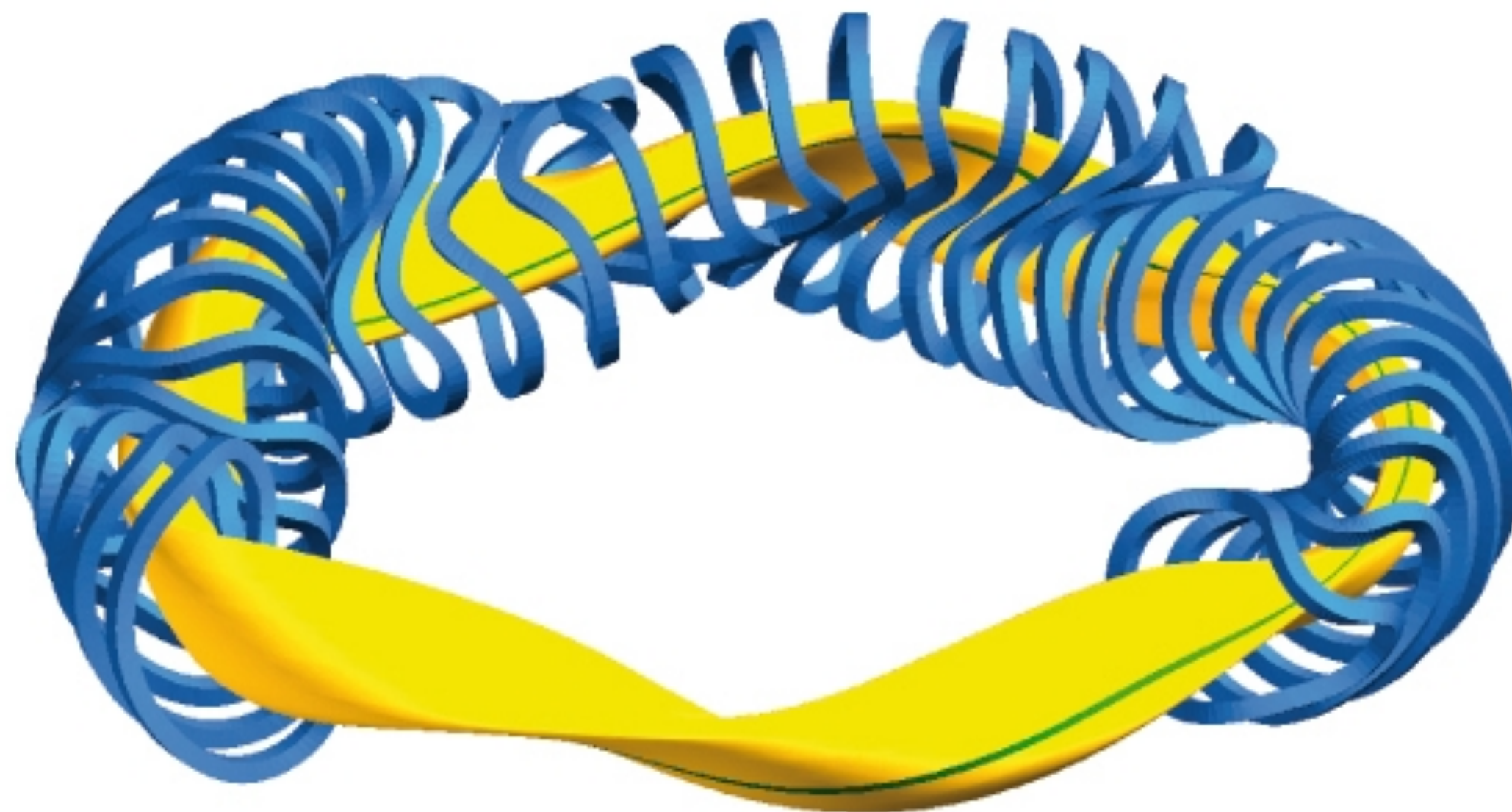
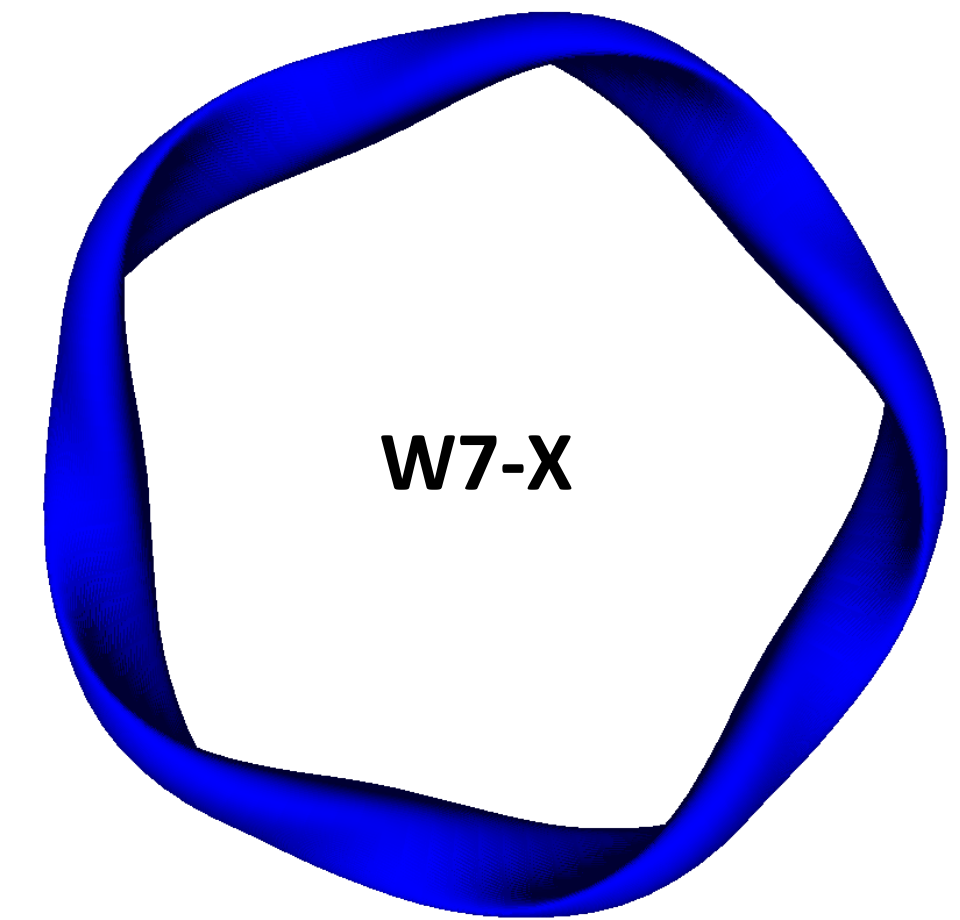
# Wendelstein 7-X (W7-X) stellarator

- W7-X is well optimised to avoid MHD activity.
- 5 field periods, major radius  $R=5.5$  m, minor radius  $r=0.53$  m.



# Wendelstein 7-X (W7-X) stellarator

- W7-X is well optimised to avoid MHD activity.
- 5 field periods, major radius  $R=5.5$  m, minor radius  $r=0.53$  m.
- Electron-cyclotron resonance heating (ECRH)  $\approx 10$  MW, largest one in the world.
- Normally, there is no toroidal current except for ECCD (electron-cyclotron-wave driven current) experiments and - at finite beta - the bootstrap current, which is a self-generated current driven by pressure and density gradients in the plasma, caused by the collisions between trapped and passing particles.

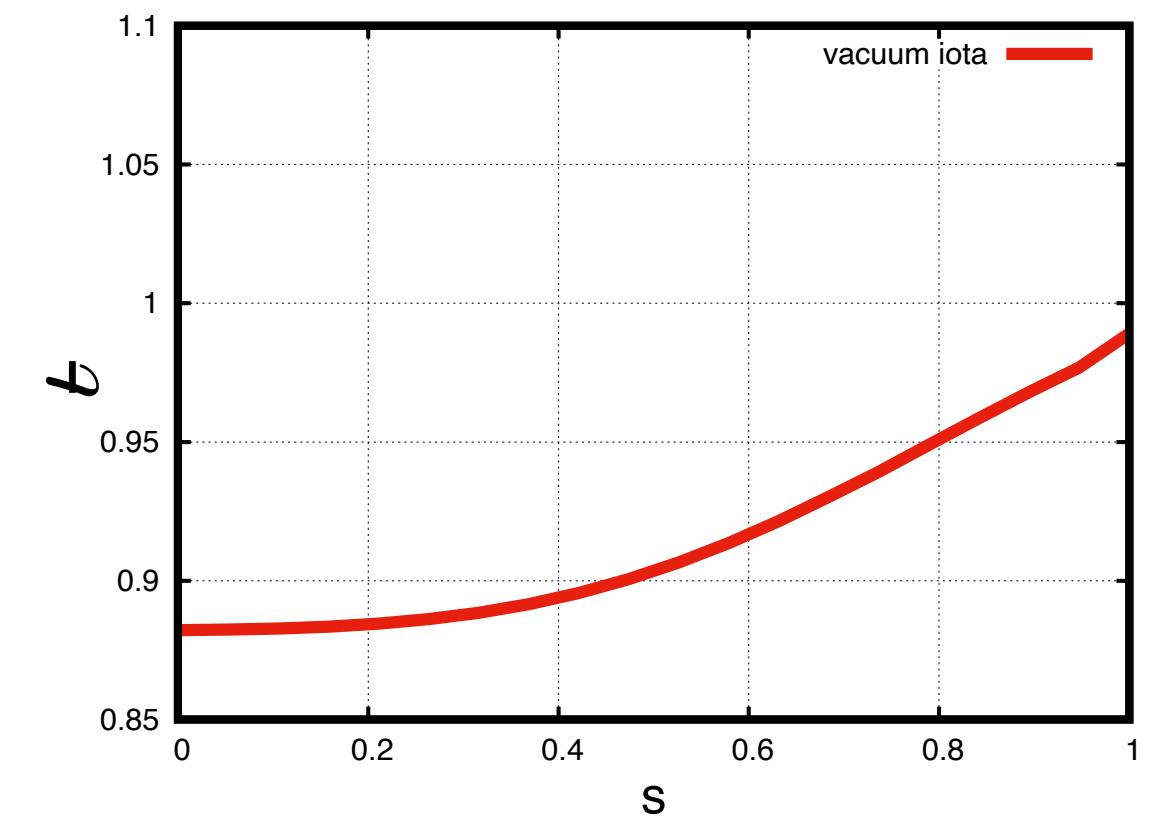


# Motivation



1. Rotational transform,  $t$  (if nested flux surfaces exist):  $t = \frac{d\psi}{d\phi}$  where  $\psi$  is the poloidal magnetic flux, and  $\phi$  the toroidal magnetic

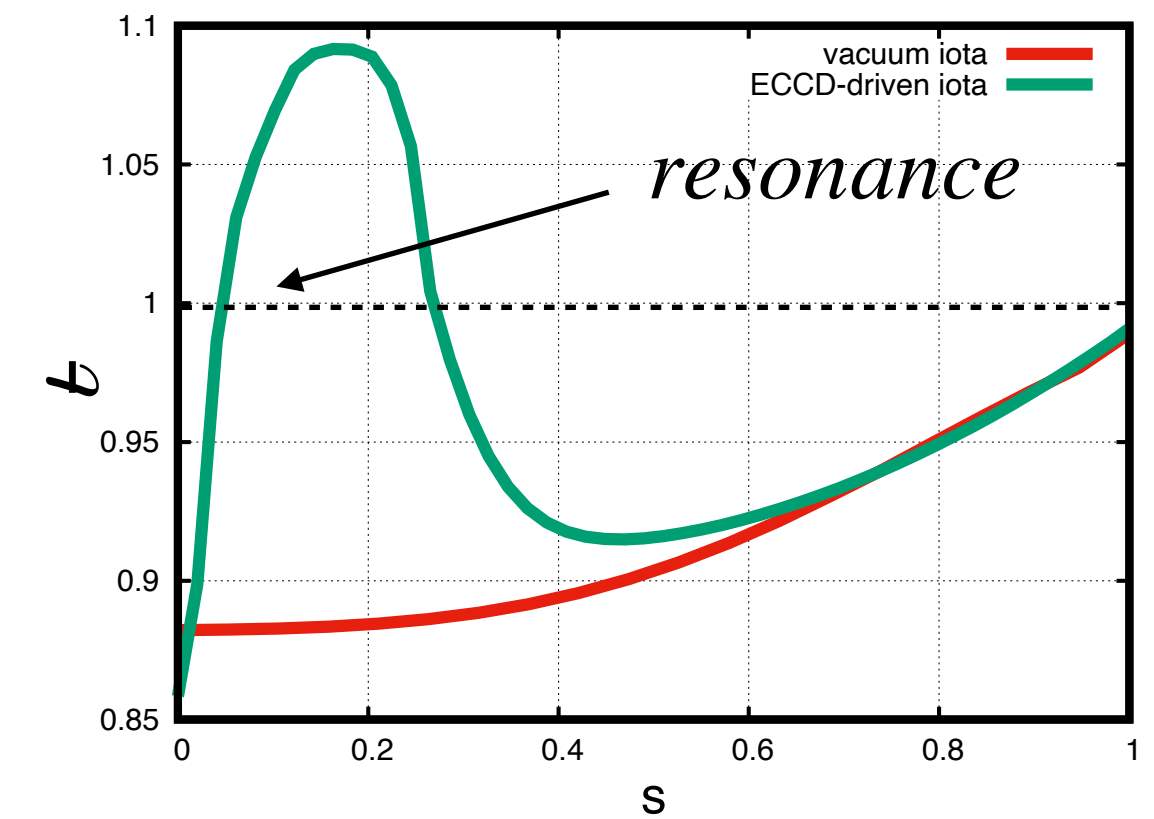
flux,  $s = \left(\frac{r_{eff}}{a}\right)^2$ . In W7-X, vacuum  $t$  has an almost flat radial profile and does not cross any major rational resonance.



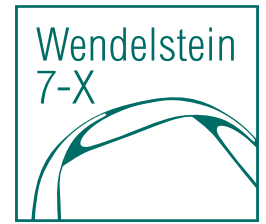
# Motivation



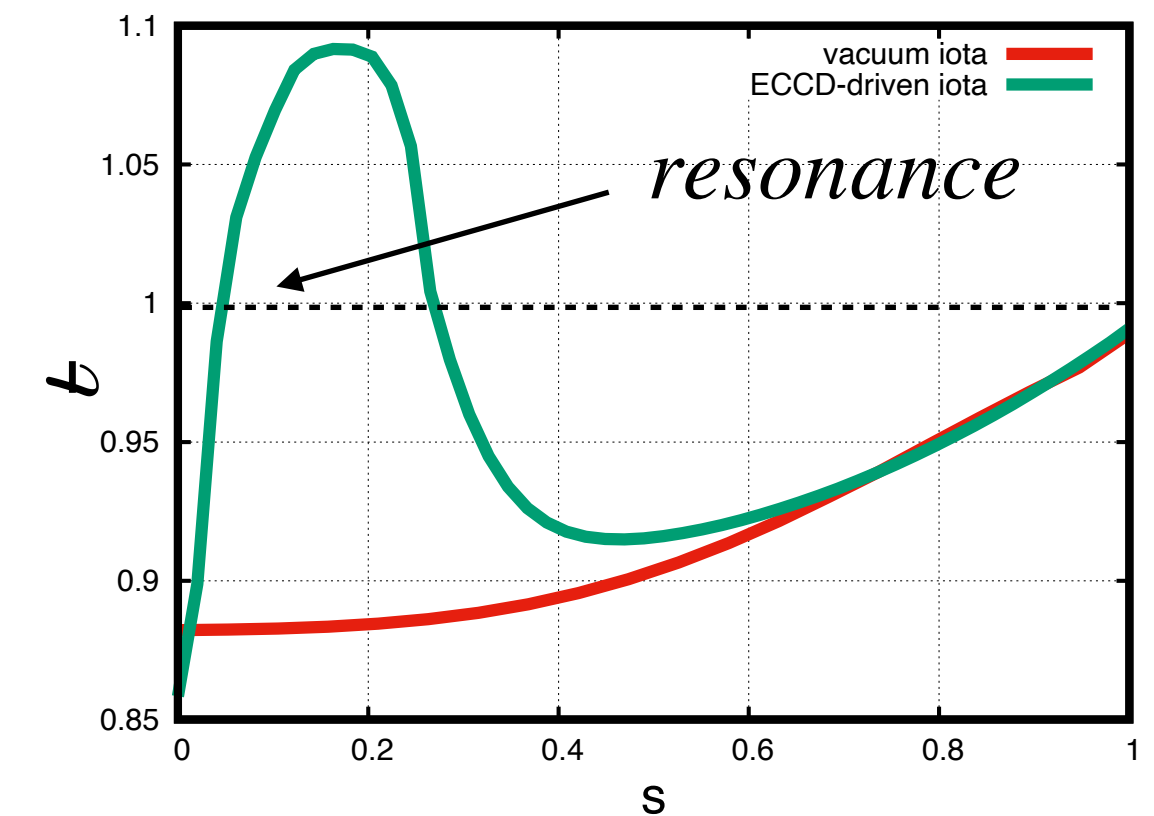
1. Rotational transform,  $t$  (if nested flux surfaces exist):  $t = \frac{d\psi}{d\phi}$  where  $\psi$  is the poloidal magnetic flux, and  $\phi$  the toroidal magnetic flux,  $s = \left(\frac{r_{eff}}{a}\right)^2$ . In W7-X, vacuum  $t$  has an almost flat radial profile and does not cross any major rational resonance.
2. During plasma operation the  $t$  - profile can be varied by ECCD. The resulting current modifies the iota profile, which can lead to MHD-activity if passing major rational values.



# Motivation

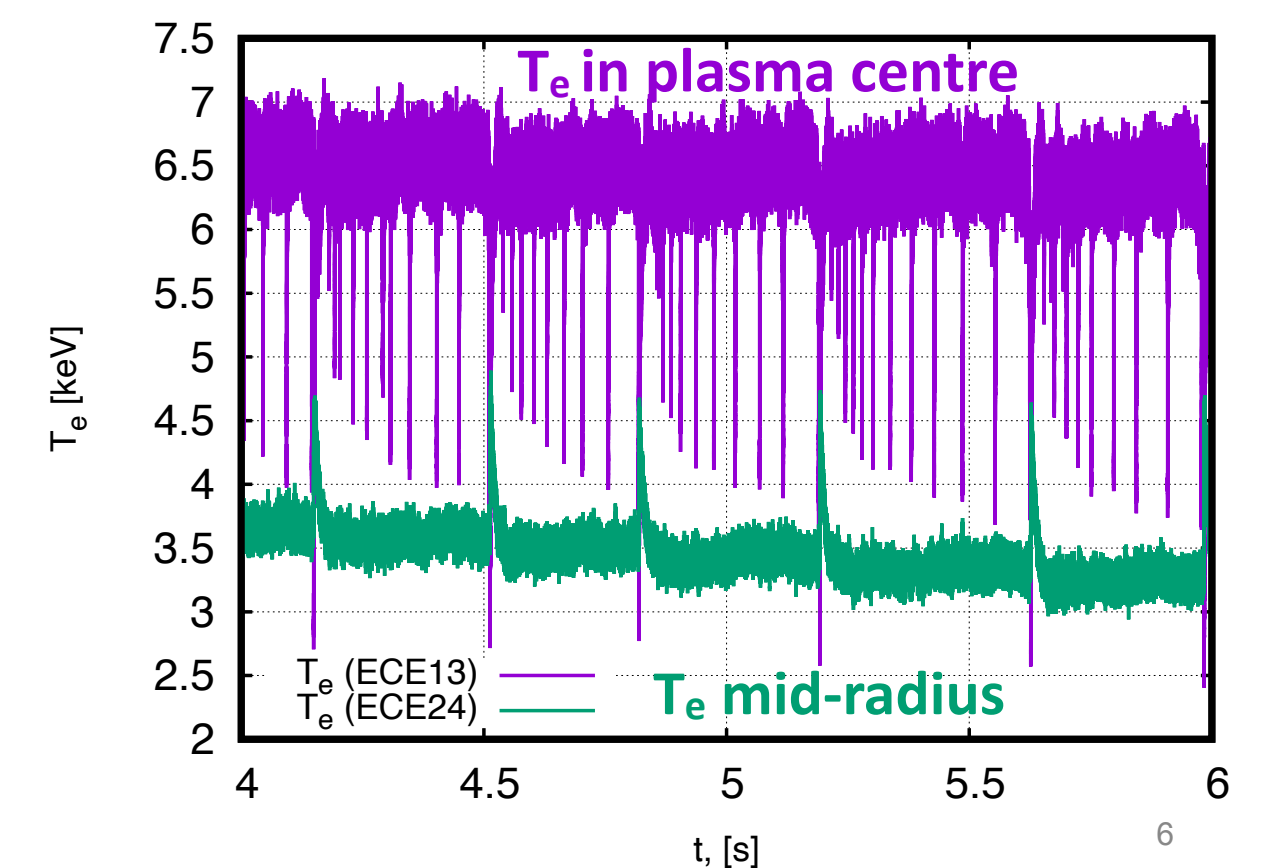


- Rotational transform,  $t$  (if nested flux surfaces exist):  $t = \frac{d\psi}{d\phi}$  where  $\psi$  is the poloidal magnetic flux, and  $\phi$  the toroidal magnetic flux,  $s = \left(\frac{r_{eff}}{a}\right)^2$ . In W7-X, vacuum  $t$  has an almost flat radial profile and does not cross any major rational resonance.
- During plasma operation the  $t$  - profile can be varied by ECCD. The resulting current modifies the iota profile, which can lead to MHD-activity if passing major rational values.
- In W7-X discharges with ECCD, phenomena reminiscent of tokamak “sawtooth” instabilities are observed: **medium-sized and small crashes**. There are also examples of discharges where related events lead to termination of the entire plasma.



The question addressed in this work is what happens to the plasma as a result of these instabilities?

Do we have sufficiently accurate and/or fast tools to predict the evolution of the plasma under these conditions?



## 1. Simplified tool to assess the signature features of crash cycles in W7-X:

- Two type of crashes will be considered: medium and small ones. Two types of crashes will be considered: medium and small.

## 2. Non-linear resistive MHD to assess specific mode dynamics:

- The focus will remain on medium-sized crashes.

## 1. Simplified tool to assess the signature features of crash cycles in W7-X:

- Two type of crashes will be considered: medium and small ones. Two types of crashes will be considered: medium and small.

## 2. Non-linear resistive MHD to assess specific mode dynamics:

- The focus will remain on medium-sized crashes.

# Conservation of helical flux in relaxations

Several models for sawtooth crashes:

Taylor (1975), Kadomtsev (1975), Bhattacharjee (1980&1982,) Waelbroeck (1989), Porcelli (1996).

Helical flux,  $\chi = \psi/l_r - \phi$ , reorganisation (a.k.a. Kadomtsev) model: dominant mode helical flux is conserved while the flux profile becomes monotonic.

- plasma volume conservation

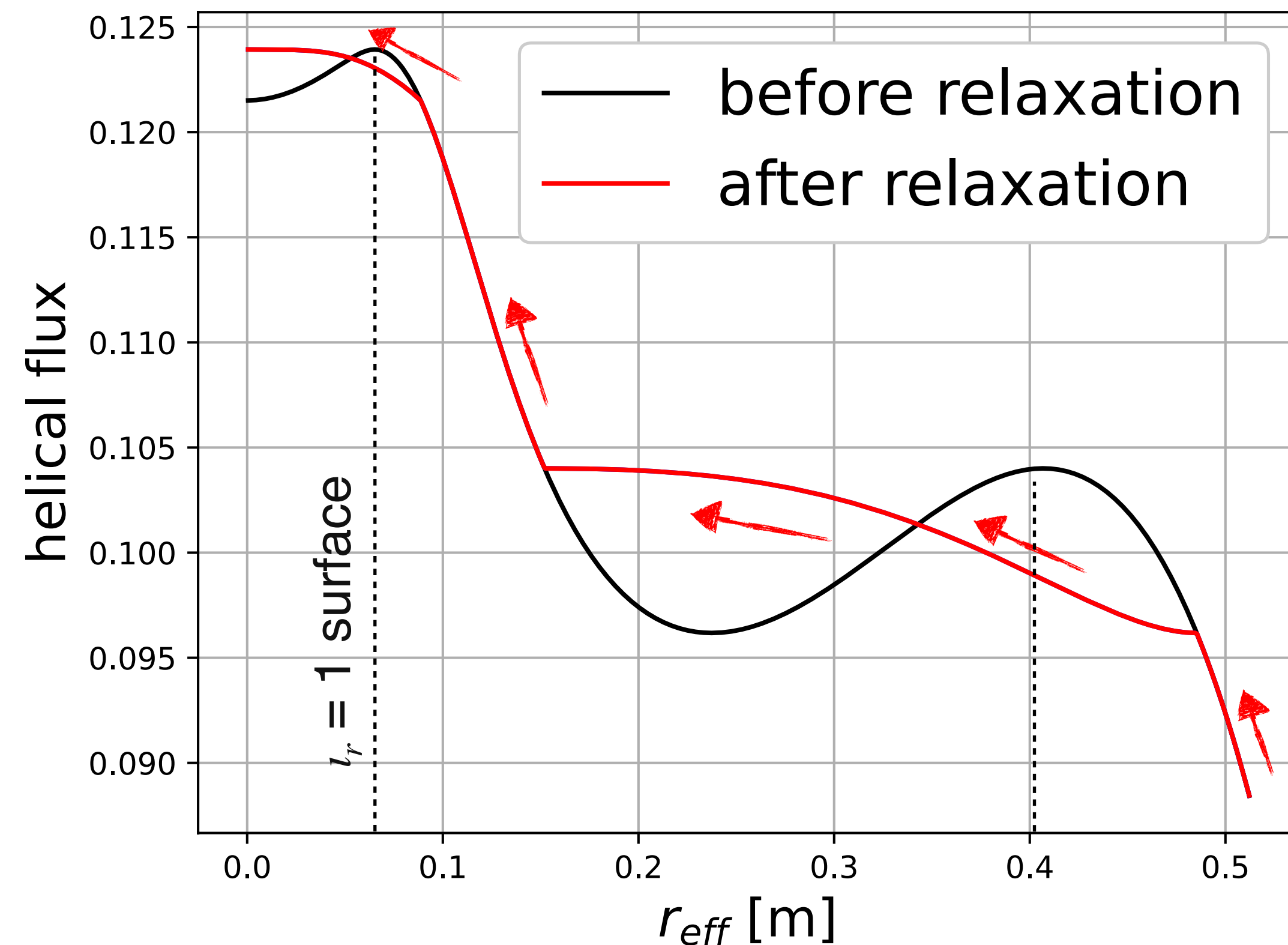
$$rdr = r_1 dr_1 + r_2 dr_2$$

- reconnected helical flux

$$d\chi_\infty = d\chi_1 = d\chi_2$$

- lower magnetic energy state

- current sheets



# Flux diffusion model with relaxations

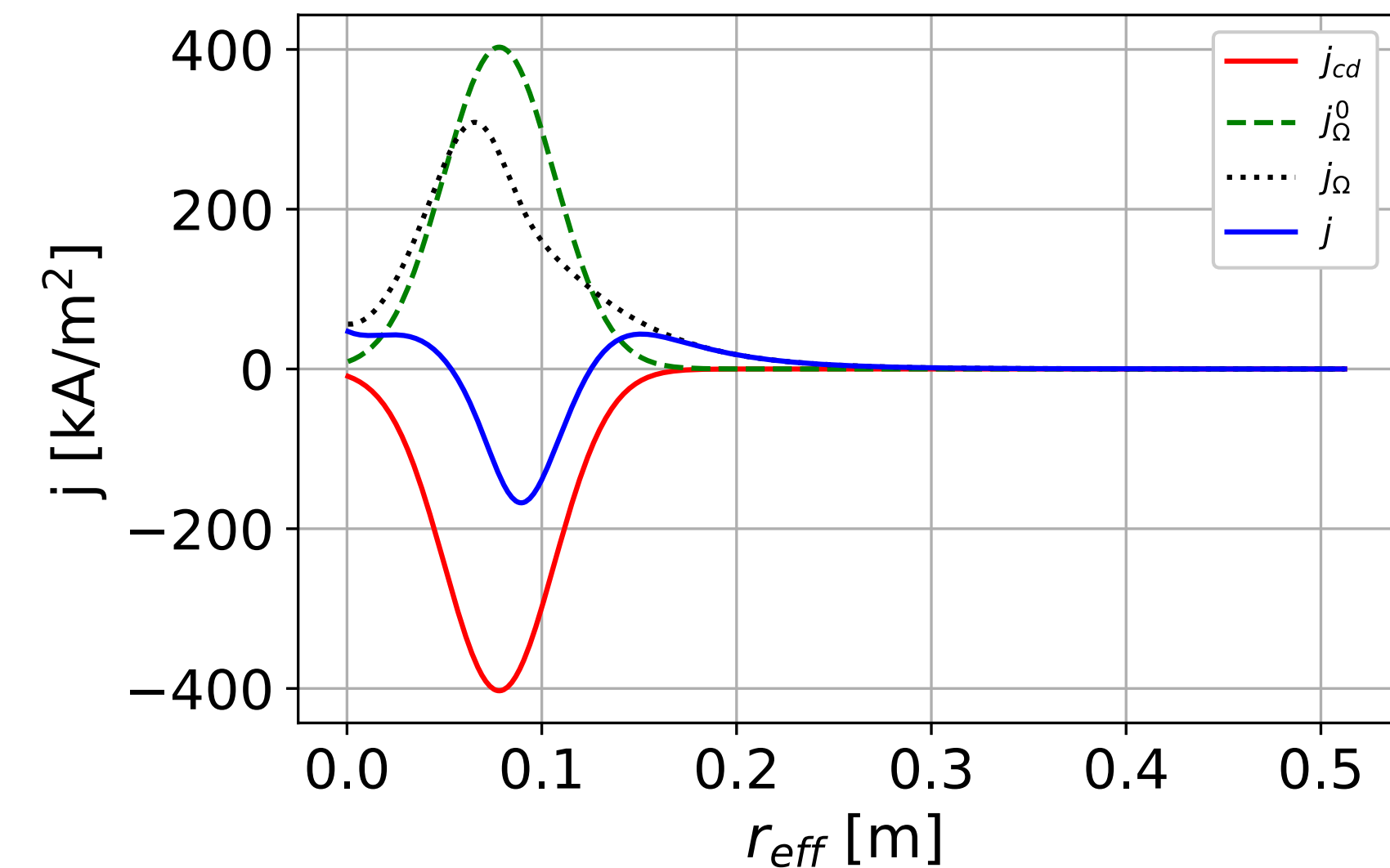
Following Strand & Houlberg (2001), we write the evolution equation for the poloidal flux  $\psi$ :

$$\sigma_{\parallel} \frac{\partial \psi}{\partial t} = \frac{J^2 R_0}{\mu_0 \rho} \frac{\partial}{\partial \rho} \frac{S_{11}}{J} \frac{\partial \psi}{\partial \rho} - \frac{V'}{2\pi \rho} j_{CD},$$

Ohm's law for the toroidal current density:

$$j(r, t) = \sigma_{\parallel} E(r, t) + j_{CD}$$

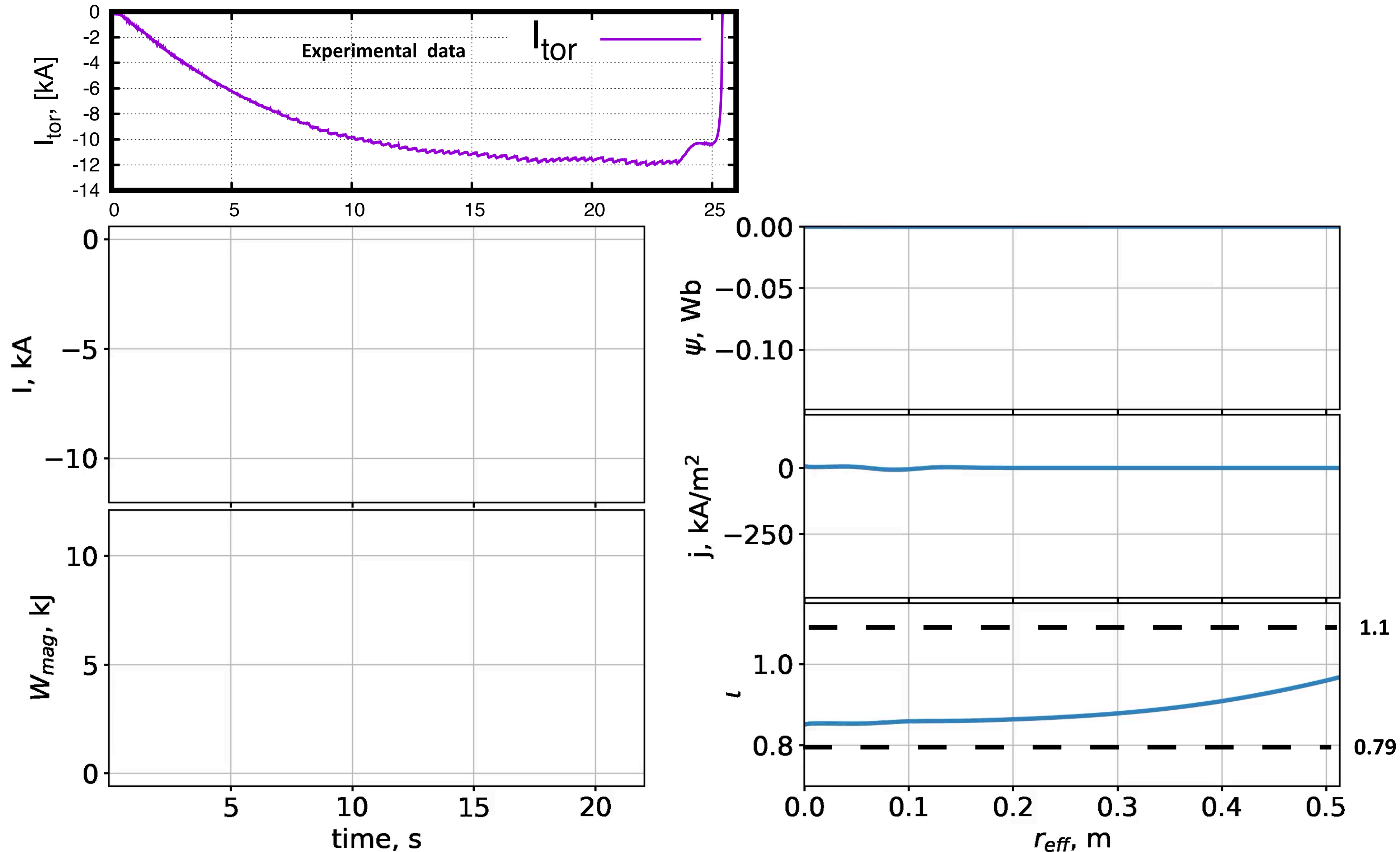
where  $\sigma_{\parallel}$  is the parallel conductivity,  $\mu_0$  is the permeability constant,  $r$  and  $R_0$  are minor and major plasma radius.



Once  $\iota$  reaches “instability”-target value  $\iota_{relax}$  (in this case:  $\iota_{relax} > 1$  or  $\iota_{relax} < 5/6$ ), flux reorganisation is triggered. Then diffusive evolution of the post-crash flux profile is calculated until the  $\iota_{relax}$  is reached again [1].

[1] Aleynikova, Hudson, Helander, et al. 61(12) (2021): 126040.

# Application of the model (XP20171206.025)

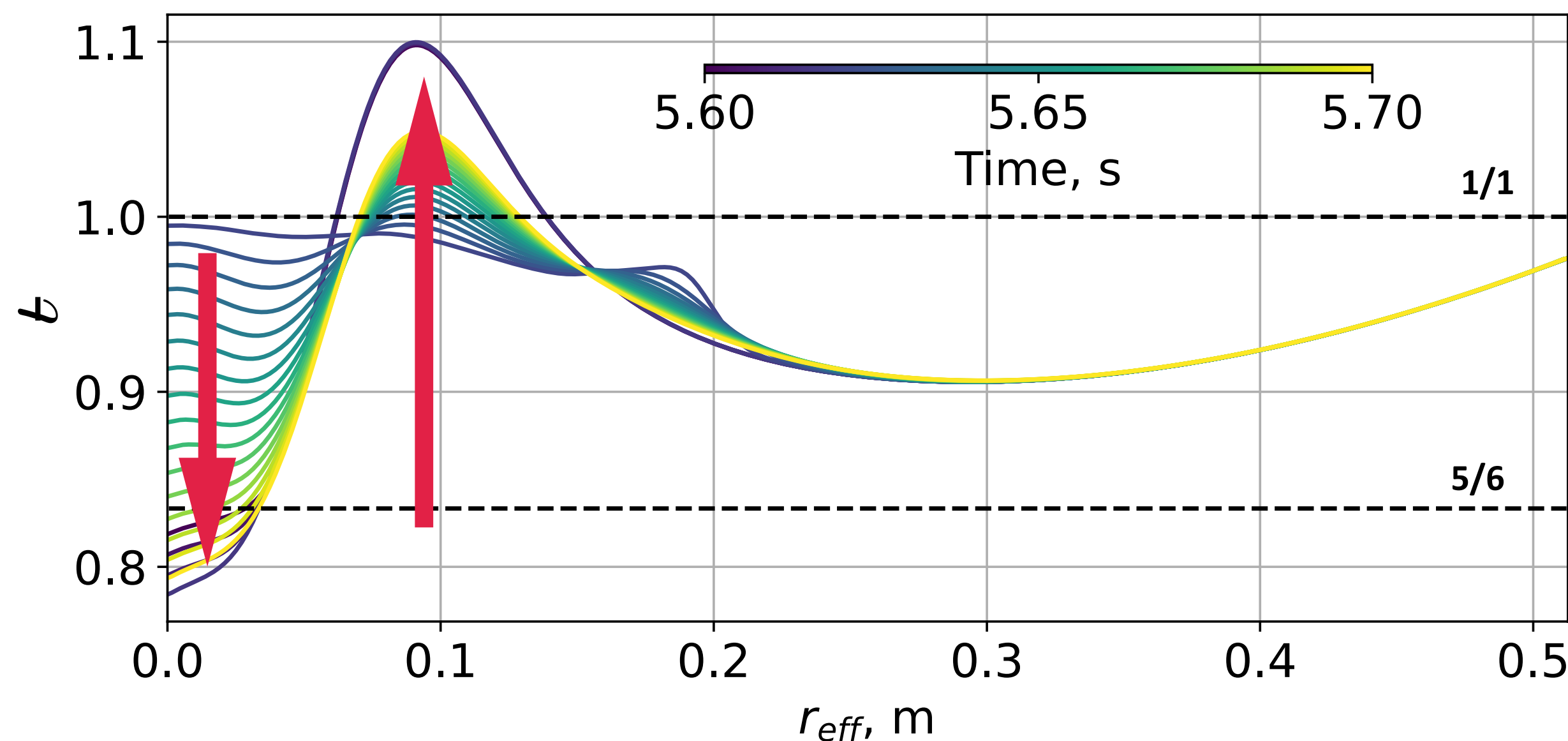


Free parameter of the modelling:

$$l_{relax 1} = 1.1$$

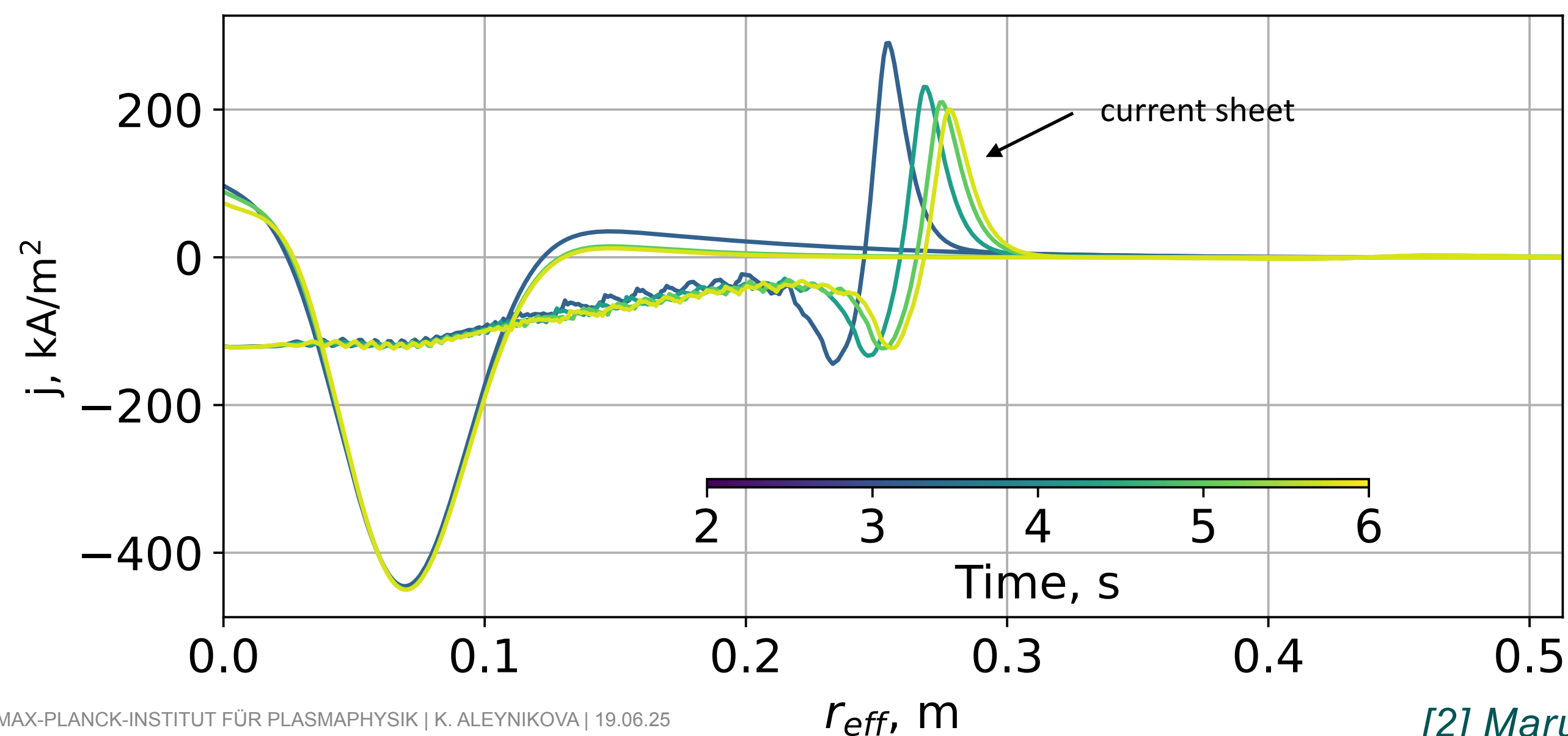
$$l_{relax 5/6} = 0.79$$

# Application of the model (XP20171206.025)



In the beginning of the experiment 14 kA ECCD is applied around  $r_{eff} \approx 0.08\text{m}$ .

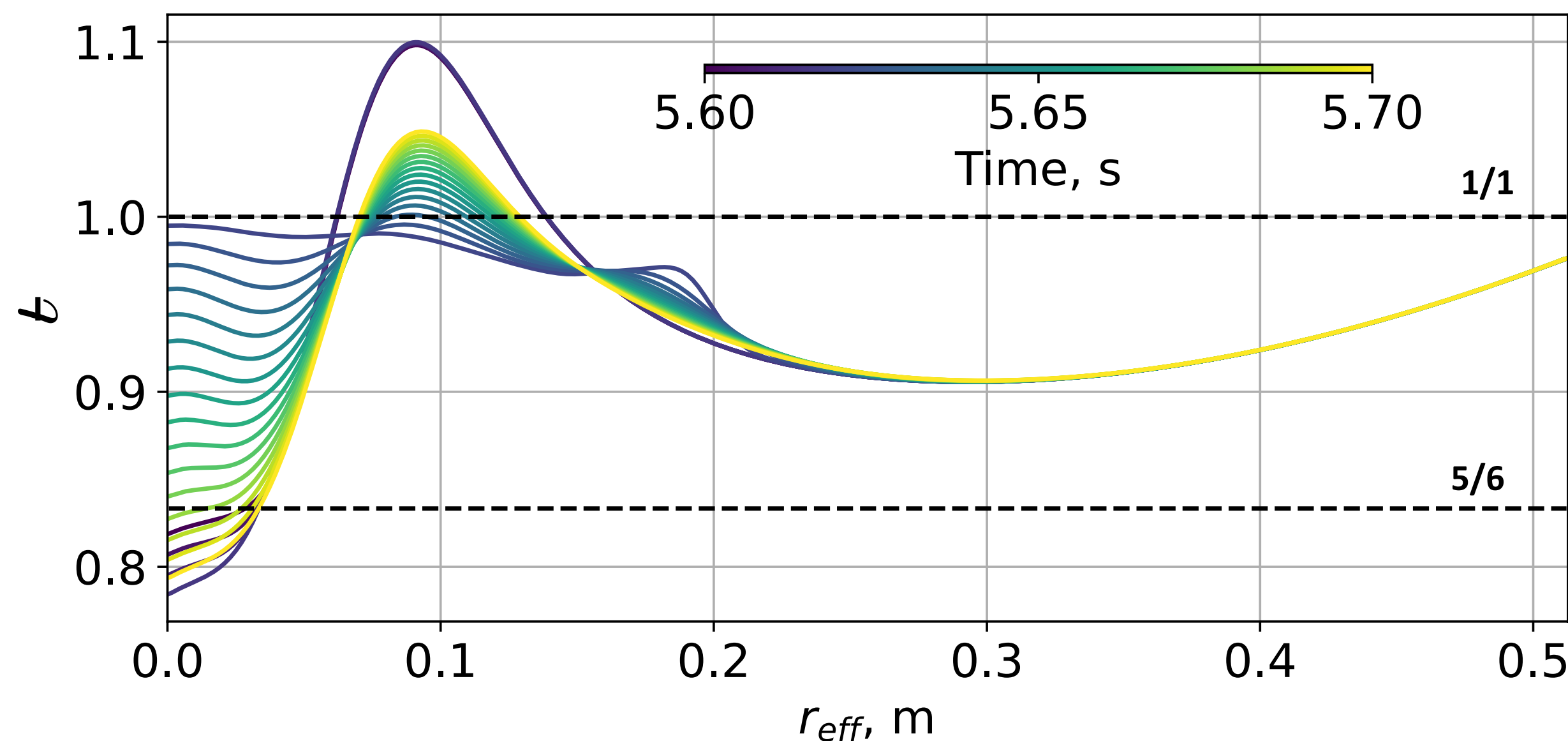
The ECCD current density has been calculated with the Travis ray-tracing code [2].



The plasma current and iota evolution is calculated from the flux diffusion equation with relaxations.

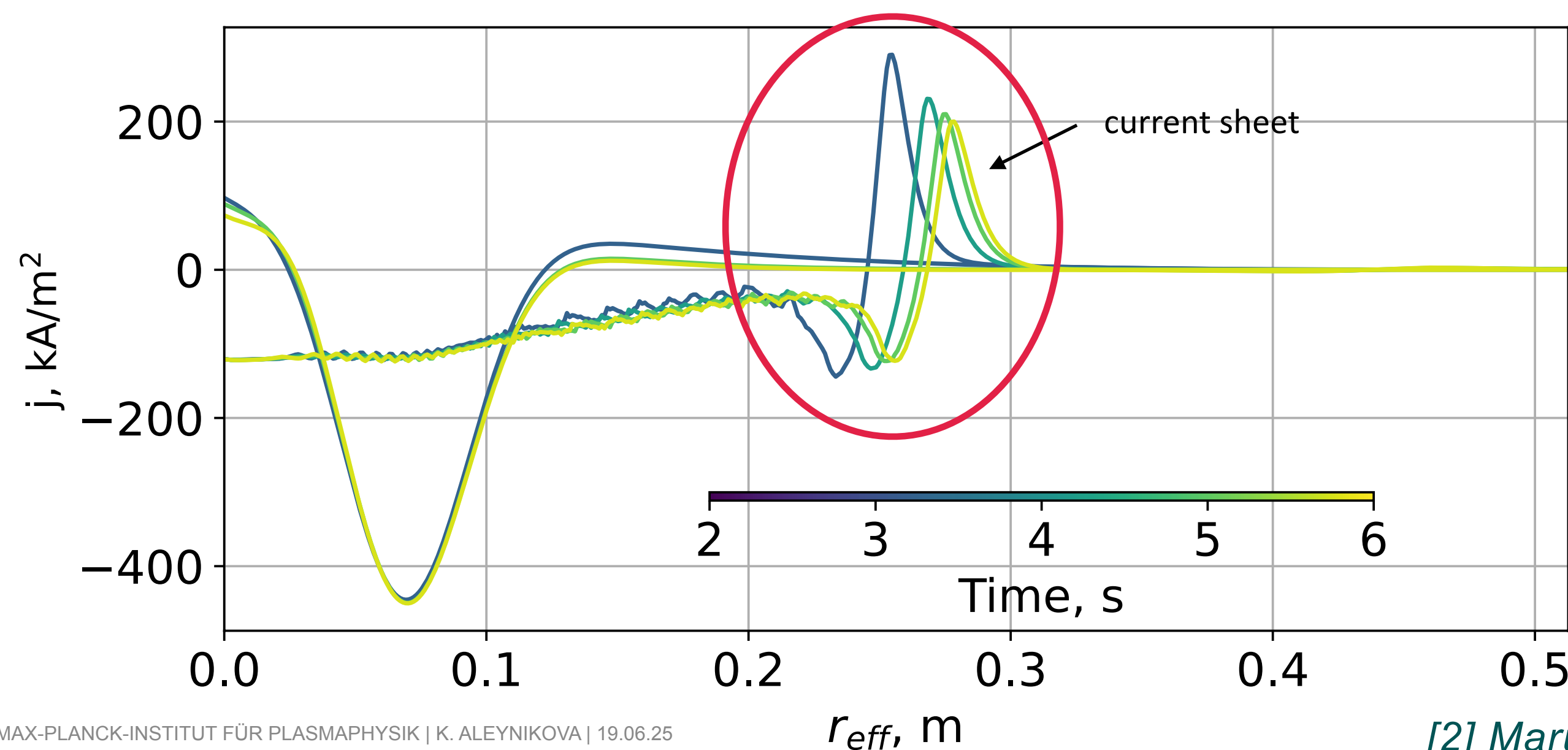
Time evolution is colour-coded.

# Application of the model (XP20171206.025)



In the beginning of the experiment 14 kA ECCD is applied around  $r_{eff} \approx 0.08\text{m}$ .

The ECCD current density has been calculated with the Travis ray-tracing code [\*].

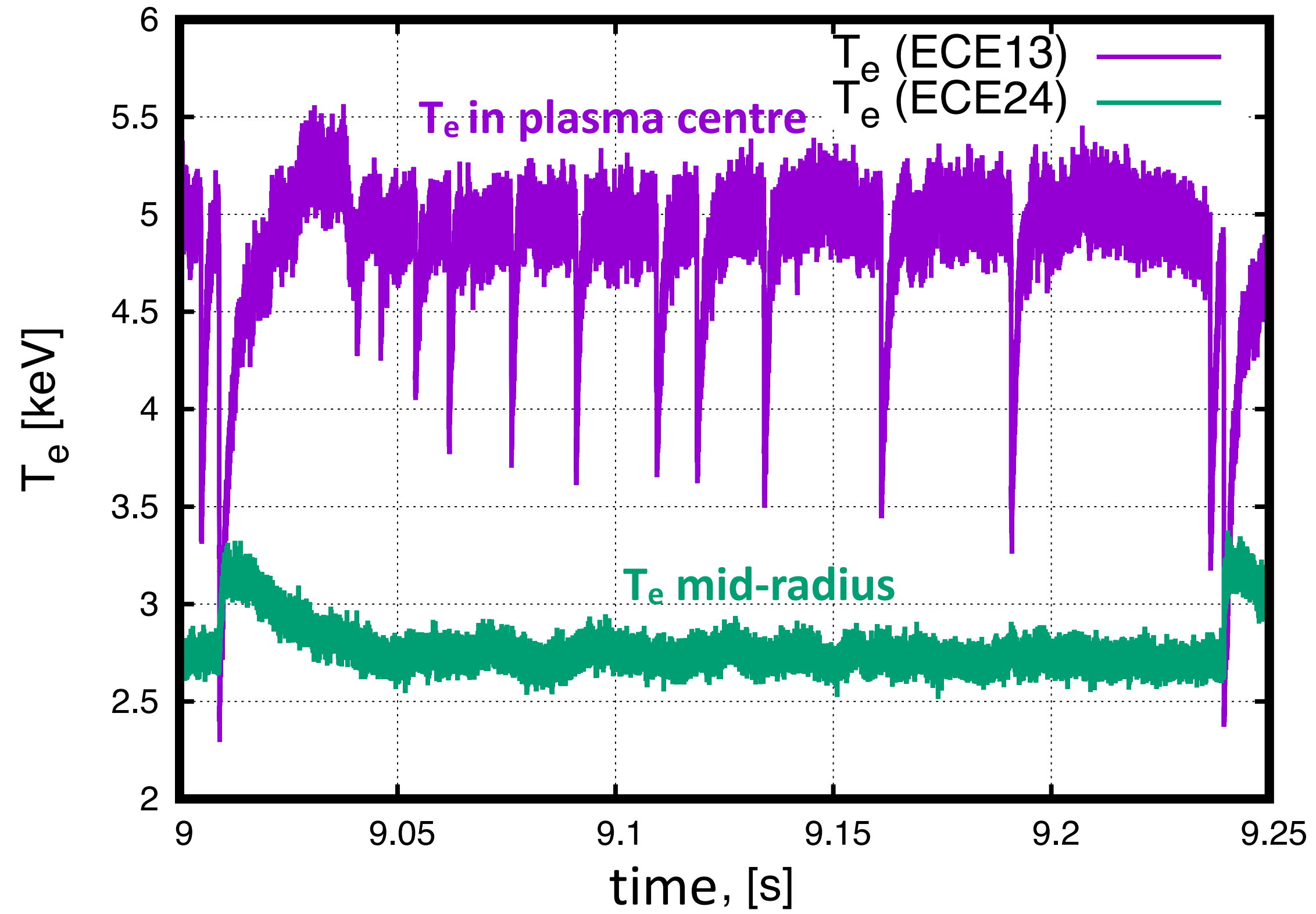


The plasma current and iota evolution is calculated from the flux diffusion equation with relaxations.

Time evolution is colour-coded.

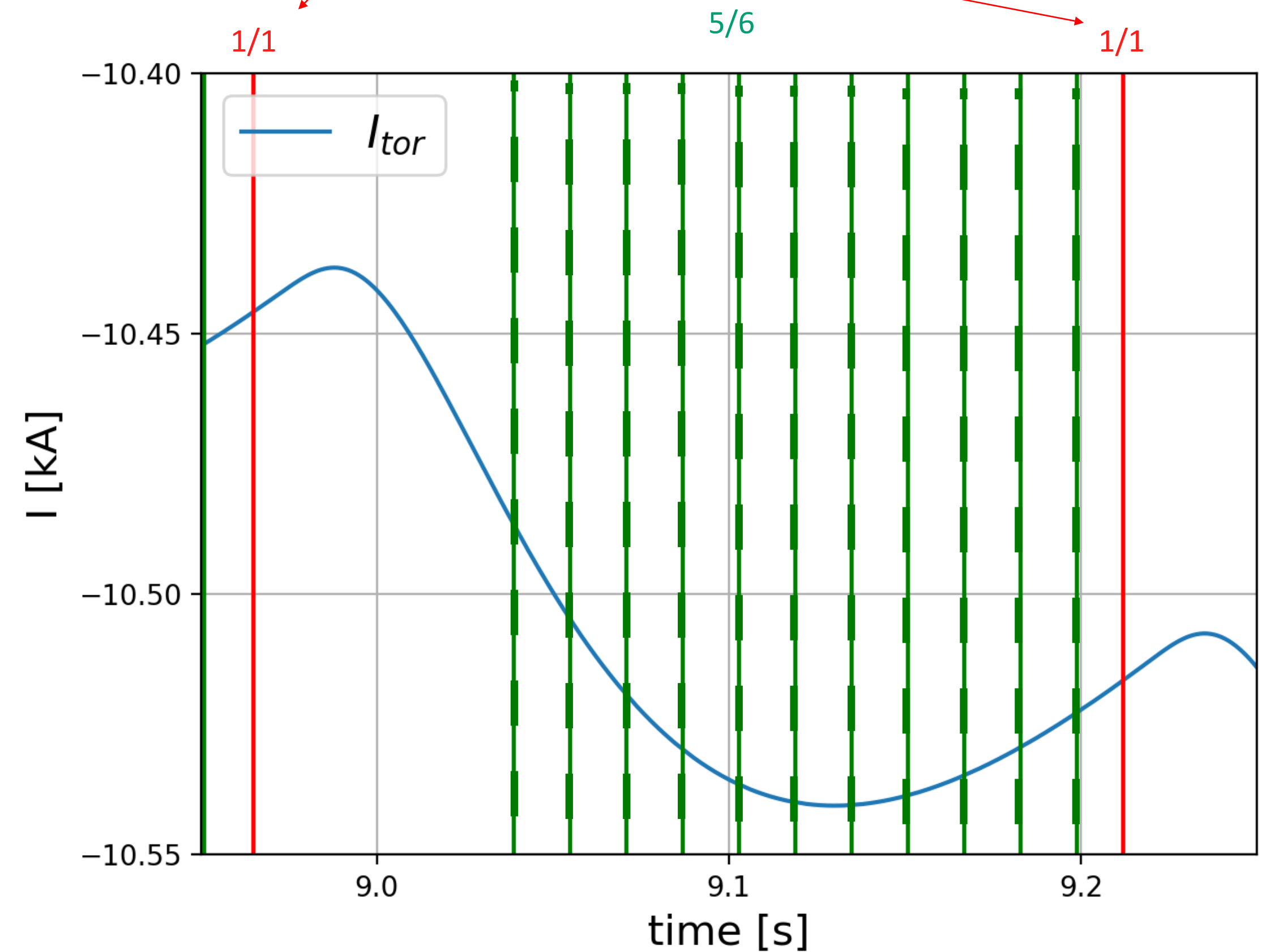
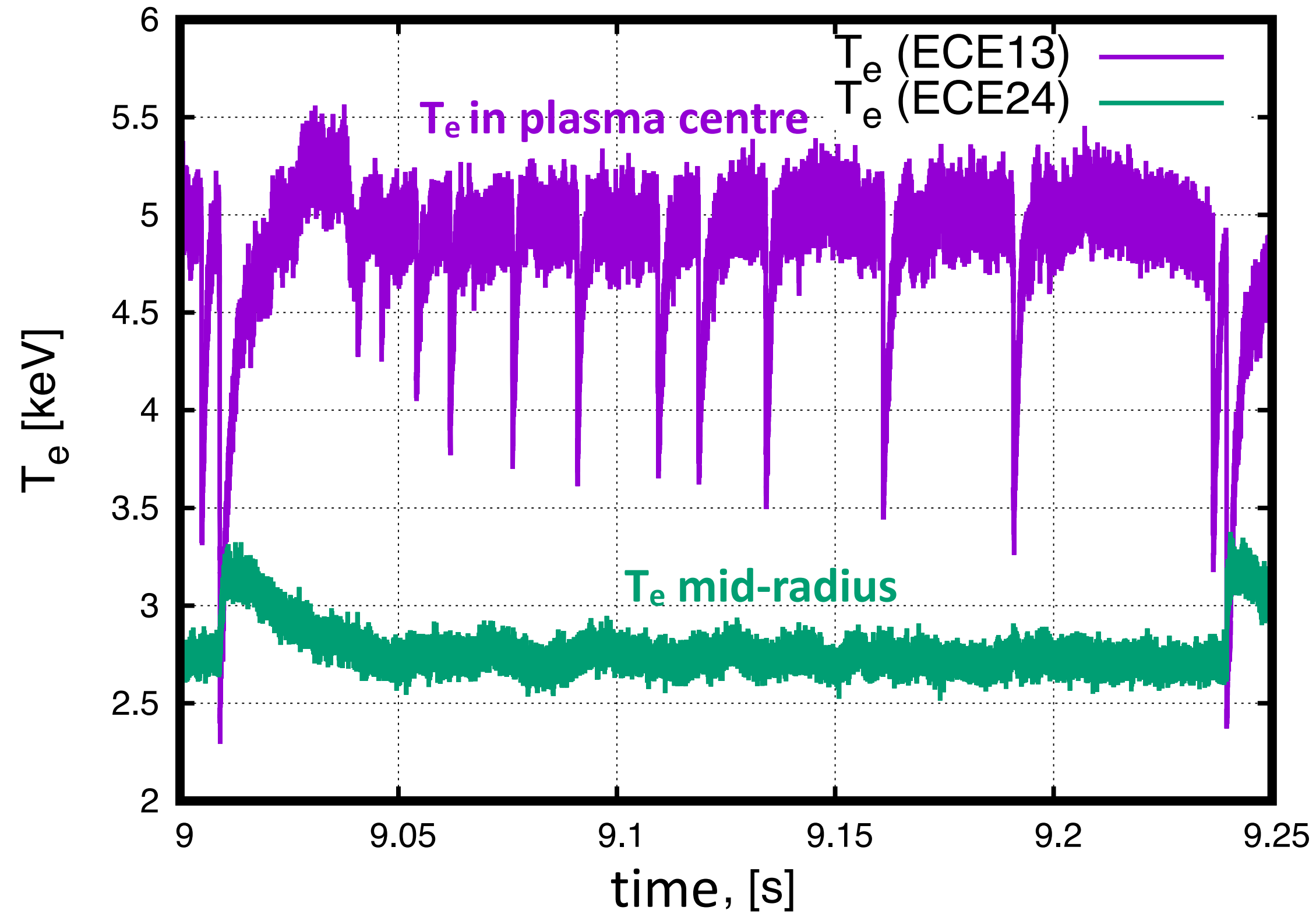
Mixing area is getting larger.

# Application of the model (XP20171206.025)



# Application of the model (XP20171206.025)

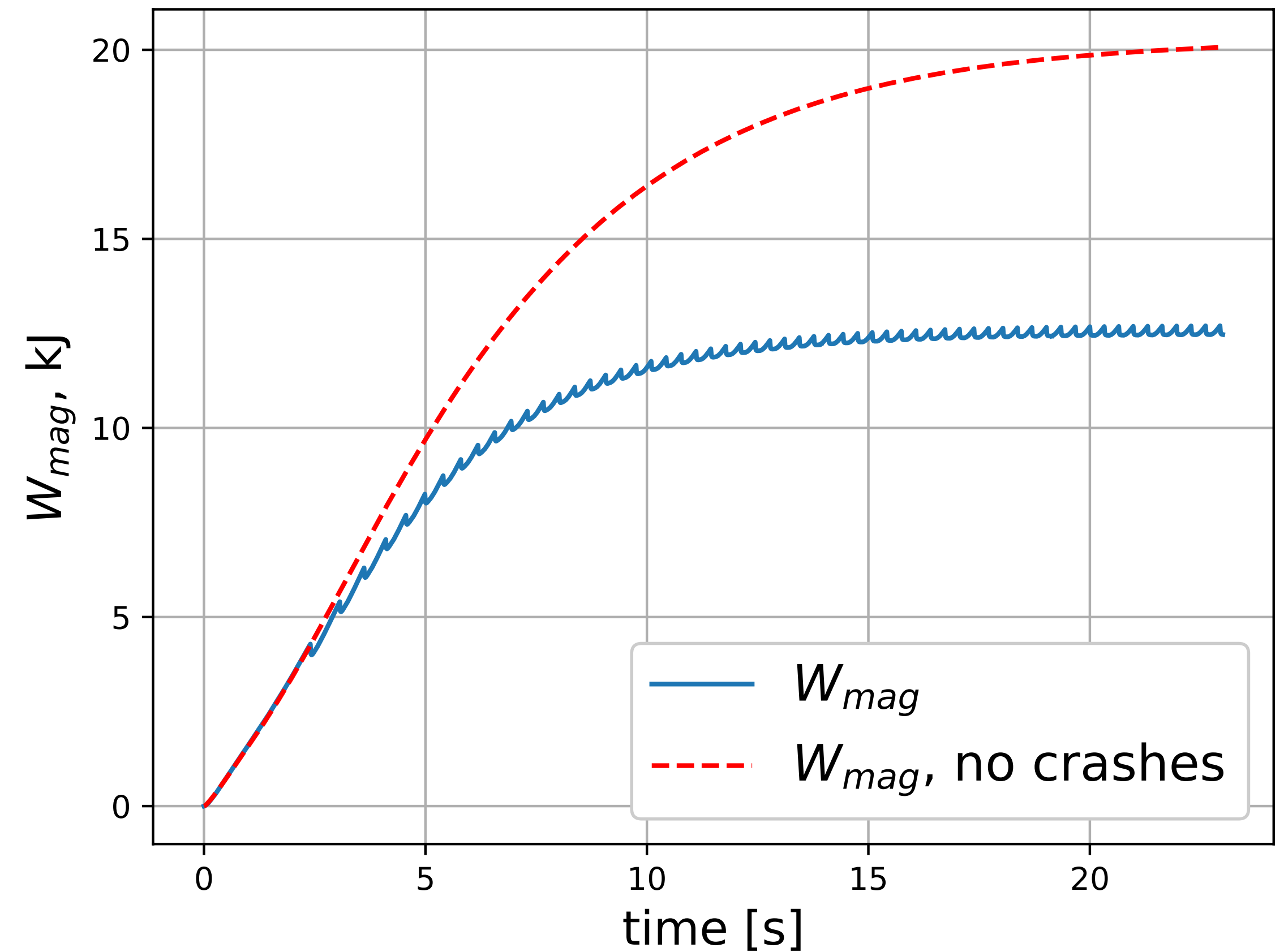
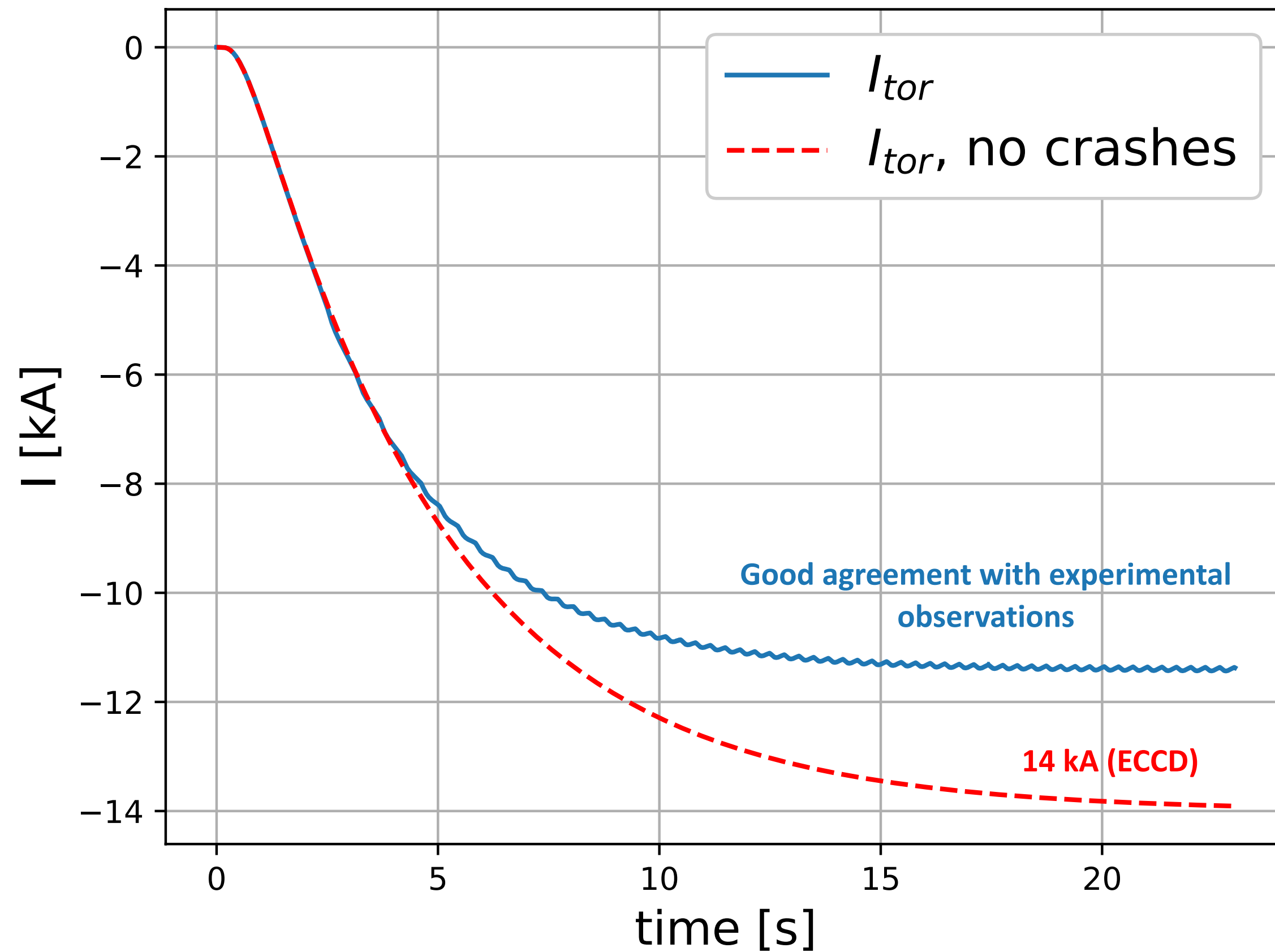
Two type of crashes: associated with  $\ell=1$  resonant surface and  $\ell=5/6$ .



The shape is due to resistive evolution of the current sheet

5/6 resonance (not only 1/1) is important.

# Current saturation with and without crashes (XP20171206.025)



Toroidal current saturates at a lower value due to continuous magnetic energy dissipation via MHD crashes.

## 1. Simplified tool to assess the signature features of crash cycles in W7-X:

- Two type of crashes will be considered: medium and small ones. Two types of crashes will be considered: medium and small.

## 2. Non-linear resistive MHD to assess specific mode dynamics:

- The focus will remain on medium-sized crashes.

# JOREK, stellarator geometry



- JOREK [3] is a finite element nonlinear MHD code.
- For the stellarator extension [4], the grid becomes  $\phi$ -dependent.
- The physics model is reduced MHD, single and two-temperature ( $T_i$  and  $T_e$ ) models are available.  $v_{par}$  was recently implemented [5] however is not used in these calculations.

## REDUCED MHD

$$\vec{B} = \nabla\chi + \nabla\Psi \times \nabla\chi + \nabla\Omega \times \nabla\psi_v,$$

$$\vec{v} = \frac{\nabla\Phi \times \nabla\chi}{B_v^2} + v_{||}\vec{B} + \nabla^\perp\zeta.$$

### Equations which are solved:

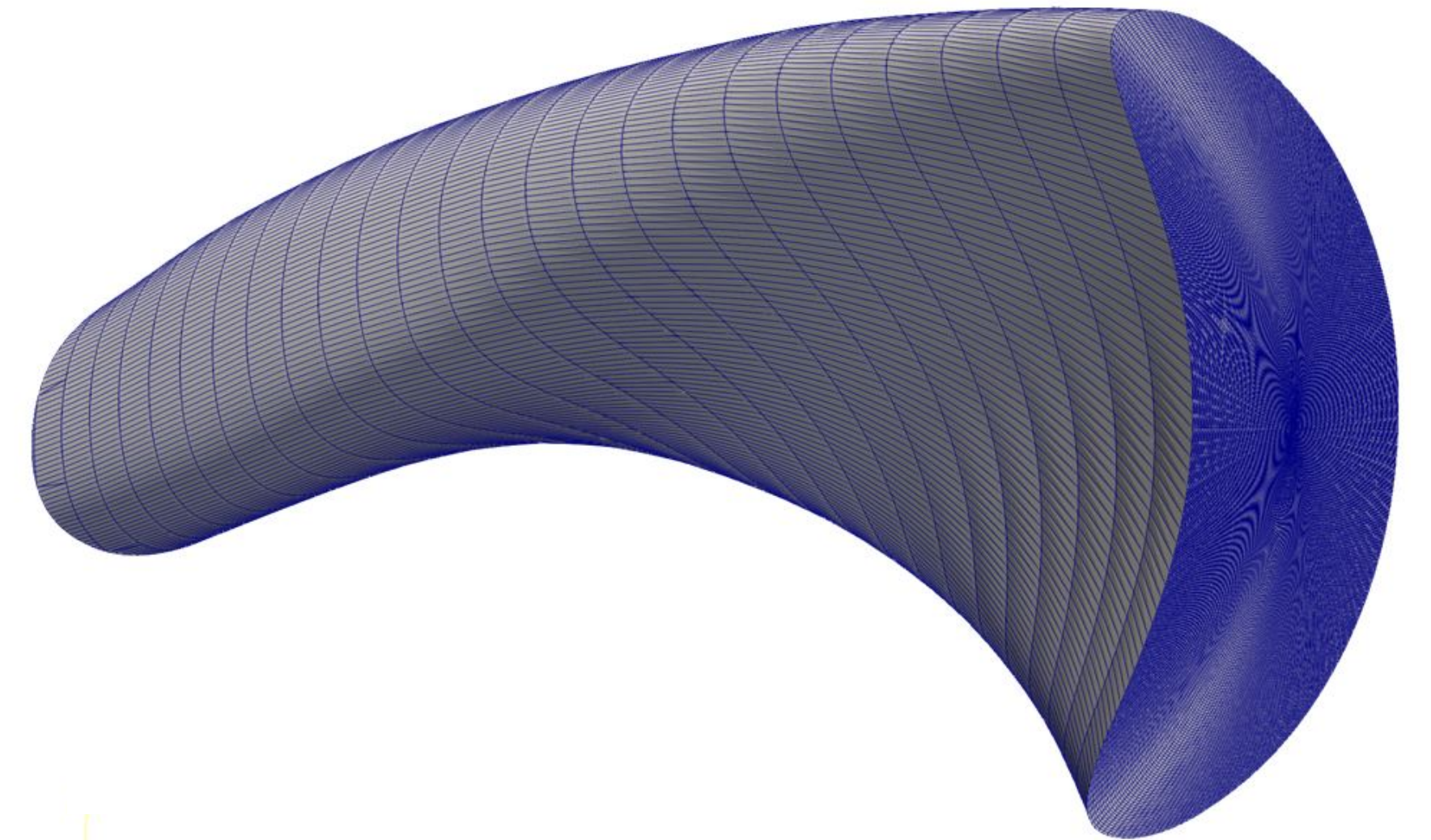
$$\frac{\partial\rho}{\partial t} = -B_v \left[ \frac{\rho}{B_v^2}, \Phi \right] + P,$$

$$\nabla \cdot \left( \frac{\rho}{B_v^2} \nabla^\perp \frac{\partial\Phi}{\partial t} \right) = \frac{B_v}{2} \left[ \frac{\rho}{B_v^2}, \frac{(\Phi, \Phi)}{B_v^2} \right] + B_v \left[ \frac{\rho\omega}{B_v^4}, \Phi \right] - \nabla \cdot \left( \frac{P}{B_v^2} \nabla^\perp \Phi \right) + \nabla \cdot (j\mathbf{B}) + B_v \left[ \frac{1}{B_v^2}, p \right] + \nabla \cdot (\mu_\perp \nabla^\perp \omega) - \Delta^\perp (\mu_{num} \Delta^\perp \omega),$$

$$\rho \frac{\partial T}{\partial t} = -\frac{1}{B_v} [\rho T, \Phi] - \gamma \rho T B_v \left[ \frac{1}{B_v^2}, \Phi \right] + \nabla \cdot \left[ \kappa_\perp \nabla_\perp T + \kappa_\parallel \nabla_\parallel \nabla_\parallel T + \frac{pD_\perp}{\rho} \nabla_\perp \rho + \frac{pD_\parallel}{\rho} \nabla_\parallel \rho \right] + (S_e + \eta_{Ohm} B_v^2 j^2) - T \frac{\partial\rho}{\partial t},$$

$$\frac{\partial\psi}{\partial t} = \frac{\partial^\parallel \Phi - [\Psi, \Phi]}{B_v} - \eta (j - j_{source}) + \nabla \cdot (\eta_{num} \nabla^\perp j),$$

where  $P = \nabla \cdot (D_\perp \nabla_\perp \rho + D_\parallel \nabla_\parallel \rho) + S_\rho$ ,  $j$  and the plasma vorticity,  $\omega$ , are given by  $j = \Delta^* \Psi$  and  $\omega = \Delta^\perp \Phi$ .

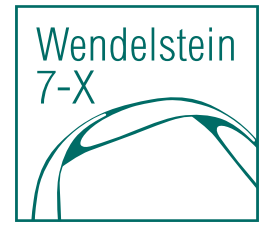


[3] G. Huysmans, et al, Nucl. Fusion 47, 659, 2007.

[4] N. Nikulsin et al., Physics of Plasmas 29, 063901, 2022.

[5] R. Ramasamy, et al. Nuclear Fusion, 64 086030, 2024.

# JOREK, stellarator geometry



- JOREK [3] is a finite element nonlinear MHD code.
- For the stellarator extension [4], the grid becomes  $\phi$ -dependent.
- The physics model is reduced MHD, single and two-temperature ( $T_i$  and  $T_e$ ) models are available.  $v_{par}$  was recently implemented [5] however is not used in these calculations.

## REDUCED MHD

$$\vec{B} = \nabla\chi + \nabla\Psi \times \nabla\chi + \nabla\Omega \times \nabla\psi_v,$$

$$\vec{v} = \frac{\nabla\Phi \times \nabla\chi}{B_v^2} + v_{||}\vec{B} + \nabla^\perp\zeta.$$

### Equations which are solved:

$$\frac{\partial\rho}{\partial t} = -B_v \left[ \frac{\rho}{B_v^2}, \Phi \right] + P,$$

$$\nabla \cdot \left( \frac{\rho}{B_v^2} \nabla^\perp \frac{\partial\Phi}{\partial t} \right) = \frac{B_v}{2} \left[ \frac{\rho}{B_v^2}, \frac{(\Phi, \Phi)}{B_v^2} \right] + B_v \left[ \frac{\rho\omega}{B_v^4}, \Phi \right] - \nabla \cdot \left( \frac{P}{B_v^2} \nabla^\perp \Phi \right) + \nabla \cdot (j\mathbf{B}) + B_v \left[ \frac{1}{B_v^2}, p \right] + \nabla \cdot (\mu_\perp \nabla^\perp \omega) - \Delta^\perp (\mu_{num} \Delta^\perp \omega),$$

$$\rho \frac{\partial T}{\partial t} = -\frac{1}{B_v} [\rho T, \Phi] - \gamma \rho T B_v \left[ \frac{1}{B_v^2}, \Phi \right] + \nabla \cdot \left[ \kappa_\perp \nabla_\perp T + \kappa_\parallel \nabla_\parallel \nabla_\parallel T + \frac{pD_\perp}{\rho} \nabla_\perp \rho + \frac{pD_\parallel}{\rho} \nabla_\parallel \rho \right] + (S_e + \eta_{ohm} B_v^2 j^2) - T \frac{\partial\rho}{\partial t},$$

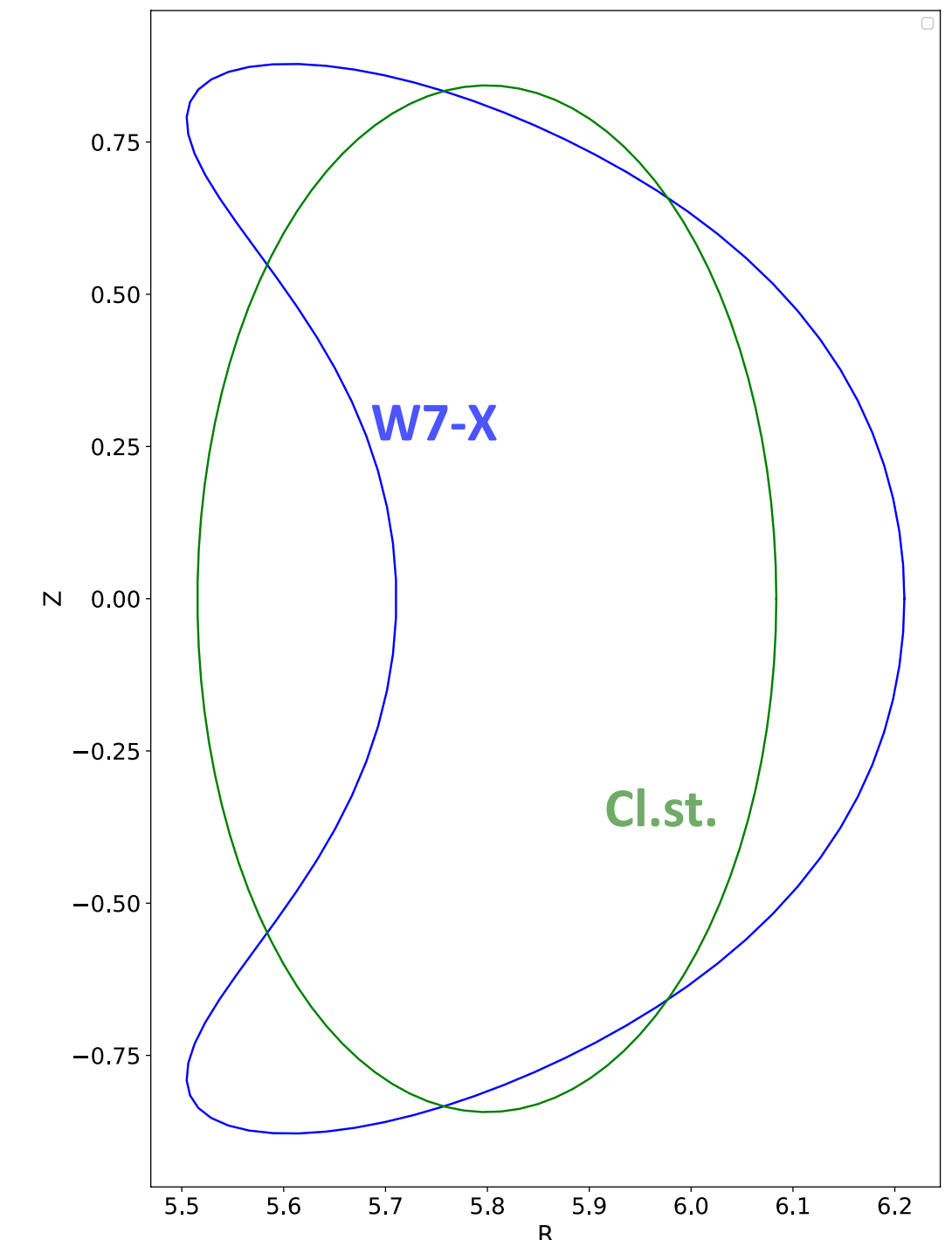
$$\frac{\partial\psi}{\partial t} = \frac{\partial^\parallel \Phi - [\Psi, \Phi]}{B_v} - \eta (j - j_{source}) + \nabla \cdot (\eta_{num} \nabla^\perp j),$$

where  $P = \nabla \cdot (D_\perp \nabla_\perp \rho + D_\parallel \nabla_\parallel \rho) + S_\rho, j$  and the plasma vorticity,  $\omega$ , are given by  $j = \Delta^* \Psi$  and  $\omega = \Delta^\perp \Phi$ .

[3] G. Huysmans, et al, Nucl. Fusion 47, 659, 2007.

[4] N. Nikulsin et al., Physics of Plasmas 29, 063901, 2022.

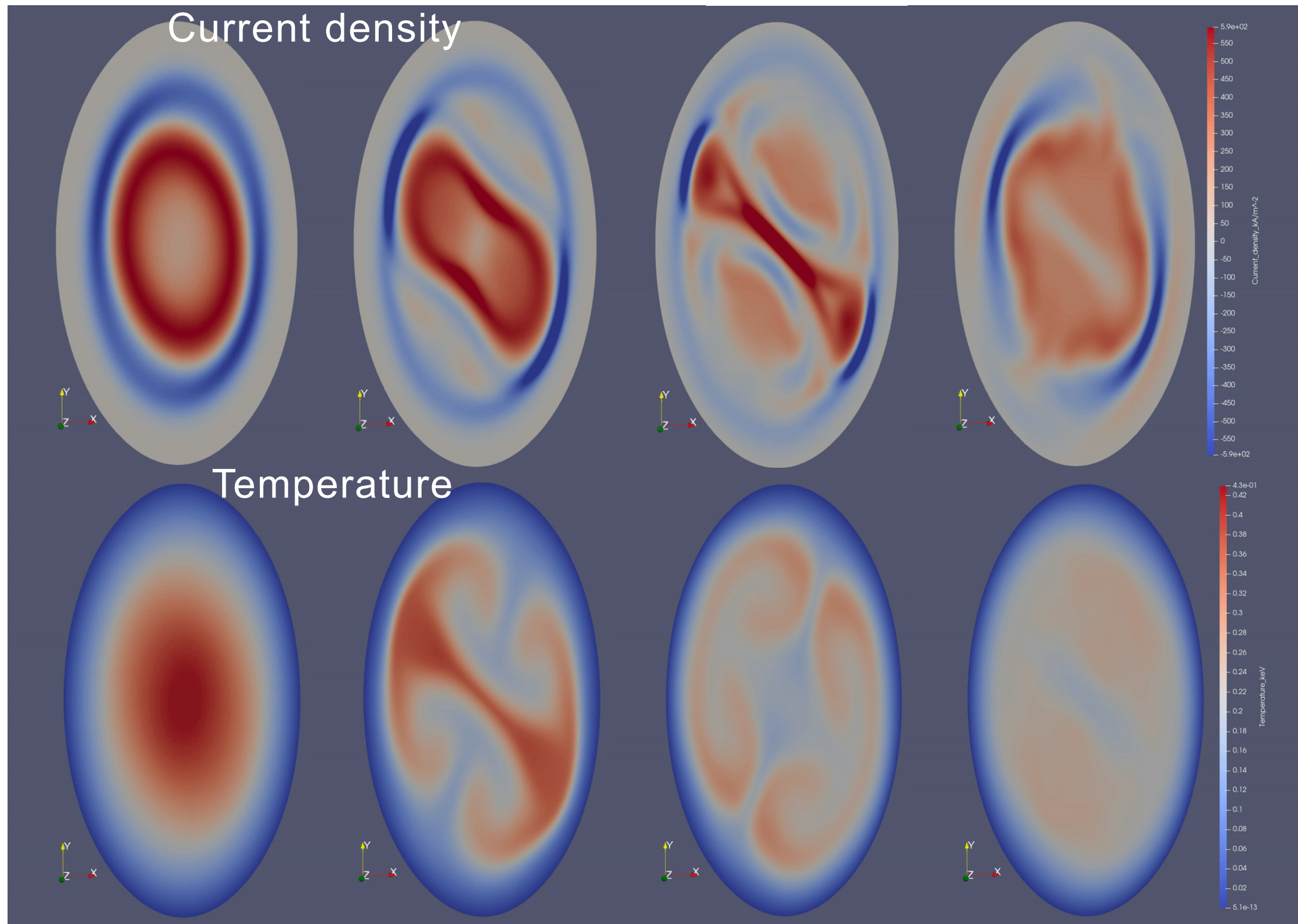
[5] R. Ramasamy, et al. Nuclear Fusion, 64 086030, 2024.



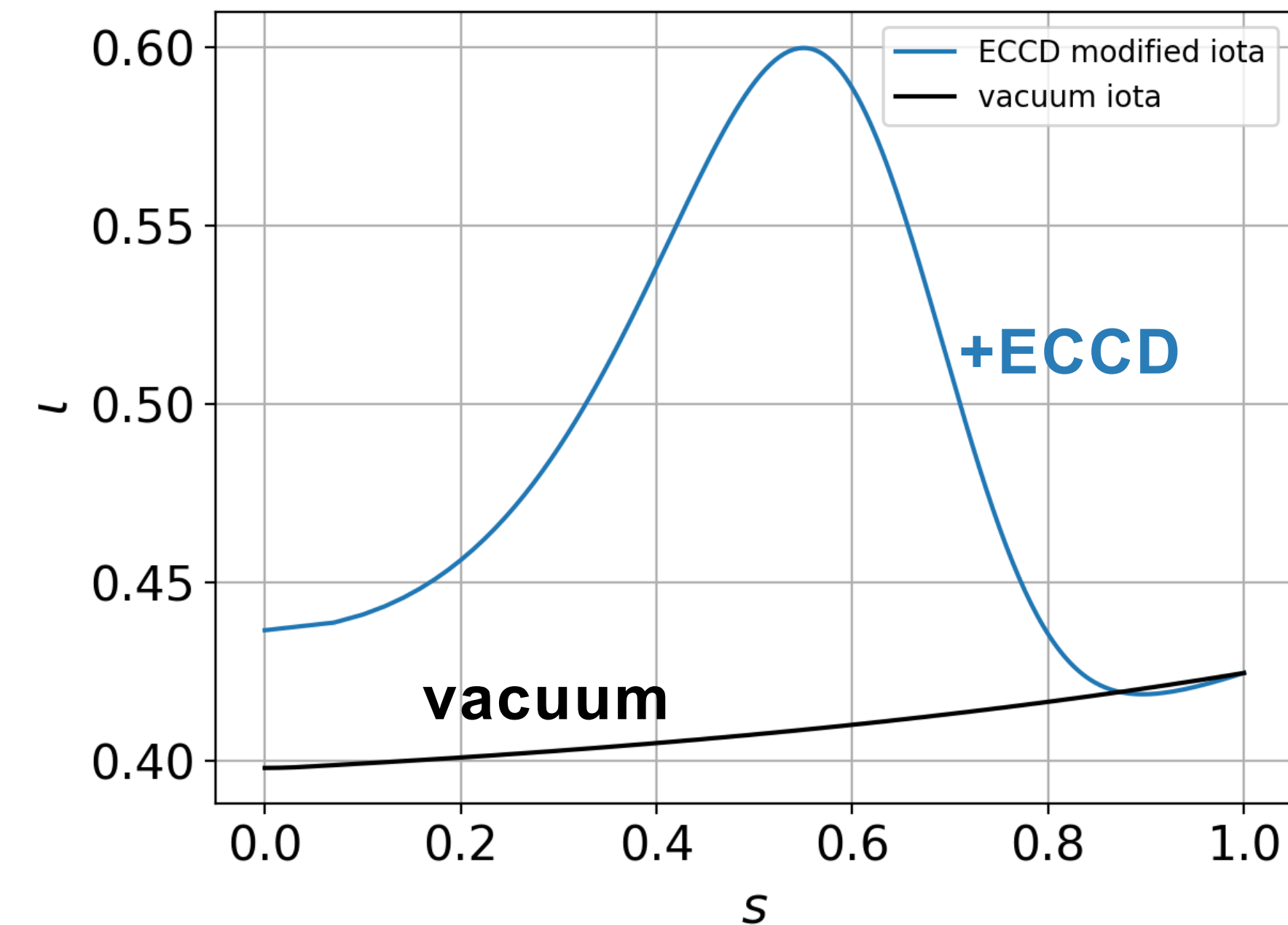
# Sawtooth crashes in a stellarator: nonlinear double kink mode evolution



Crash dynamics:



W7-A equilibrium is modified such that the vacuum rotational transform comes from elongation only and is quite flat. Then electron cyclotron current drive is applied.

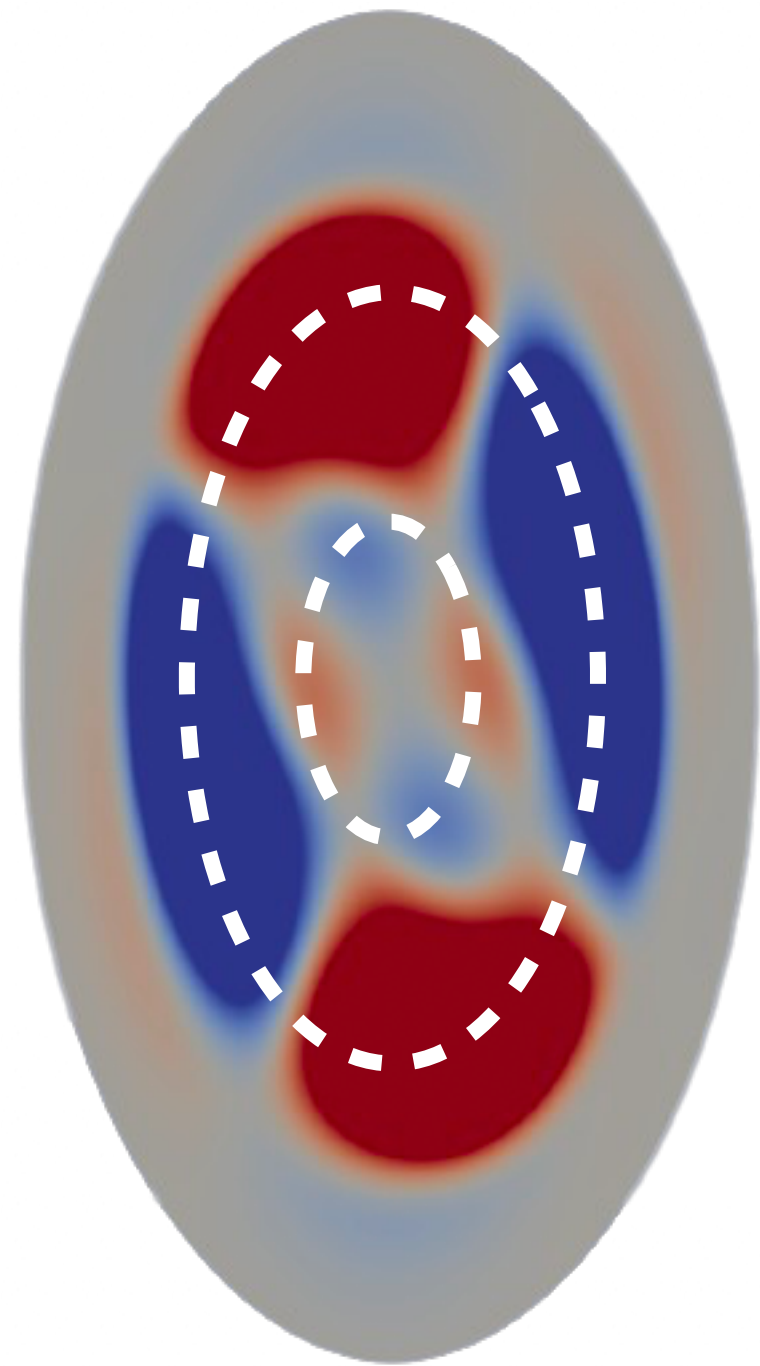


Current source is included, thus recovery of the current density profile can be observed. Sawtooth crash cycles can be reproduced.

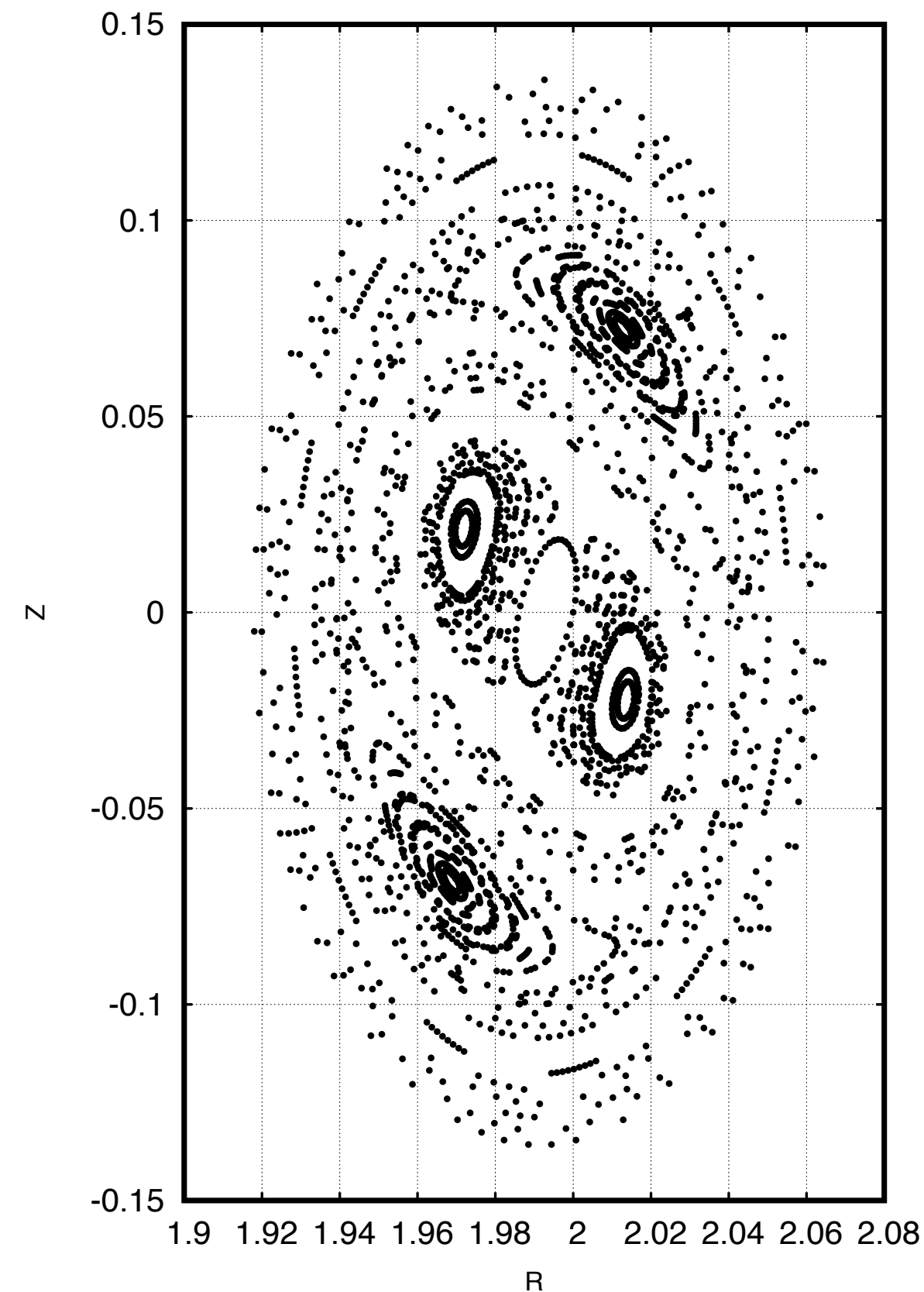
# Sawtooth crashes in a stellarator: nonlinear double kink mode evolution



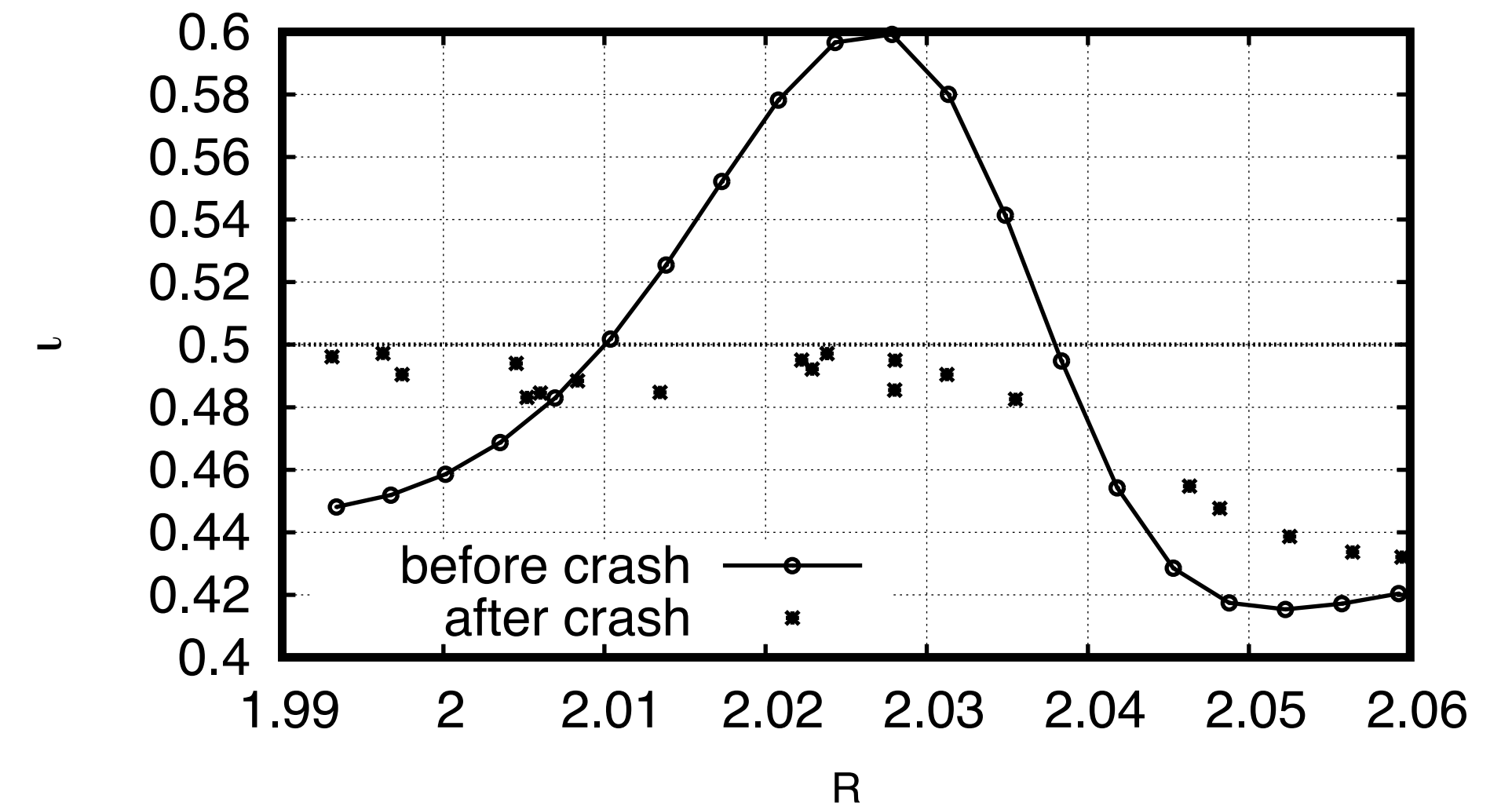
Velocity stream function.  
Pre-crash  $\iota = 0.5$  is marked.  
The characteristic (2,1) structure of the mode is clearly visible.



Poincaré plot showing double tearing/kink mode.



$\iota$ -profile before and after the crash



$$\beta = 0.1 \%$$

$$\eta = 0.5 * 10^{-6} [\Omega * m]$$

$$\mu = 2.90 * 10^{-7} [kg/(m * s)]$$

In addition, hyperviscosity  $\mu_h = 2.90 * 10^{-13} [kg/(m * s)]$

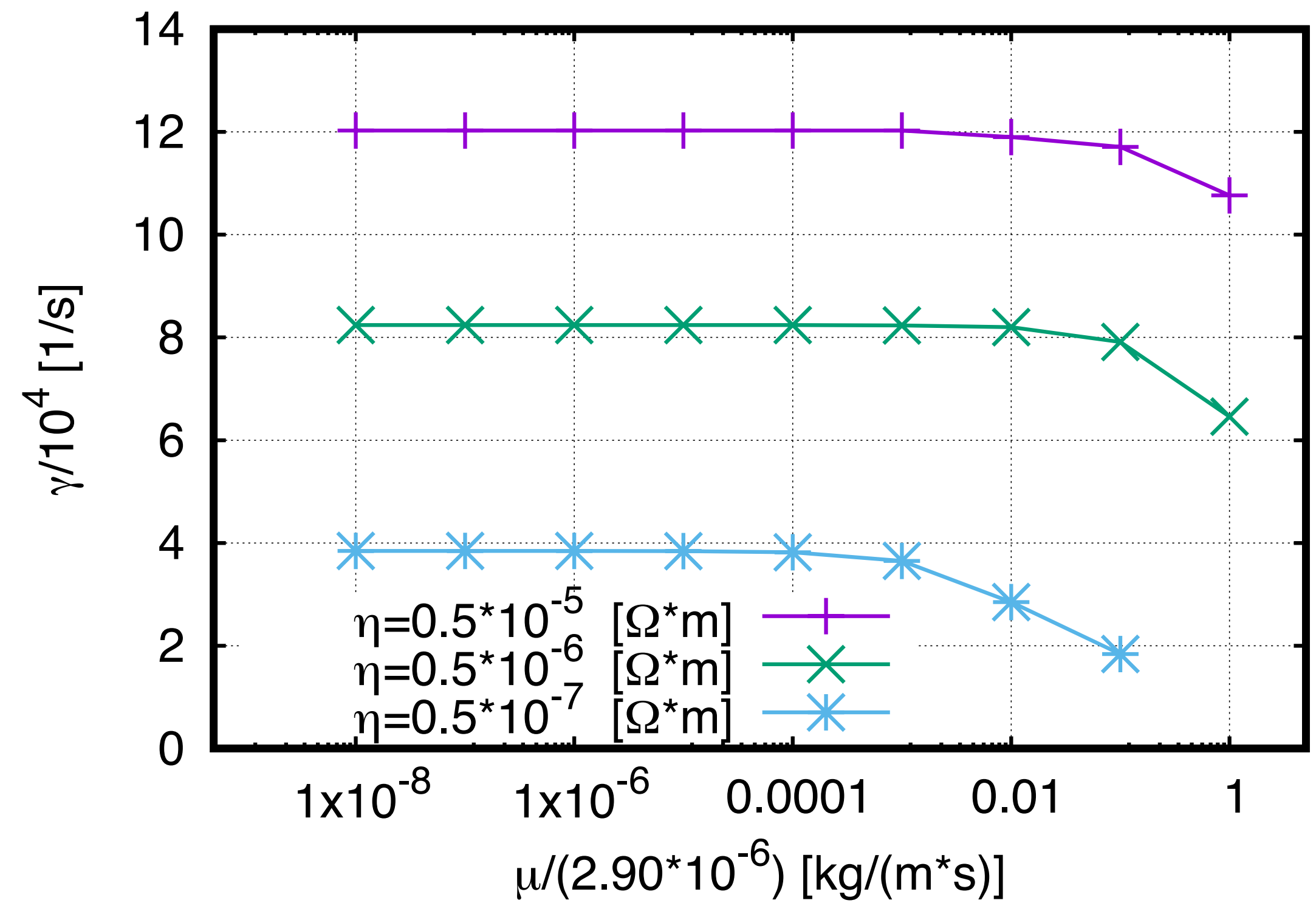
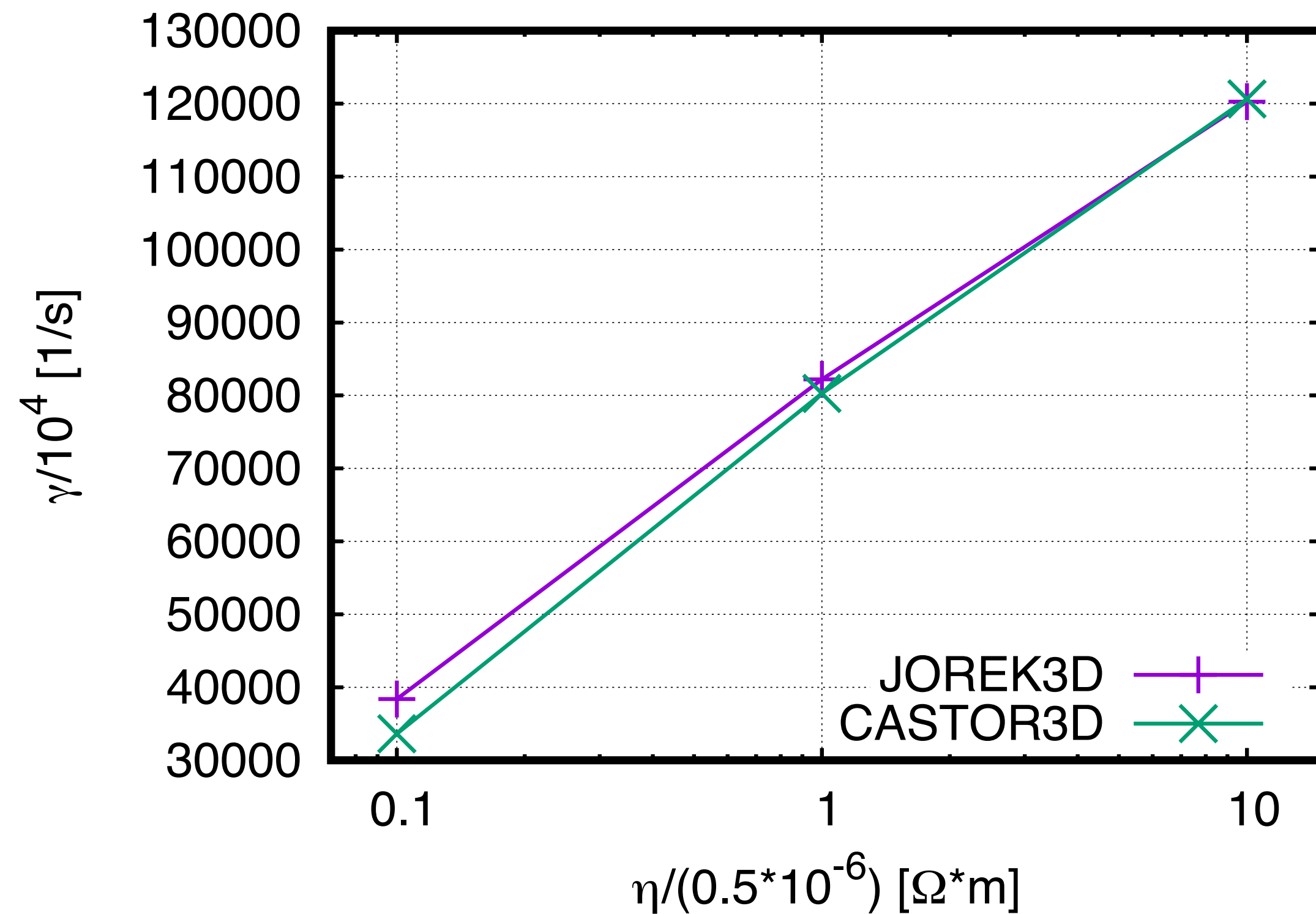
and hyper-resistivity  $\eta_h = 0.5 * 10^{-12} [\Omega * m^2]$

were applied.

# Benchmarks: CASTOR3D and M3D-C1



To verify validity of the results a benchmark with another MHD code is necessary. Here such a study is presented and discrepancy between two codes is minimal.



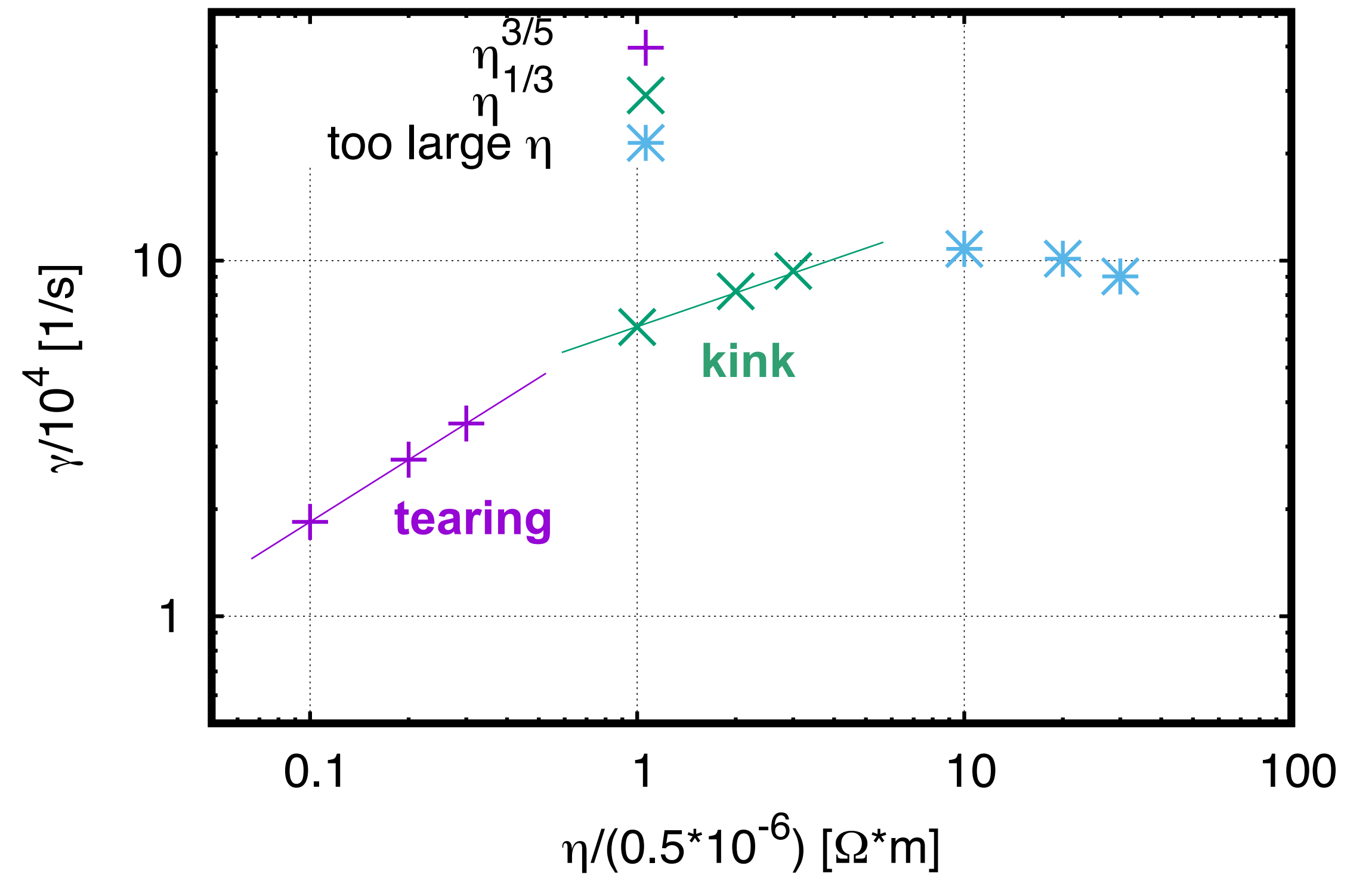
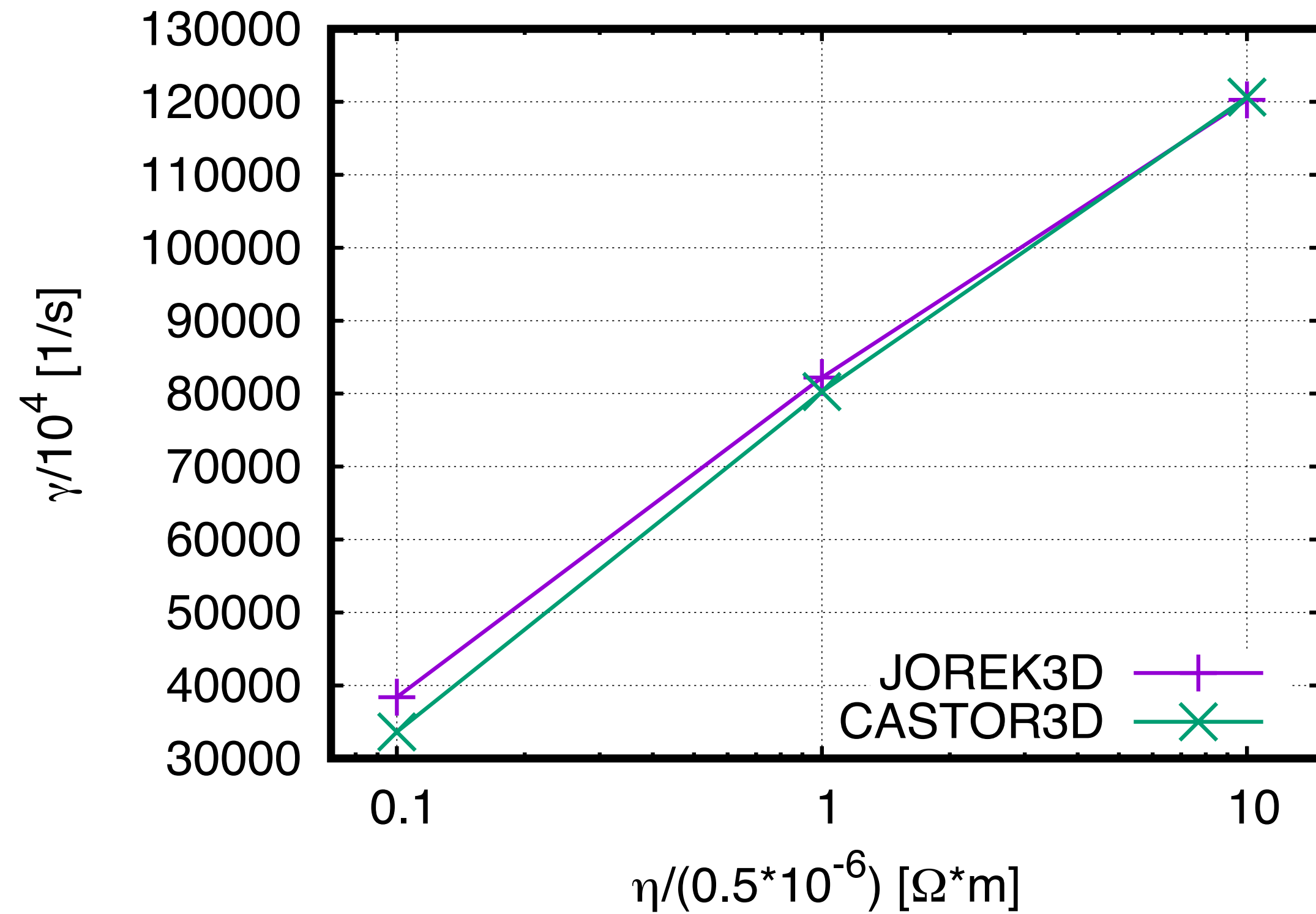
Note that CASTOR3D [6] has no identical viscosity terms thus viscosity independent limit in JOREK was found.

[6] Strumberger and Günter, Nuclear Fusion 57/1 (2016): 016032.

# Benchmarks: CASTOR3D and M3D-C1



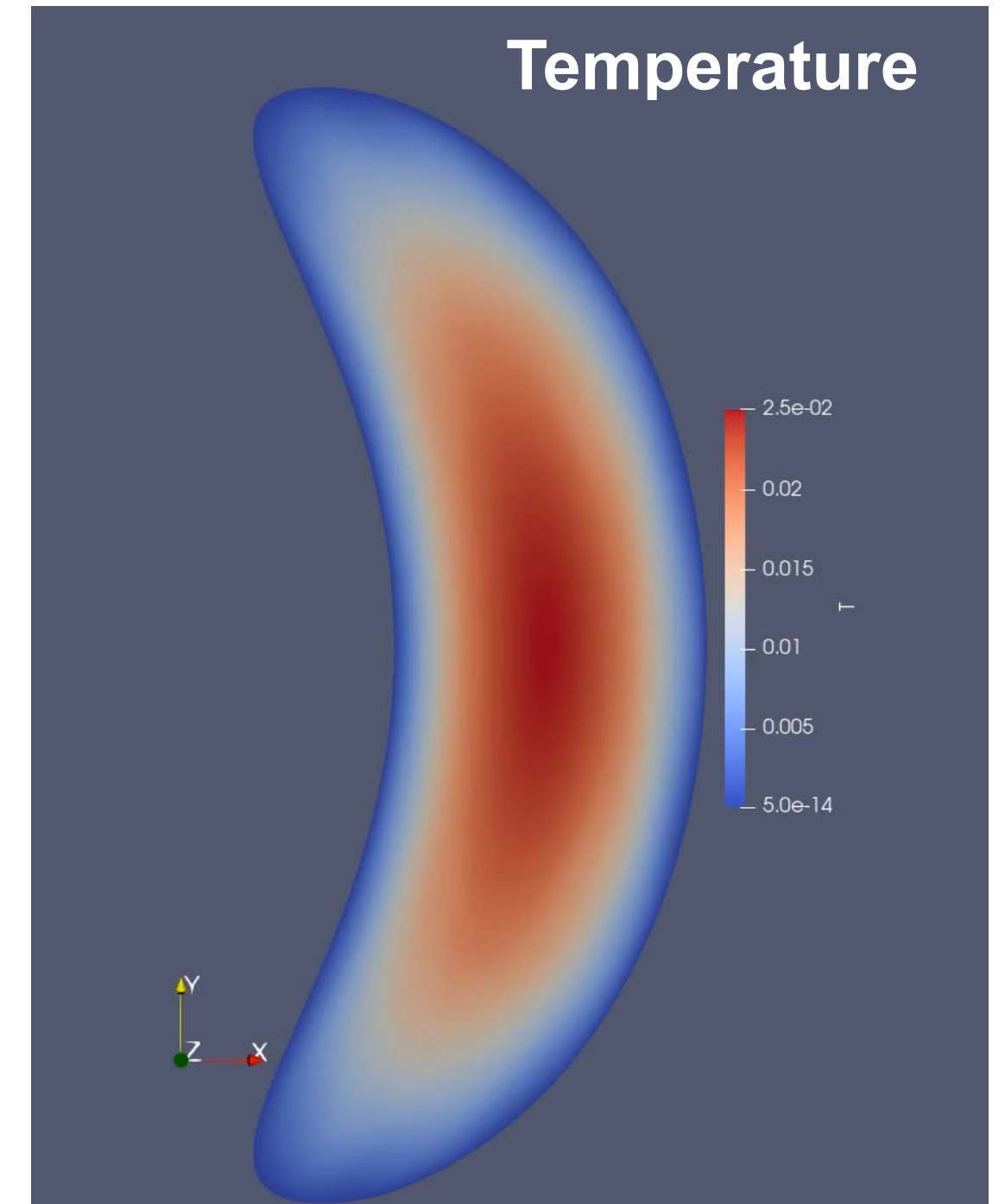
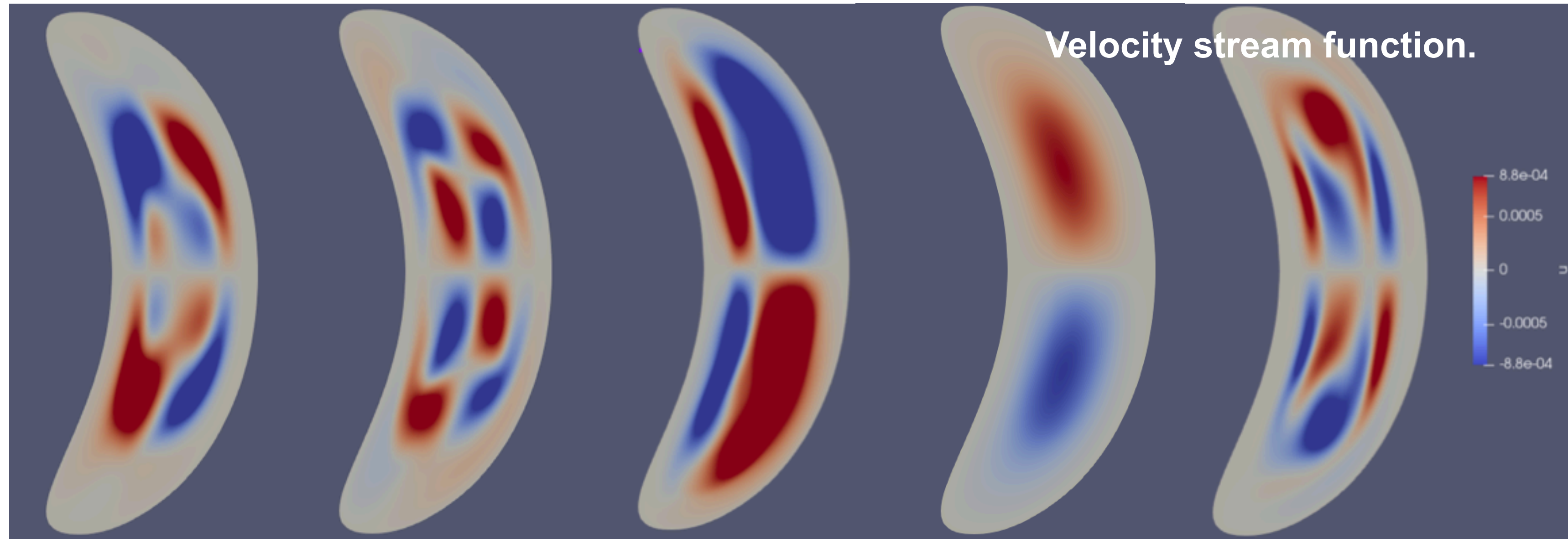
To verify validity of the results a benchmark with another MHD code is necessary. Here such a study is presented and discrepancy between two codes is minimal.



Studying growth rate dependence on resistivity demonstrated transition from double tearing mode to resistive double kink mode.

# W7-X, sawtooth-like crash

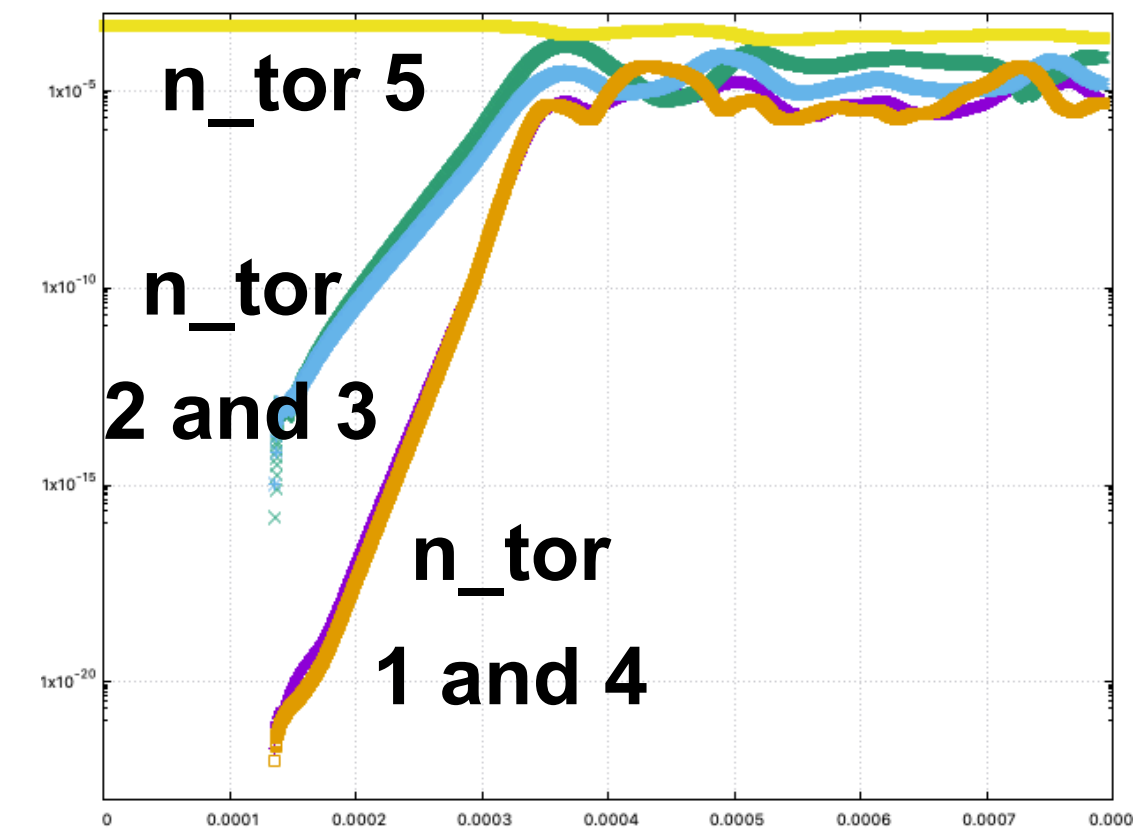
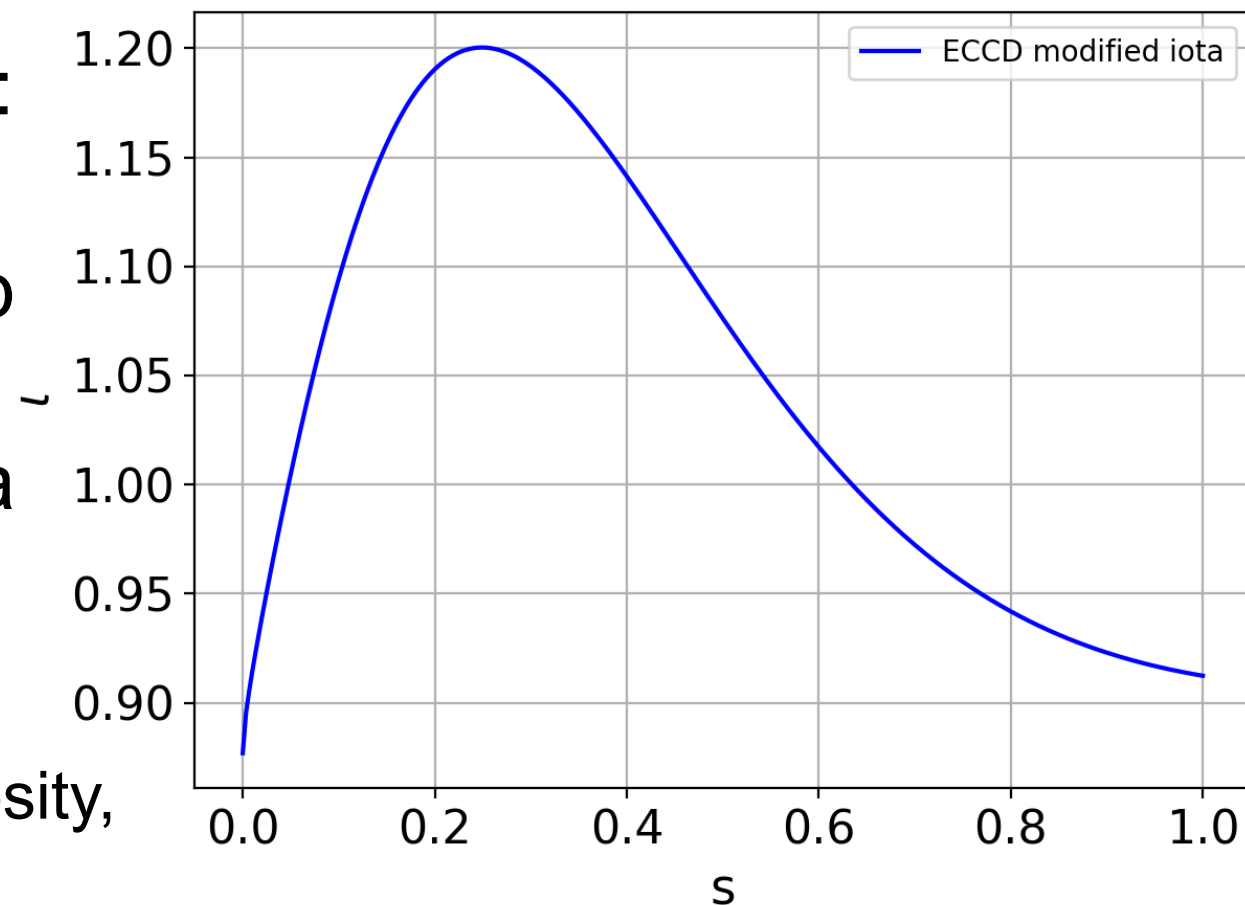
The first production run, with still a relatively wide iota hump, exhibits (2,2) mode activity. However, according to the energy plot, (2,2) and (1,1) modes are in competition during non-linear evolution.



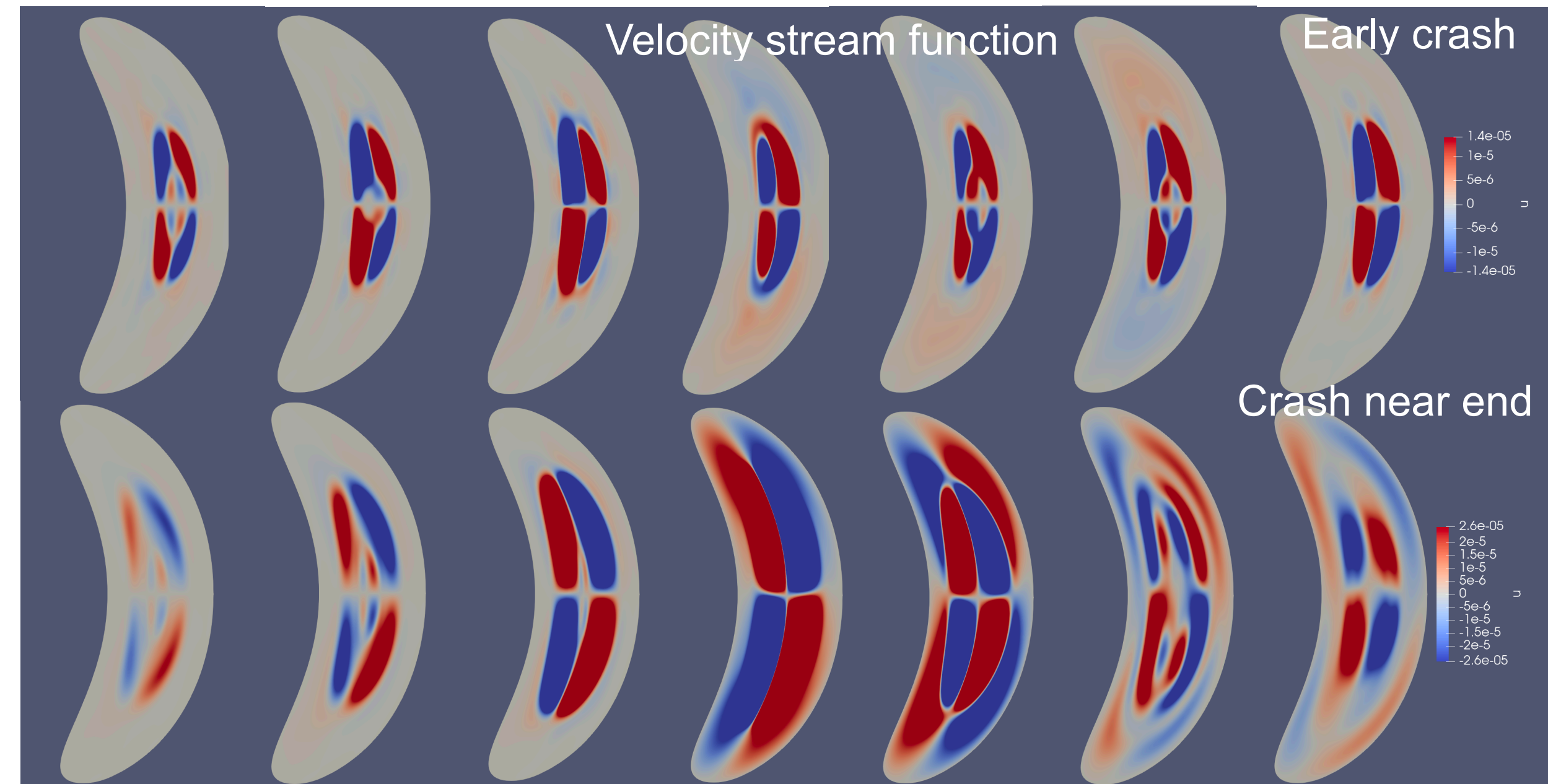
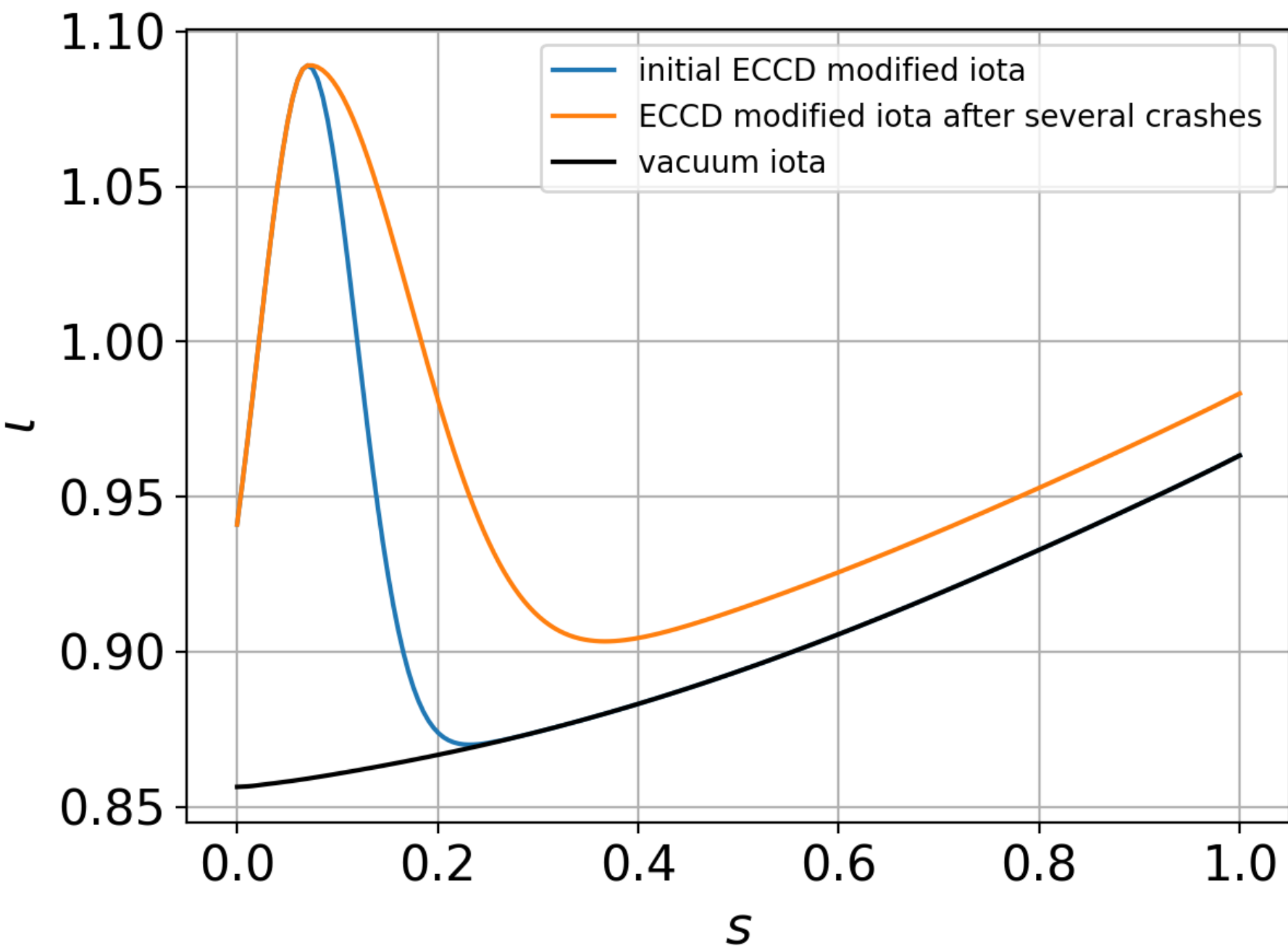
The reason why the (1,1) mode is not dominant could be attributed to:

- 1) A relatively high resistivity in this simulation (to speed up calculations).
- 2) A rather high beta value. For the rMHD model utilized here, a non-negligible beta value might act to stabilize the (1,1) mode.

$$\beta = 0.3\%, \eta = 0.5 * 10^{-5} [\Omega * m], \mu = 2.90 * 10^{-6} [kg/(m * s)], \text{ hyper-viscosity, } \mu_h = 2.90 * 10^{-12} [kg/(m * s)], \text{ hyper-resistivity } \eta_h = 0.5 * 10^{-11} [\Omega * m^2]$$



# W7-X, sawtooth-like crash

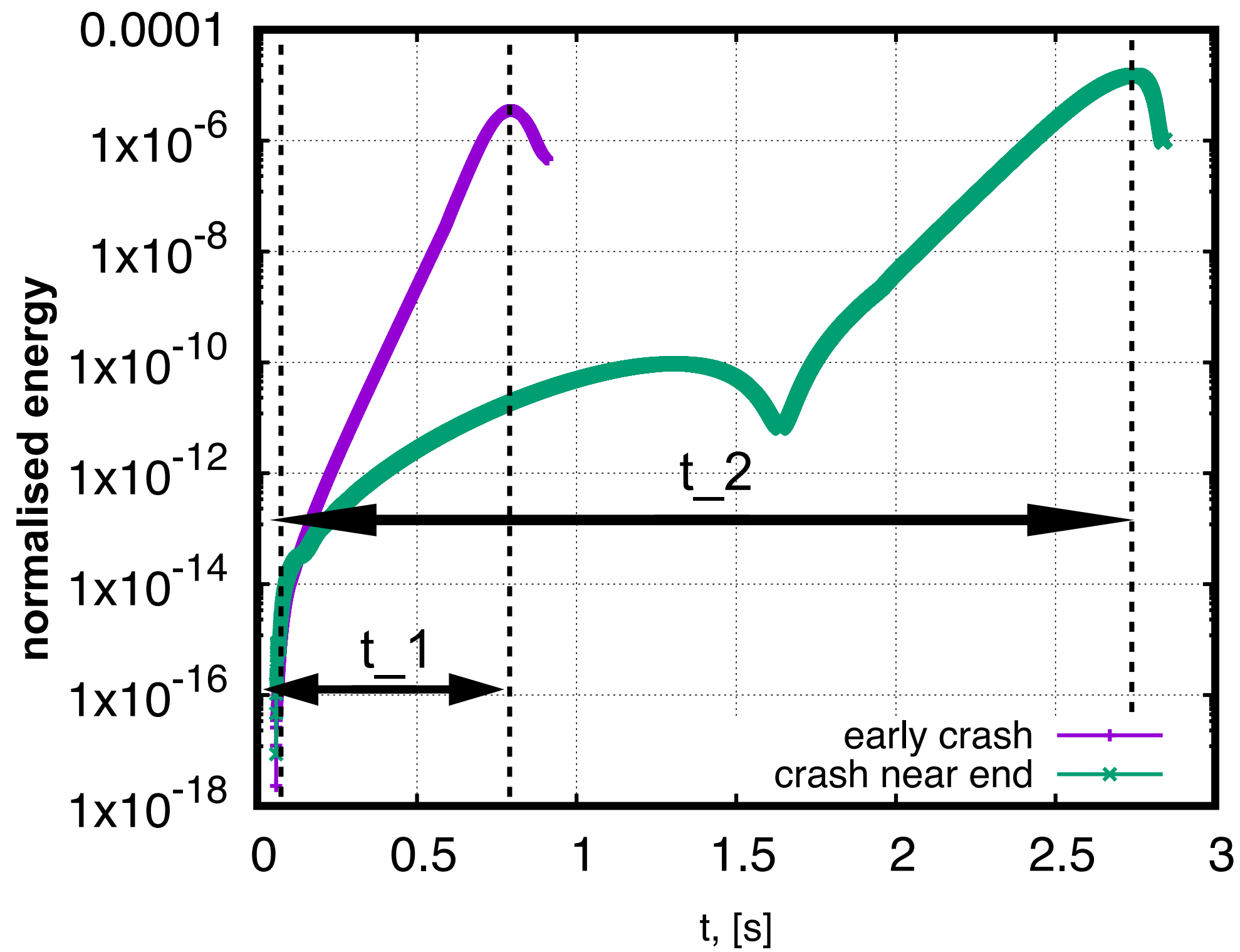


The characteristic double (2,2) structure of the mode is clearly visible for both types of crashes.

The mixing areas (and corresponding iotas) are calculated from the flux diffusion equation with relaxation, using ECCD current density profiles obtained from the Travis code. Two iota profiles were obtained: one at an early stage of the discharge (approximately 300 ms) and another near the end (around 8 s).

The (1,1) mode remains mostly dominated by the (2,2) mode in both cases.

# W7-X, sawtooth-like crash



$$t_1 = 0.75 \text{ ms}$$

$$t_2 = 2.75 \text{ ms}$$

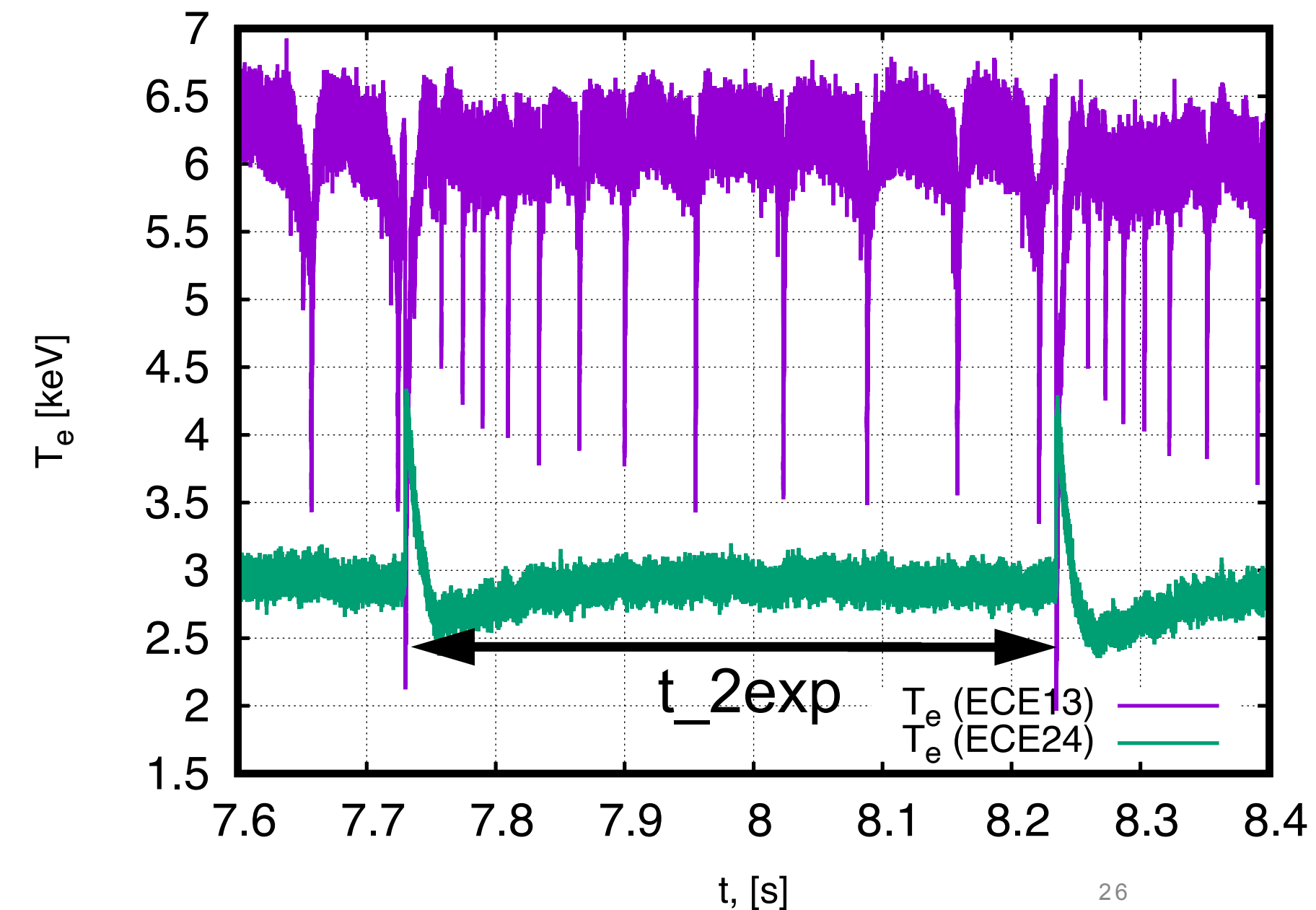
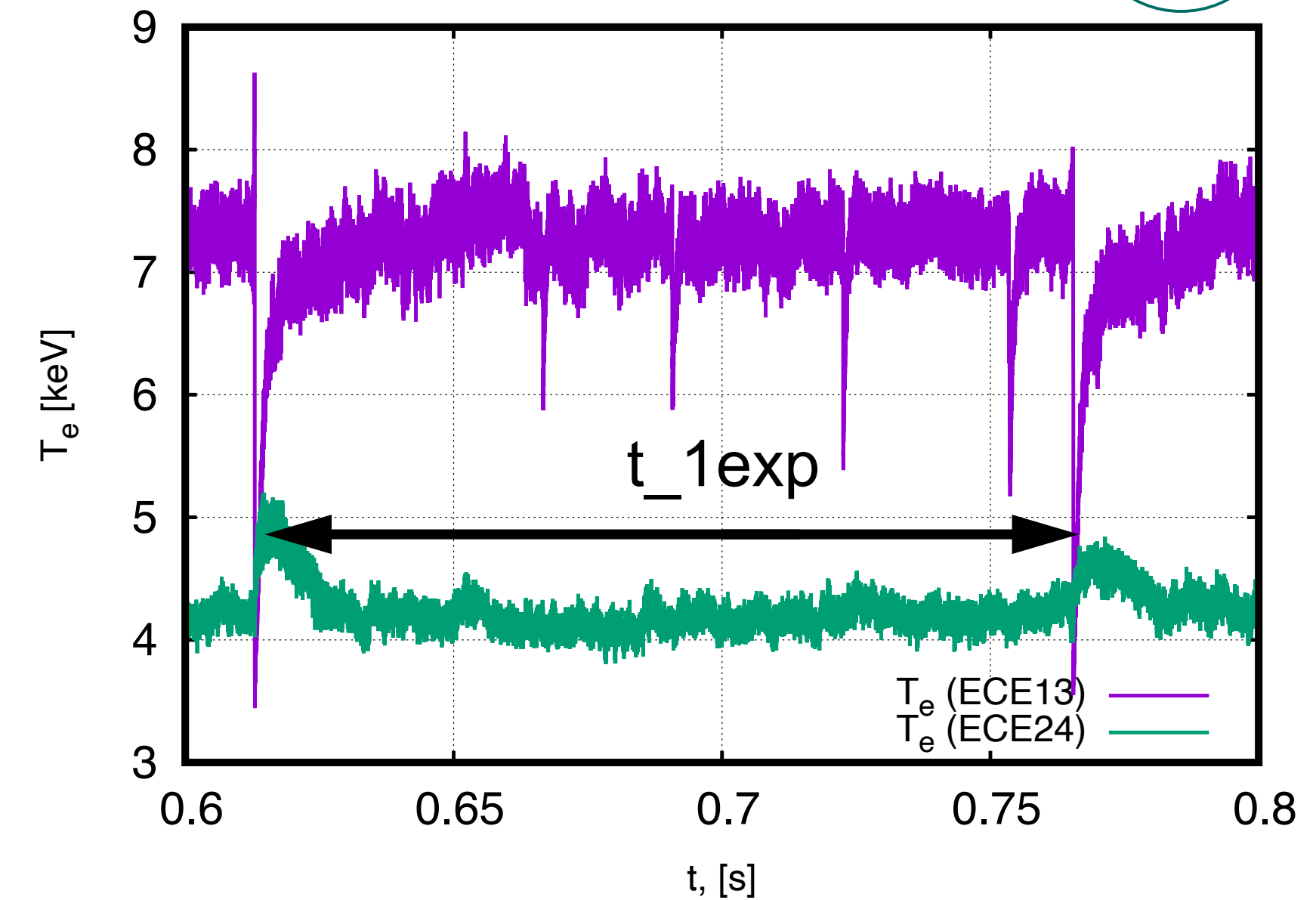
$$t_1/t_2 = 0.27$$

$$t_{1\text{exp}} = 150 \text{ ms}$$

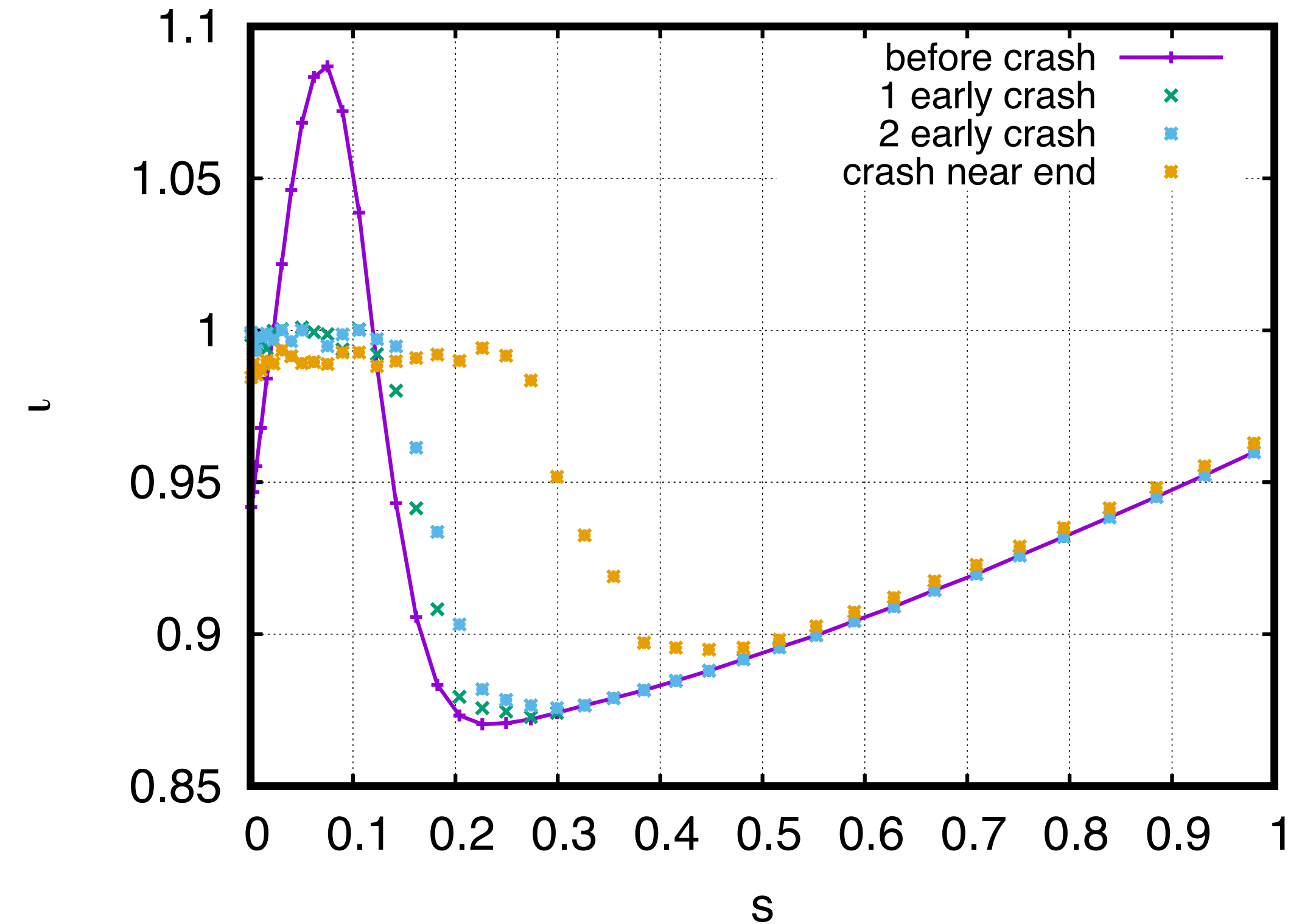
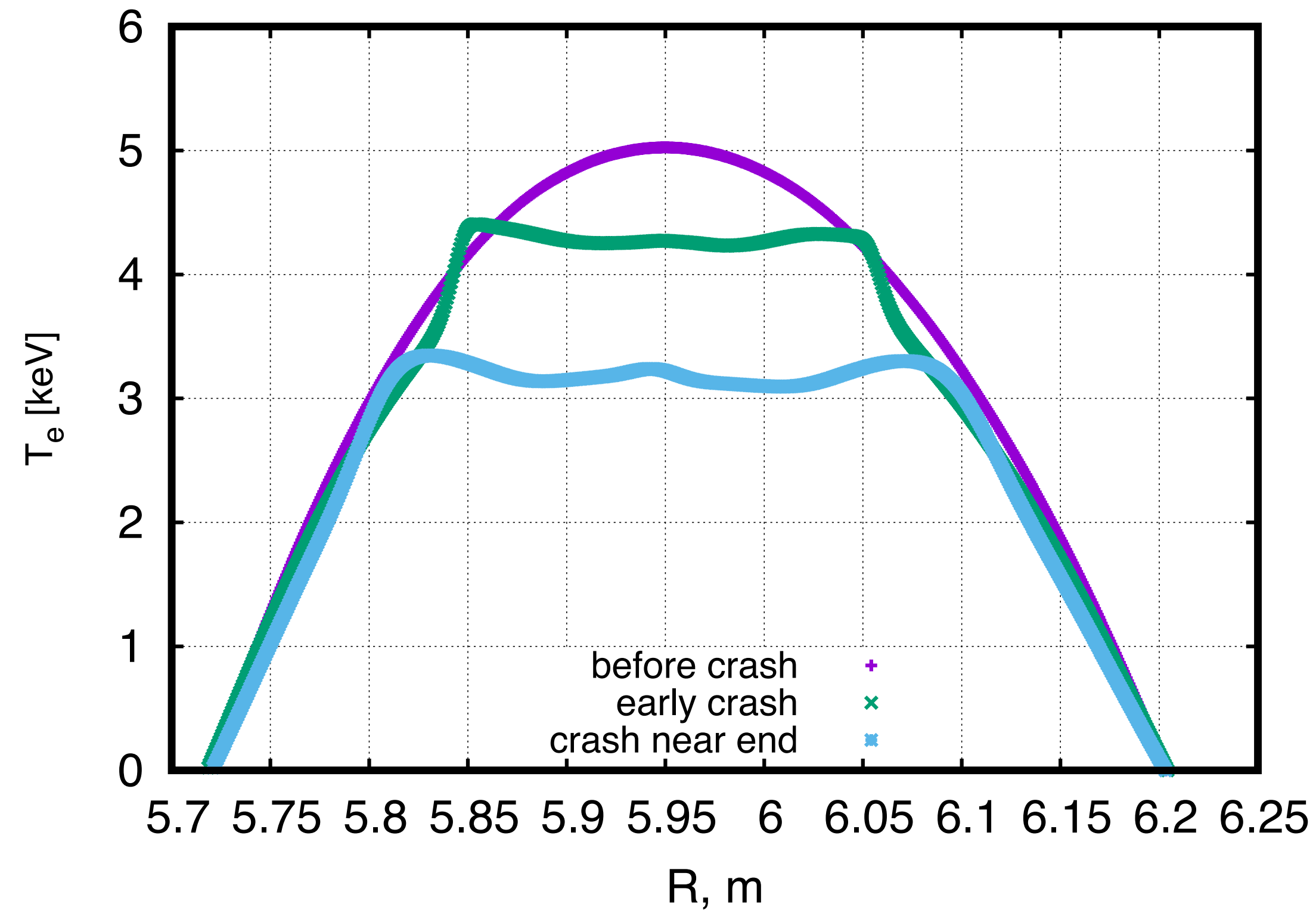
$$t_{2\text{exp}} = 500 \text{ ms}$$

$$t_{1\text{exp}}/t_{2\text{exp}} = 0.3$$

The timing of these crashes - defined as the ratio between the time to reach the medium crash at the beginning of the discharge ( $t_1$ ) and the time to reach the medium crash closer to the end of the discharge ( $t_2$ ) - is clearly visible in the energy plot and closely matches the experimental data ( $t_{1\text{exp}}/t_{2\text{exp}}$ ), taking into account the increased resistivity used to accelerate the simulations.



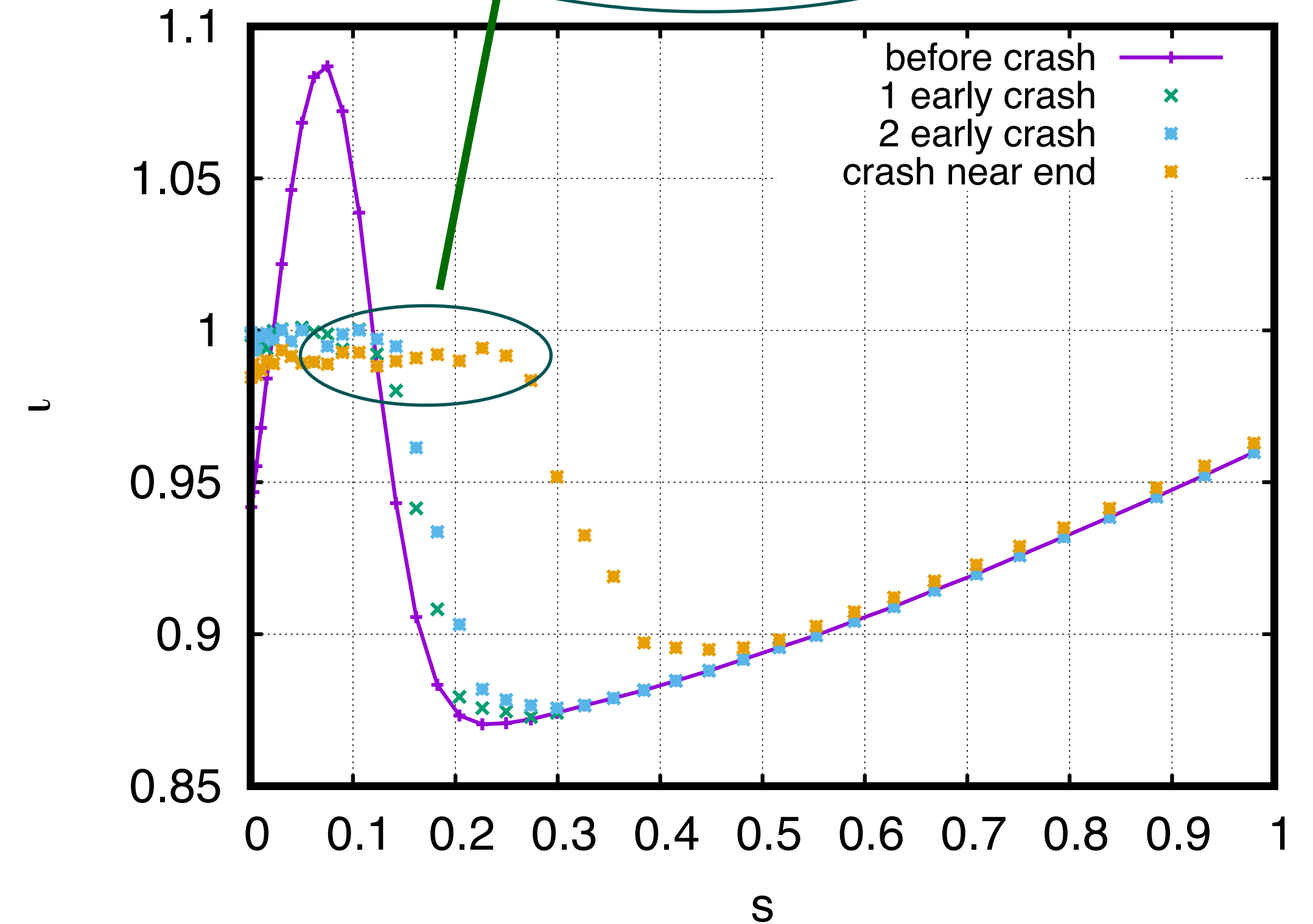
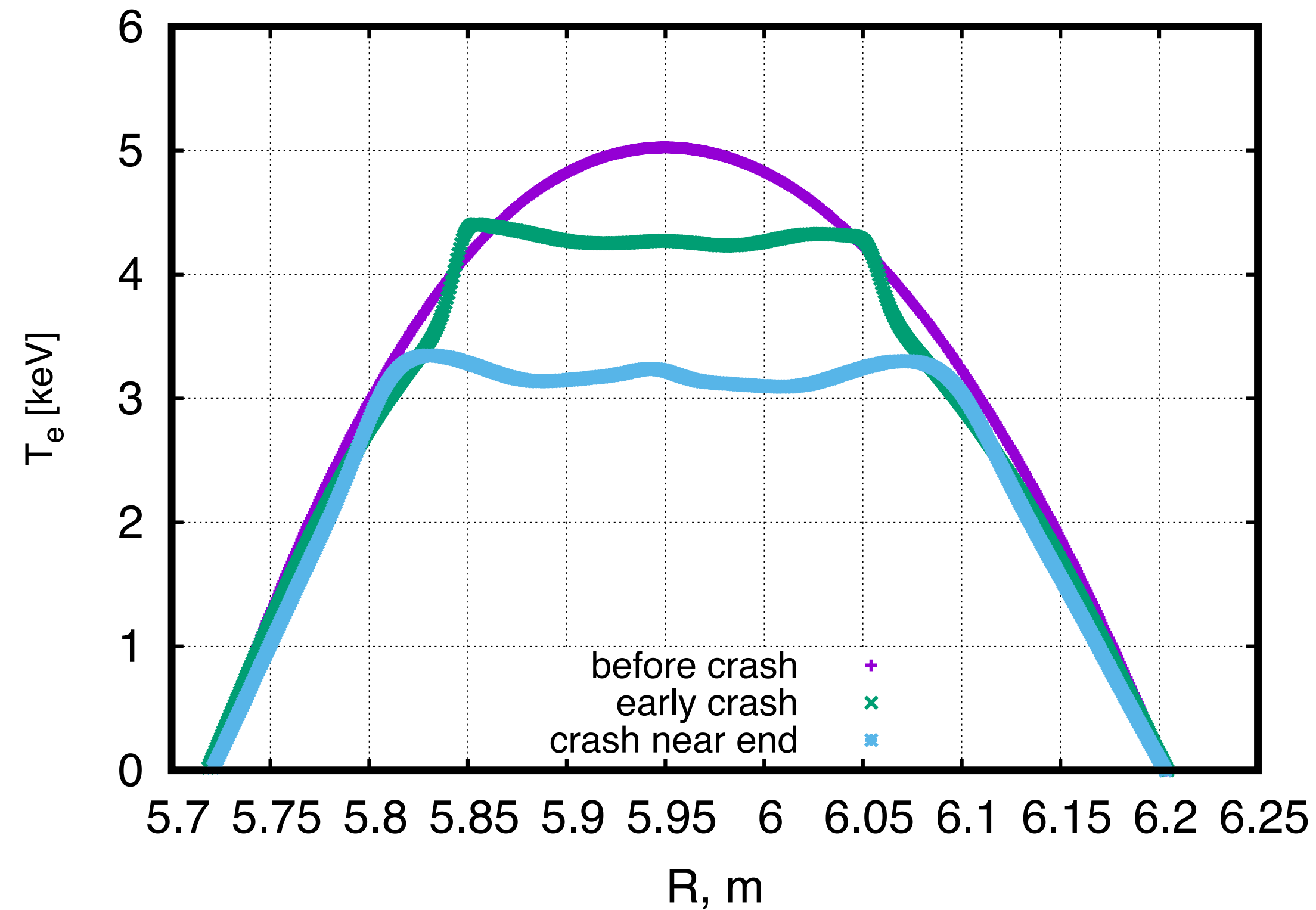
# Post-crash temperature and iota profiles



The inversion radius of the temperature change ( $r_{\text{inv}}/a$ ) shows good compatibility with experimental data when experimentally relevant plasma  $\beta$  is used.

The rotational transform after the crash is flat, settling around the  $\iota = 1$  value for earlier crashes and below it for a crash closer to the end of the discharge.

# Post-crash temperature and iota profiles



The inversion radius of the temperature change ( $r_{inv}/a$ ) shows good compatibility with experimental data when experimentally relevant plasma  $\beta$  is used.

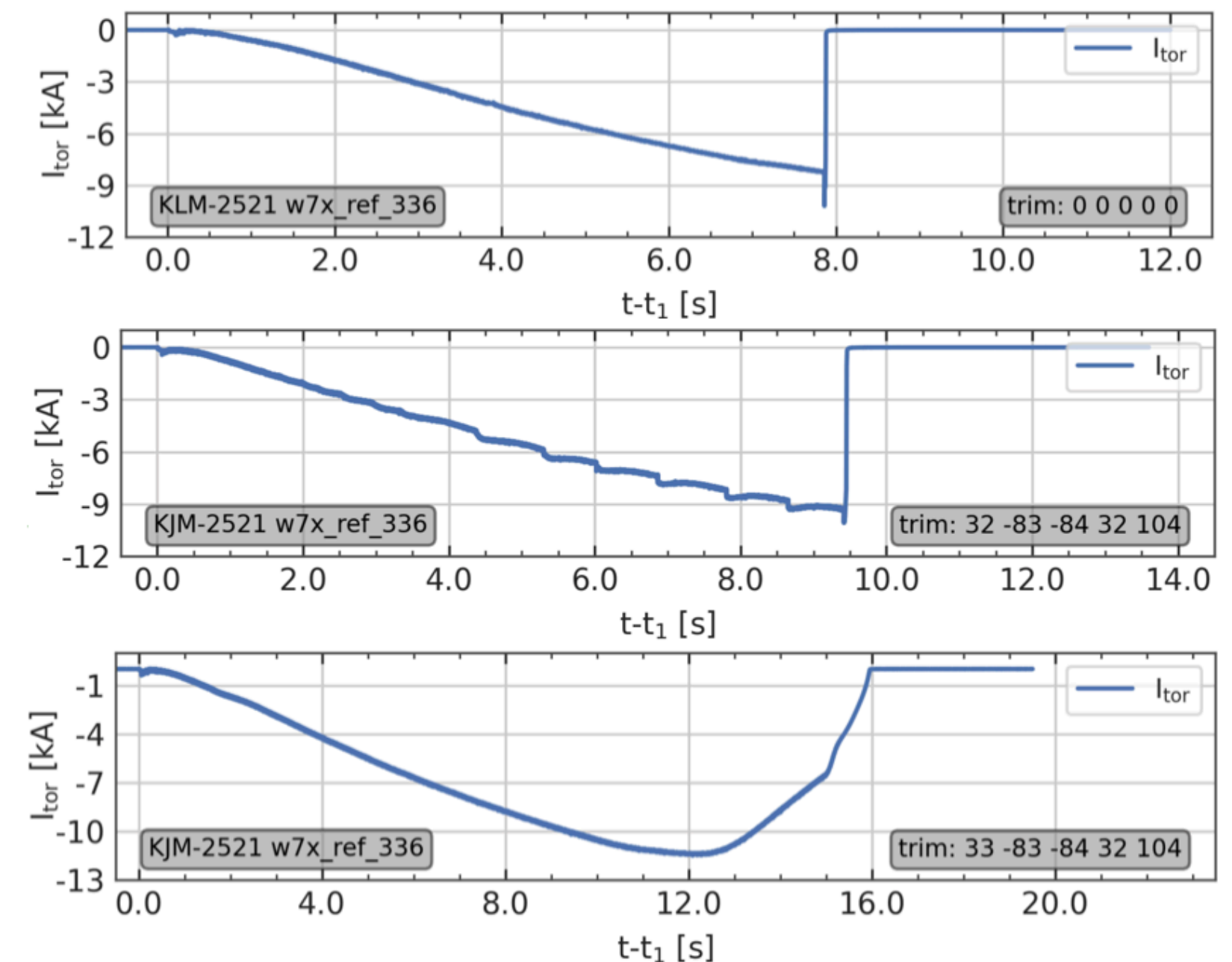
The rotational transform after the crash is flat, settling around the  $\iota = 1$  value for earlier crashes and below it for a crash closer to the end of the discharge.

**Mixing area increases due to crashes as expected.**

# Conclusion



1. A flux diffusion model with relaxation was developed and applied to sawtooth cycles in W7-X.
2. Two types of ECCD-induced crashes—small and medium—were successfully simulated. Their characteristic scales match experimental data, suggesting different resonant origins.
3. Medium crashes were also studied using the non-linear MHD code JOREK, supporting the simplified model's result: mixing area gets larger.
4. The inversion radius ( $r_{\text{inv}}/a$ ) and the relative timing between medium crashes early and late in the discharge ( $t_1/t_2$ ) show good agreement with experiments.
5. This work lays the foundation for studying sawtooth-like oscillations in W7-X, which include small, medium, and **large crashes - the latter linked to plasma termination.**



Toroidal current vs time termination dynamics in W7-X different configurations and different ECCD settings.



# Back up slides

# JOREK, stellarator geometry

- JOREK [\*] is a finite element nonlinear MHD code.
- Equations solved in weak form: original equations are multiplied by a test function and integrated over domain.
- Time-stepping: Crank-Nicholson, Gears or implicit Euler schemes.
- For the stellarator extension [\*\*], the grid becomes  $\phi$ -dependent.
- The equilibrium is not calculated inside JOREK, but imported from the GVEC code [\*\*\*].
- The physics model is reduced MHD, single and two-temperature ( $T_i$  and  $T_e$ ) models are available.  $v_{par}$  was recently implemented [\*\*\*\*] however is not used in these calculations.

## REDUCED MHD

$$\vec{B} = \nabla\chi + \nabla\Psi \times \nabla\chi + \nabla\Omega \times \nabla\psi_v,$$

$$\vec{v} = \frac{\nabla\Phi \times \nabla\chi}{B_v^2} + v_{||}\vec{B} + \nabla^\perp\zeta.$$

### Equations which are solved:

$$\frac{\partial\rho}{\partial t} = -B_v \left[ \frac{\rho}{B_v^2}, \Phi \right] + P,$$

$$\nabla \cdot \left( \frac{\rho}{B_v^2} \nabla^\perp \frac{\partial\Phi}{\partial t} \right) = \frac{B_v}{2} \left[ \frac{\rho}{B_v^2}, \frac{(\Phi, \Phi)}{B_v^2} \right] + B_v \left[ \frac{\rho\omega}{B_v^4}, \Phi \right] - \nabla \cdot \left( \frac{P}{B_v^2} \nabla^\perp \Phi \right) + \nabla \cdot (j\mathbf{B}) + B_v \left[ \frac{1}{B_v^2}, p \right] + \nabla \cdot (\mu_\perp \nabla^\perp \omega) - \Delta^\perp (\mu_{num} \Delta^\perp \omega),$$

$$\rho \frac{\partial T}{\partial t} = -\frac{1}{B_v} [\rho T, \Phi] - \gamma \rho T B_v \left[ \frac{1}{B_v^2}, \Phi \right] + \nabla \cdot \left[ \kappa_\perp \nabla_\perp T + \kappa_\parallel \nabla_\parallel \nabla_\parallel T + \frac{pD_\perp}{\rho} \nabla_\perp \rho + \frac{pD_\parallel}{\rho} \nabla_\parallel \rho \right] + (S_e + \eta_{Ohm} B_v^2 j^2) - T \frac{\partial\rho}{\partial t},$$

$$\frac{\partial\psi}{\partial t} = \frac{\partial^\parallel \Phi - [\Psi, \Phi]}{B_v} - \eta (j - j_{source}) + \nabla \cdot (\eta_{num} \nabla^\perp j),$$

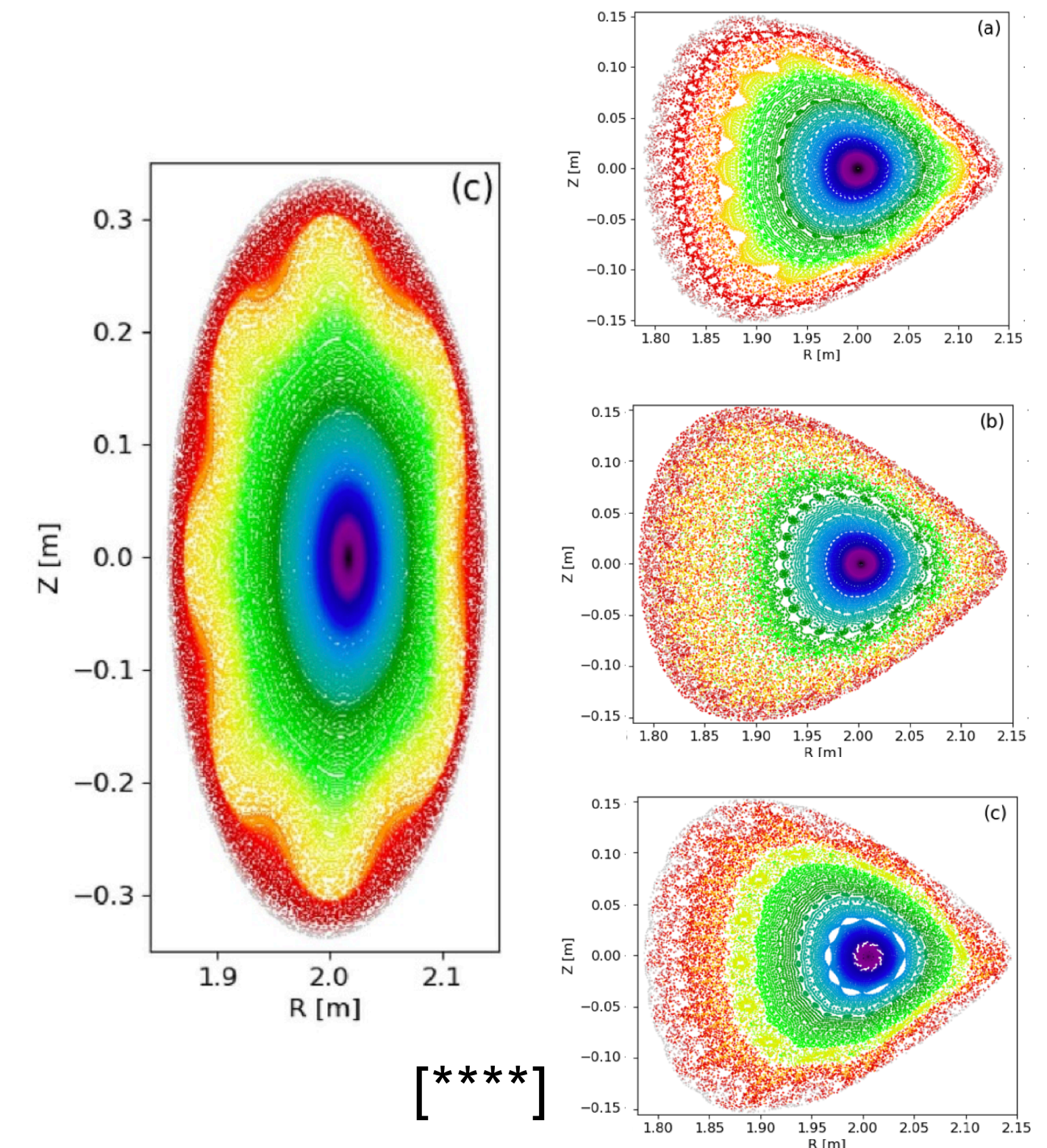
where  $P = \nabla \cdot (D_\perp \nabla_\perp \rho + D_\parallel \nabla_\parallel \rho) + S_\rho$ ,  $j$  and the plasma vorticity,  $\omega$ , are given by  $j = \Delta^* \Psi$  and  $\omega = \Delta^\perp \Phi$ .

[\*] G. Huysmans, et al, Nucl. Fusion 47, 659, 2007.

[\*\*] N. Nikulsin et al., Physics of Plasmas 29, 063901, 2022.

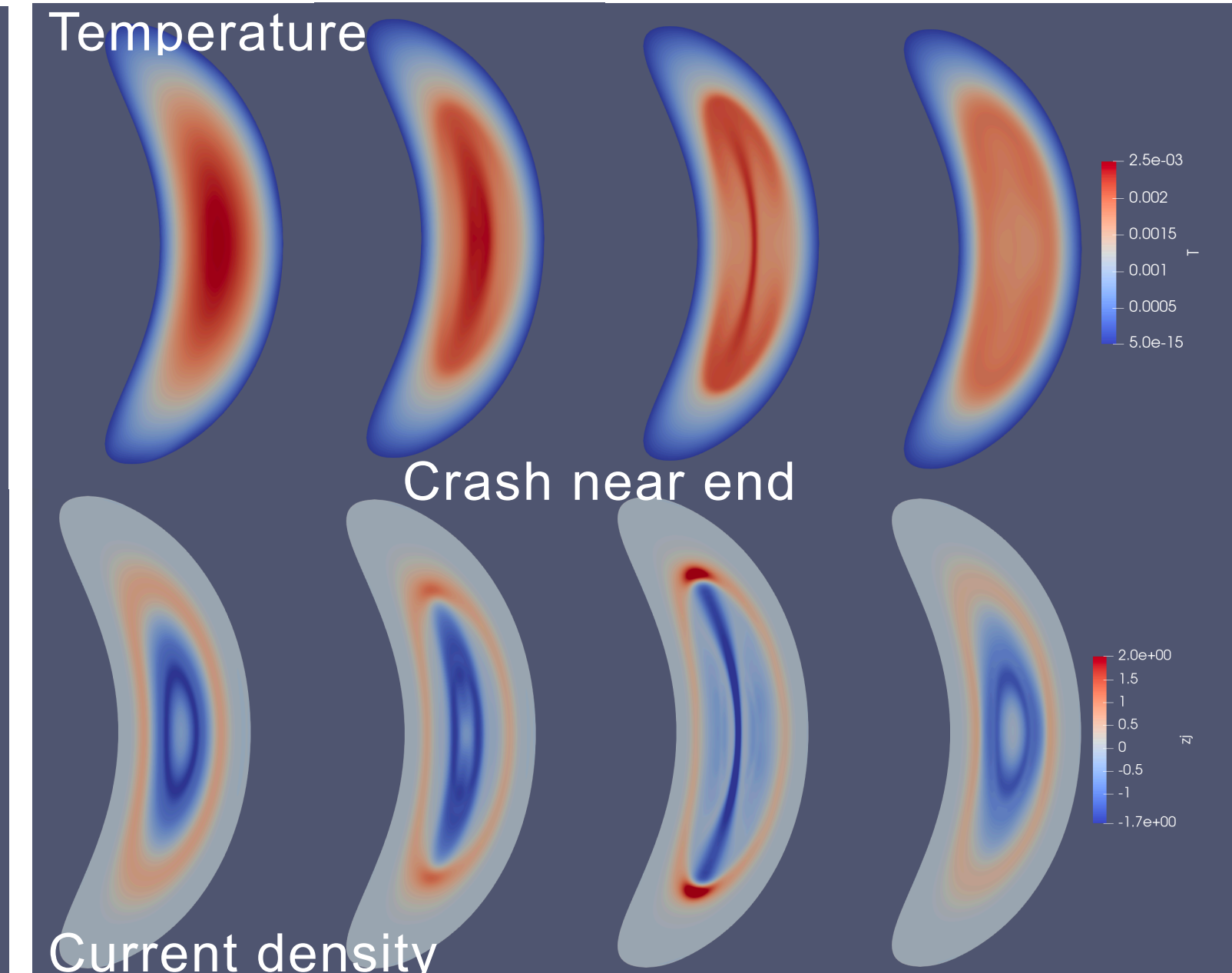
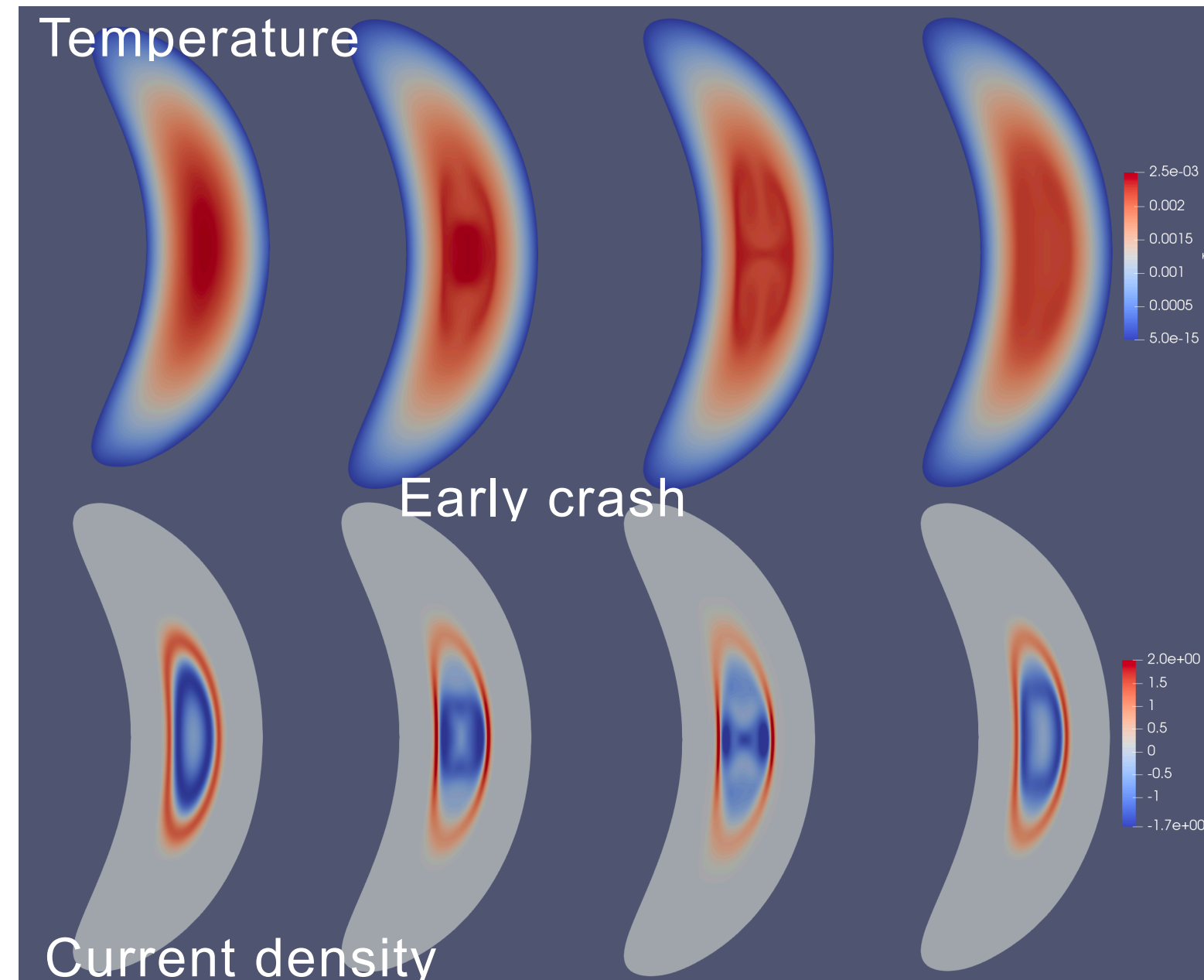
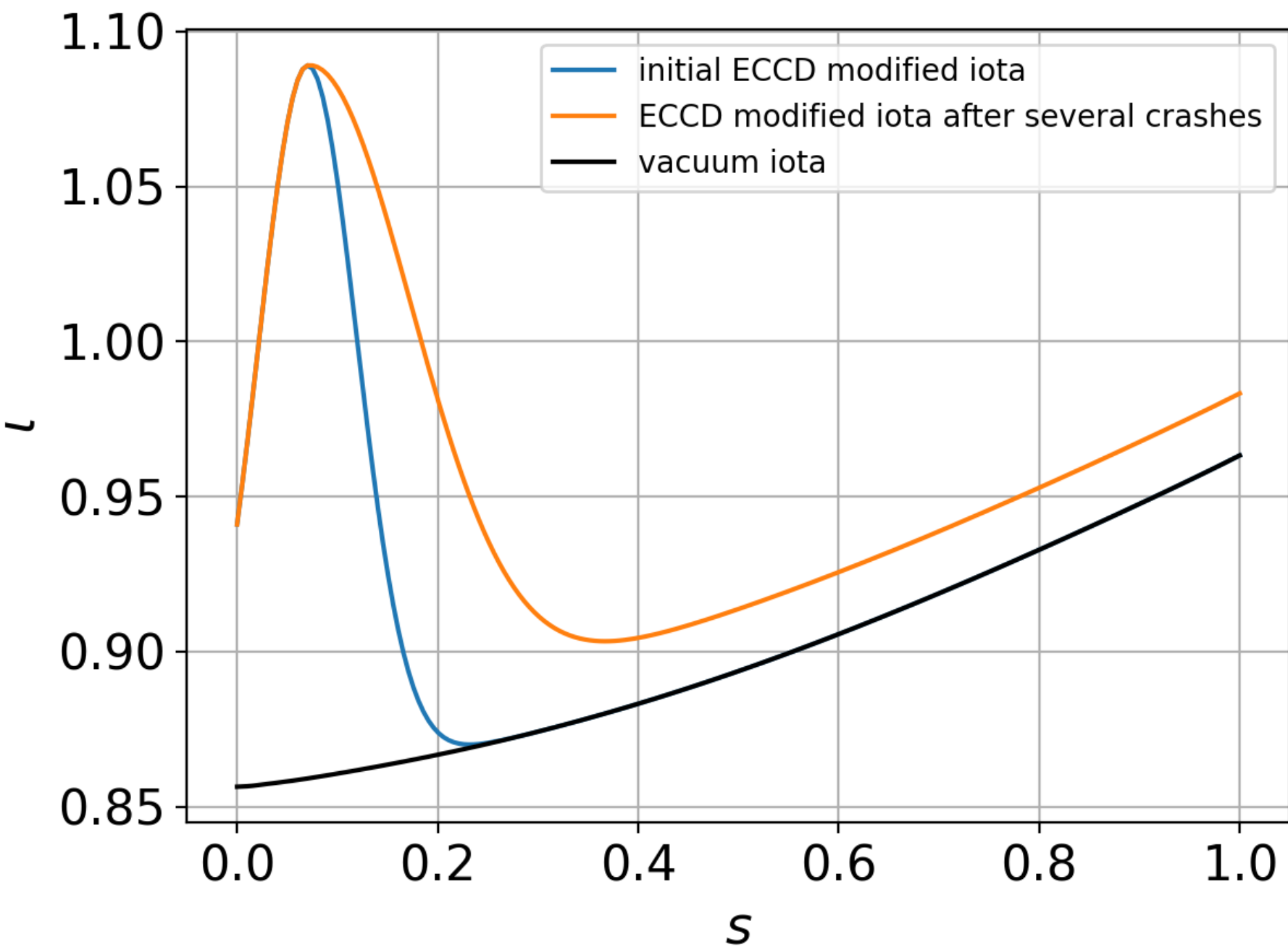
[\*\*\*] F. Hindenlang, et al, Simons hour talk, 2019.

[\*\*\*\*] R. Ramasamy, et al. Nuclear Fusion, 64 086030, 2024.



[\*\*\*\*]

# W7-X, sawtooth-like crash



The mixing areas (and corresponding iotas) are calculated from the flux diffusion equation with relaxation, using ECCD current density profiles obtained from the Travis code. Two iota profiles were obtained: one at an early stage of the discharge (approximately 300 ms) and another near the end (around 8 s).

# JOREK, stellarator geometry

- JOREK [\*] is a finite element nonlinear MHD code.
- Equations solved in weak form: original equations are multiplied by a test function and integrated over domain.
- Time-stepping: Crank-Nicholson, Gears or implicit Euler schemes.
- For the stellarator extension [\*\*], the grid becomes  $\phi$ -dependent.
- The equilibrium is not calculated inside JOREK, but imported from the GVEC code [\*\*\*].
- The physics model is reduced MHD, single and two-temperature ( $T_i$  and  $T_e$ ) models are available.  $v_{par}$  was recently implemented [\*\*\*\*] however is not used in these calculations.

## REDUCED MHD

$$\vec{B} = \nabla\chi + \nabla\Psi \times \nabla\chi + \nabla\Omega \times \nabla\psi_v,$$

$$\vec{v} = \frac{\nabla\Phi \times \nabla\chi}{B_v^2} + v_{\parallel}\vec{B} + \nabla^{\perp}\zeta.$$

### Equations which are solved:

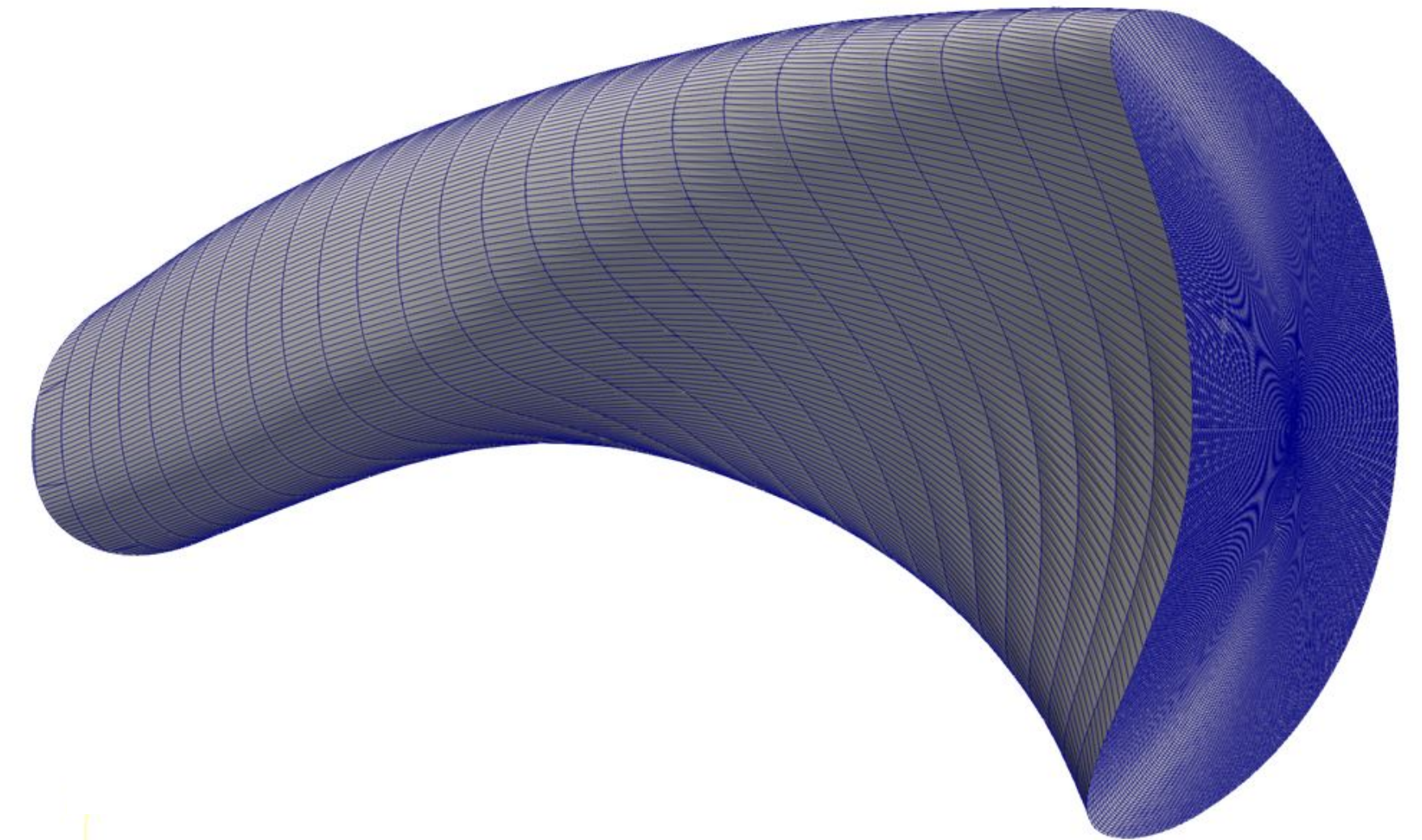
$$\frac{\partial\rho}{\partial t} = -B_v \left[ \frac{\rho}{B_v^2}, \Phi \right] + P,$$

$$\nabla \cdot \left( \frac{\rho}{B_v^2} \nabla^{\perp} \frac{\partial\Phi}{\partial t} \right) = \frac{B_v}{2} \left[ \frac{\rho}{B_v^2}, \frac{(\Phi, \Phi)}{B_v^2} \right] + B_v \left[ \frac{\rho\omega}{B_v^4}, \Phi \right] - \nabla \cdot \left( \frac{P}{B_v^2} \nabla^{\perp} \Phi \right) + \nabla \cdot (j\mathbf{B}) + B_v \left[ \frac{1}{B_v^2}, p \right] + \nabla \cdot (\mu_{\perp} \nabla^{\perp} \omega) - \Delta^{\perp} (\mu_{num} \Delta^{\perp} \omega),$$

$$\rho \frac{\partial T}{\partial t} = -\frac{1}{B_v} [\rho T, \Phi] - \gamma \rho T B_v \left[ \frac{1}{B_v^2}, \Phi \right] + \nabla \cdot \left[ \kappa_{\perp} \nabla_{\perp} T + \kappa_{\parallel} \nabla_{\parallel} \nabla_{\parallel} T + \frac{pD_{\perp}}{\rho} \nabla_{\perp} \rho + \frac{pD_{\parallel}}{\rho} \nabla_{\parallel} \rho \right] + (S_e + \eta_{Ohm} B_v^2 j^2) - T \frac{\partial\rho}{\partial t},$$

$$\frac{\partial\psi}{\partial t} = \frac{\partial^{\parallel}\Phi - [\Psi, \Phi]}{B_v} - \eta (j - j_{source}) + \nabla \cdot (\eta_{num} \nabla^{\perp} j),$$

where  $P = \nabla \cdot (D_{\perp} \nabla_{\perp} \rho + D_{\parallel} \nabla_{\parallel} \rho) + S_{\rho}$ ,  $j$  and the plasma vorticity,  $\omega$ , are given by  $j = \Delta^* \Psi$  and  $\omega = \Delta^{\perp} \Phi$ .



[\*] G. Huysmans, et al, Nucl. Fusion 47, 659, 2007.

[\*\*] N. Nikulsin et al., Physics of Plasmas 29, 063901, 2022.

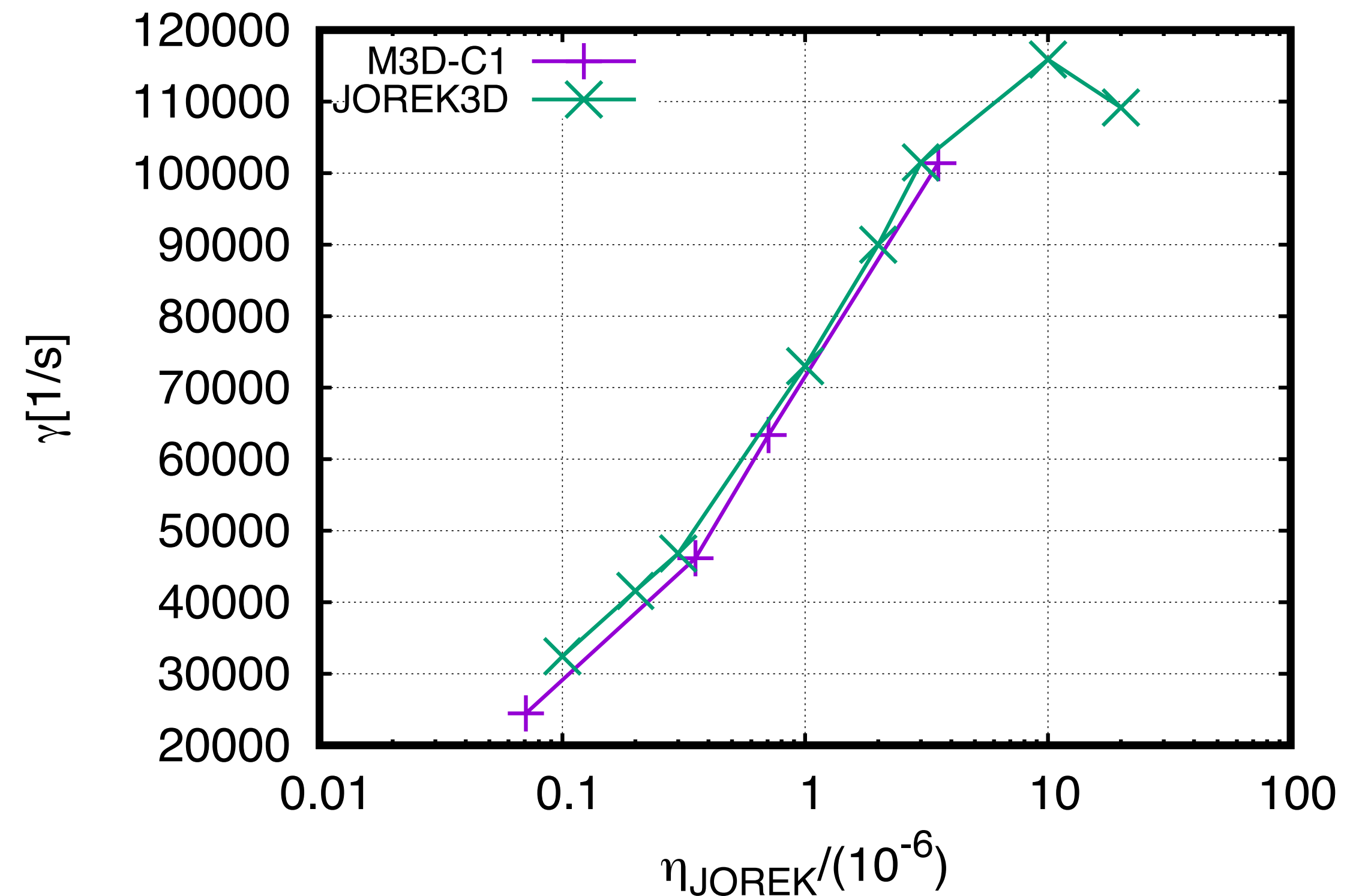
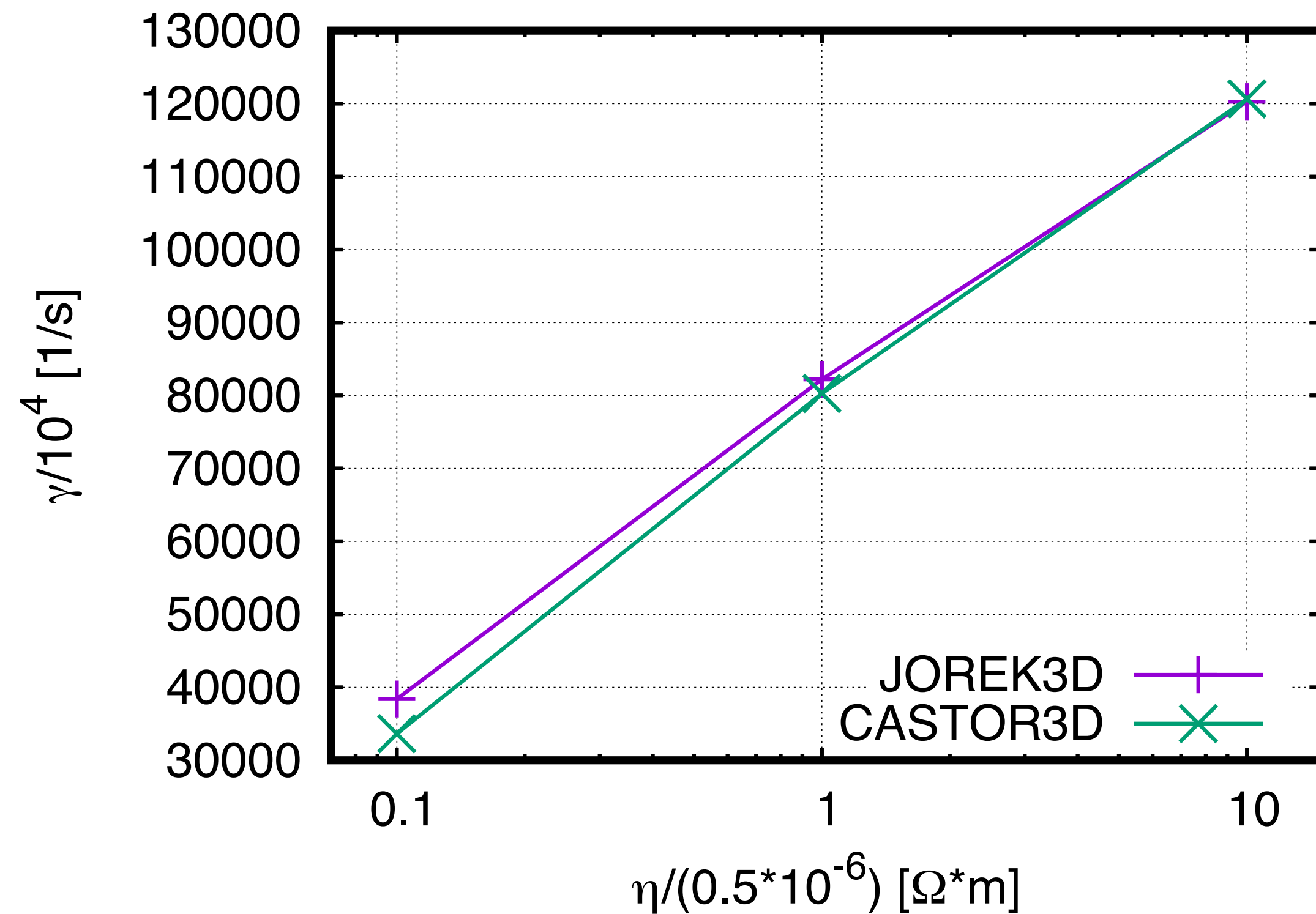
[\*\*\*] F. Hindenlang, et al, Simons hour talk, 2019.

[\*\*\*\*] R. Ramasamy, et al. Nuclear Fusion, 64 086030, 2024.

# Benchmarks: CASTOR3D and M3D-C1



Note that CASTOR3D [\*] has no identical viscosity terms thus viscosity independent limit in JOREK was found.  
Viscosity in all cases for M3D-C1 [\*\*] benchmark is  $1\text{E-}06 \cdot 0.364831 \text{ kg}/(\text{m}\cdot\text{s})$ .

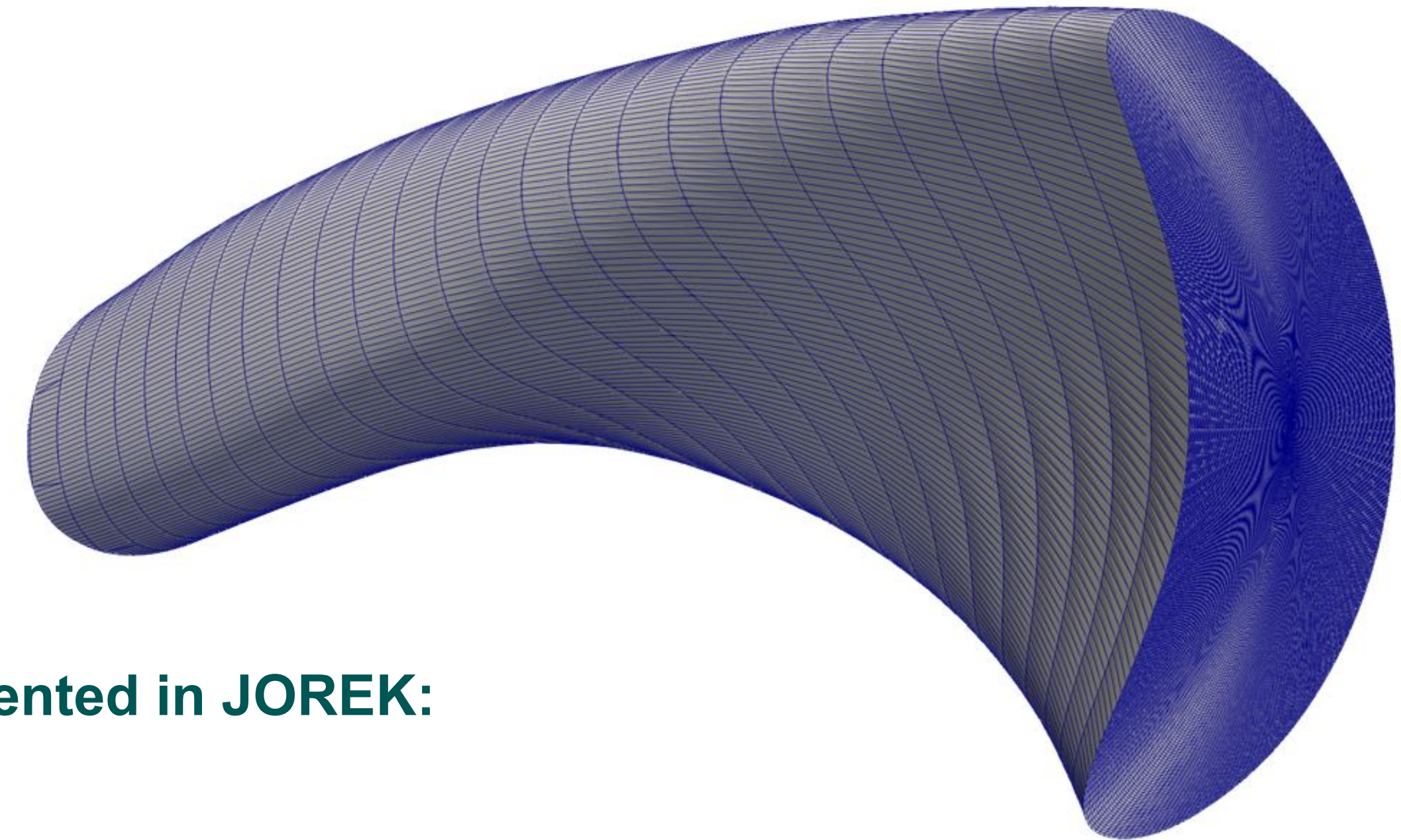


[\*] Strumberger and Günter, Nuclear Fusion 57/1 (2016): 016032.

[\*\*] Jardin, Ferraro, Breslau, et al. Computational Science & Discovery 5, no. 1 (2012): 014002.

# JOREK3D code

- For the stellarator extension, the grid becomes  $\phi$ -dependent.
- The equilibrium is not calculated inside JOREK, but imported from the GVEC code [\*].
- The physics model presently is reduced MHD without  $v_{||}$  (equivalent to 199 model for the tokamak); single and two-temperature ( $T_i$  and  $T_e$ ) models are available.
- A reduced MHD model for stellarators was derived and implemented in JOREK:
  - \* Energy is conserved
  - \*  $\nabla \cdot \vec{B} = 0$  is satisfied
  - \* Force balance error is insignificant
- The model was validated for tearing and ballooning modes in Wendelstein 7-A [\*\*], and shows good agreement with linear full MHD results.



[\*] F. Hindenlang, et al, Simons hour talk, 2019.

[\*\*] N. Nikulsin et al, PoP, 26(10), 102109, 2019; JPP, 87(3), 855870301, 2021 and PoP, 29(6), 063901, 2022.



# Reduced MHD

- **Nonlinear MHD simulations are computationally expensive.**
- **Reduced MHD models are less expensive:**
  - No fast magnetosonic waves > larger time step
  - Reduction of number of unknowns > less memory
- **Two approaches to reduced MHD:**
  - Ordering-based:** expand variables in the inverse aspect ratio  $\epsilon$ . Constraints at 0th order remove fast waves.
  - Ansatz-based:** force  $\vec{B}$  and  $\vec{v}$  to satisfy ansatzes that zero out fast waves.



# Stellarator-capable (full) MHD

Let the induced vector potential be  $\vec{A} = \Psi \nabla \chi + \Omega \nabla \psi_v$ .

**Total magnetic field (exact):**  $\vec{B} = \nabla \chi + \nabla \Psi \times \nabla \chi + \nabla \Omega \times \nabla \psi_v$ , where  $\nabla \chi$  is a background vacuum field (dominant),  $\Psi$  represents field line bending,  $\Omega$  is magnetic field compression and  $\psi_v$  is a scalar such that  $\nabla \chi = \nabla \psi_v \times \nabla \beta_v$ .

**Velocity field (exact):**  $\vec{v} = \frac{\nabla \Phi \times \nabla \chi}{B_v^2} + v_{||} \vec{B} + \nabla^\perp \zeta$ .

**Here terms correspond to ExB velocity terms, parallel flow and fluid compression terms (Alfvén waves, slow magnetosonic waves and fast magnetosonic waves).**

## Stellarator-capable (full) MHD

Let the induced vector potential be  $\vec{A} = \Psi \nabla \chi + \Omega \nabla \psi_v$ .

Total magnetic field (exact):  $\vec{B} = \nabla \chi + \nabla \Psi \times \nabla \chi + \nabla \Omega \times \nabla \psi_v$ , where  $\nabla \chi$  is a background vacuum field (dominant),  $\Psi$  represents field line bending,  $\Omega$  is magnetic field compression and  $\psi_v$  is a scalar such that  $\nabla \chi = \nabla \psi_v \times \nabla \beta_v$ .

Velocity field (exact):  $\vec{v} = \frac{\nabla \Phi \times \nabla \chi}{B_v^2} + \gamma_{\parallel} \vec{B} + \nabla_{\perp} \zeta$ .

Here terms correspond to ExB velocity terms, parallel flow and fluid compression terms (Alfvén waves, slow magnetosonic waves and fast magnetosonic waves).

# Stellarator-capable (full) MHD

Viscoresistive MHD equations with anisotropic heat flow and mass diffusion (full MHD):

$$\frac{\partial \rho}{\partial t} + \nabla \cdot (\rho \vec{v}) = P, \quad \text{Continuity equation}$$

$$\frac{\partial}{\partial t}(\rho \vec{v}) + \nabla \cdot (\rho \vec{v} \vec{v}) = \vec{j} \times \vec{B} - \nabla p + \mu \Delta \vec{v}, \quad \text{Vector momentum equation}$$

$$\frac{\partial p}{\partial t} + \vec{v} \cdot \nabla p + \gamma p \nabla \cdot \vec{v} = (\gamma - 1) \left[ \nabla \cdot \left( \kappa_{\perp} \nabla_{\perp} T + \kappa_{\parallel} \nabla_{\parallel} T + \frac{p}{\gamma - 1} \frac{D_{\perp}}{\rho} \nabla_{\perp} \rho \right) + S_e + \eta j^2 \right], \quad \text{Internal energy equation}$$

$$\frac{\partial \vec{B}}{\partial t} = - \nabla \times \vec{E}, \quad \text{Faraday's Law}$$

$$\nabla \times \vec{B} = \mu_0 \vec{j}, \quad \nabla \cdot \vec{B} = 0, \quad \vec{E} = - \vec{v} \times \vec{B} + \eta \vec{j}, \quad P = \nabla \cdot (D_{\perp} \nabla_{\perp} \rho) + S_{\rho},$$

# Stellarator-capable reduced MHD

With  $\vec{B}$  and  $\vec{v}$  now being  $\vec{B} = \nabla\chi + \nabla\Psi \times \nabla\chi$  and  $\vec{v} = \frac{\nabla\Phi \times \nabla\chi}{B_v^2}$  respectively, reduced MHD equations are:

$$\frac{\partial\rho}{\partial t} = -B_v \left[ \frac{\rho}{B_v^2}, \Phi \right] + P,$$

$$\nabla \cdot \left( \frac{\rho}{B_v^2} \nabla^\perp \frac{\partial\Phi}{\partial t} \right) = \frac{B_v}{2} \left[ \frac{\rho}{B_v^2}, \frac{(\Phi, \Phi)}{B_v^2} \right] + B_v \left[ \frac{\rho\omega}{B_v^4}, \Phi \right] - \nabla \cdot \left( \frac{P}{B_v^2} \nabla^\perp \Phi \right) + \nabla \cdot (j\mathbf{B}) + B_v \left[ \frac{1}{B_v^2}, p \right] + \nabla \cdot (\mu_\perp \nabla^\perp \omega) - \Delta^\perp (\mu_{num} \Delta^\perp \omega),$$

$$\rho \frac{\partial T}{\partial t} = -\frac{1}{B_v} [\rho T, \Phi] - \gamma \rho T B_v \left[ \frac{1}{B_v^2}, \Phi \right] + \nabla \cdot \left[ \kappa_\perp \nabla_\perp T + \kappa_\parallel \nabla_\parallel \nabla_\parallel T + \frac{pD_\perp}{\rho} \nabla_\perp \rho + \frac{pD_\parallel}{\rho} \nabla_\parallel \rho \right] + (S_e + \eta_{Ohm} B_v^2 j^2) - T \frac{\partial\rho}{\partial t},$$

$$\frac{\partial\psi}{\partial t} = \frac{\partial^\parallel \Phi - [\Psi, \Phi]}{B_v} - \eta (j - j_{source}) + \nabla \cdot (\eta_{num} \nabla^\perp j),$$

where  $P = \nabla \cdot (D_\perp \nabla_\perp \rho + D_\parallel \nabla_\parallel \rho) + S_\rho, j$  and the plasma vorticity,  $\omega$ , are given by  $j = \Delta^* \Psi$  and  $\omega = \Delta^\perp \Phi$ .